Master's thesis

NTNU
Norwegian University of Science and Technology
Faculty of Engineering
Department of Energy and Process Engineering

Mélanie Jaspart

Optimisation of offshore oil and gas processing plants based on online cricondenbar and TVP analysis

Master's thesis in Miscellaneous Courses - Faculty of Engineering
Supervisor: Even Solbraa (co-supervisor: Efstathios Skouras-Iliopoulos)

June 2019

NTNU
Norwegian University of Science and Technology

equinor

Mélanie Jaspart

Optimisation of offshore oil and gas processing plants based on online cricondenbar and TVP analysis

Master's thesis in Miscellaneous Courses - Faculty of Engineering
Supervisor: Even Solbraa (co-supervisor: Efstathios Skouras-Iliopoulos)
June 2019

Norwegian University of Science and Technology
Faculty of Engineering
Department of Energy and Process Engineering

NTNU
Norwegian University of
Science and Technology

Acknowledgments

This master's thesis report concludes my year as an exchange student at NTNU. I would like to thank the Norwegian University of Science and Technology for its welcome. My gratitude goes also to my French university, the University of Lorraine, which permitted me to study abroad.

I want also to express my great gratitude to my supervisors Even Solbraa, advisor at Equinor Research Centre and professor at NTNU, and Efstathios Skouras-Iliopoulos, principal researcher at Equinor, for their guidance and time during this work.

Background and objective

Online analysis of cricondenbar is a new technology. New field developments on the Norwegian continental shelf will need to install such online cricondenbar measurement. Online analysis of TVP is not done at the moment but could be calculated based on process simulation for the well fluid composition and flow rates. The topics of this work will be to see how to optimise an oil and gas process based on both TVP analysis and cricondenbar analysis of the rich gas. The student needs to set up an Unisim model for a given oil field. A well composition and flow rate, and export specifications will be given. The student will optimise the process for meeting specifications, energy consumption and production. In some situations, the field will optimise oil production rate, while other situations could be that we will produce as much rich gas as possible. Case studies for optimization will be defined during the thesis. The following tasks are to be considered:

1. Review standards for natural gas dew point and oil TVP/RVP/RVPE measurements
2. Review calculation methods for natural gas dew point and oil TVP/RVP/RVPE
3. Review of methods for online cricondenbar estimation
4. Review of offshore gas processes for controlling TVP and cricondenbar
5. Set up a UniSim model for an offshore plant to meet TVP and cricondenbar specifications
6. Optimization of process based on TVP and cricondenbar specification

Abstract

The focus of this work is on an oil and gas offshore plant where the extracted natural gas is processed to deliver on one hand the rich gas, and on the other hand the oil.

Such as plant is simulated thanks to the UniSim software. It includes different steps.
The first one is the transport of natural gas from the well to the inlet of the offshore platform considering pressure drop and heat transfer. At the inlet, liquid and gas are separated.
Then, the condensate stabilization unit which removes the lightest hydrocarbons from the liquid is modelled to meet an oil true vapour pressure (TVP) below 0.965 bar. This step is done by the cascade flash separation process. The TVP specification ensure a safe storage of the oil.
Vapour from this process are sent to the gas recompression train and mixed with the gas coming from the inlet separation.
Finally, the gas processing part consists of controlling the gas cricondenbar by cooling and separation processes so that it is below 110 bar. It enables to ensure to have a single phase for the rich gas transport.
This model is referred as the base case model.

Oil TVP specification is used to optimise the plant. Indeed, this work shows that the rich gas cricondenbar is never a problem, its value is always below the specification. Hence, it is not used to optimise the plant. Three distinct optimisations are done in this work.

The first one consists of maximizing the production of gas. In order to do so, more vaporization is required in the condensate stabilization unit. Hence, the pressure levels are reduced, and the condensate is heated at a higher temperature than in the base case model. Another important parameter is the choice of temperature in the gas processing part. A high temperature enables to generates more vapour. The optimized model enables to increase by 4 % the rich gas production.

The second optimisation is the increase of the production of oil. However, due the relatively high TVP in the base case model, it is not possible to increase the oil production without having a TVP off-spec. It means that the base case model is also the optimal model for oil production maximisation.

Finally, reducing the energy consumption of the offshore plant is the third optimisation done in this work. By modifying the conditions of pressure and temperature along the process the total energy consumption is reduced by 50 %. The most important parameter is the choice of temperature at which the condensate is heated.
In the context of energy consumption reduction, heat integration is achieved. It consists of using the energy released by the different fluids which need to be cooled in the process to heat the condensate in the condensate stabilization unit. Results show that the heat integration has a bigger impact on the reduction of the energy consumption in the base case model than in the model which optimises the energy demand of the plant. It is due to the fact that the energy distribution is different in the two models: thermal energy (heater energy consumption) represents half of the total energy demand of the plant in the base case model whereas it represents only 4 % in the optimized model.
Finally, different liquid recirculation loops are present in the process. This work shows that changing the location where these liquids are sent does not reduce more the energy consumption of the plant than the previous optimized model.

Additional studies show that the composition of the extracted natural gas is relevant for the optimisations. Indeed, process parameters must be changed to meet the rich gas and the oil

specifications. Moreover, in some cases, cricondenbar specification is relevant to optimise the offshore plant. This work suggests to first change the parameters that control the most the cricondenbar (the temperature levels in the gas processing part) and then modify the parameters that controls the oil TVP (the heater temperature and the last level of pressure in the condensate stabilization unit).

Since cricondenbar can be off-spec in some cases, PhaseOpt technology, which is an online tool to measure the cricondenbar directly on the field, can be used.

Table of content

List of abbreviations

ANFIS	Adaptive Neuro Fuzzy Inference System
ASTM	American Society for Testing and Materials
CBM	Coal Bed Methane
CCS	Carbone Capture and Storage
CMR	Certified Reference Material
EoS	Equation of State
HCDP	HydroCarbon Dew point
ISO	International Organization for Standardization
LNG	Liquefied Natural Gas
LPG	Liquefied Petroleum Gases
MEG	MonoEthylene Glycol
NG1	Natural Gas number 1 (chapter 5, 6 and 7)
NG2	Natural Gas number 2 (chapter 8)
NGL	Natural Gas Liquids
PNA	Paraffin-Naphtene-Aromatic
PR	Peng-Robinson
RVP	Reid Vapour Pressure
RVPE	Reid Vapour Pressure Equivalent
SRK	Soave-Redlich-Kwong
TEG	TriEthylene Glycol
TVP	True Vapour Pressure
UMR-PRU	Universal Mixing Rule – Peng Robinson UNIFAC
VPCR	Vapour Pressure of Crude oil

Nomenclature

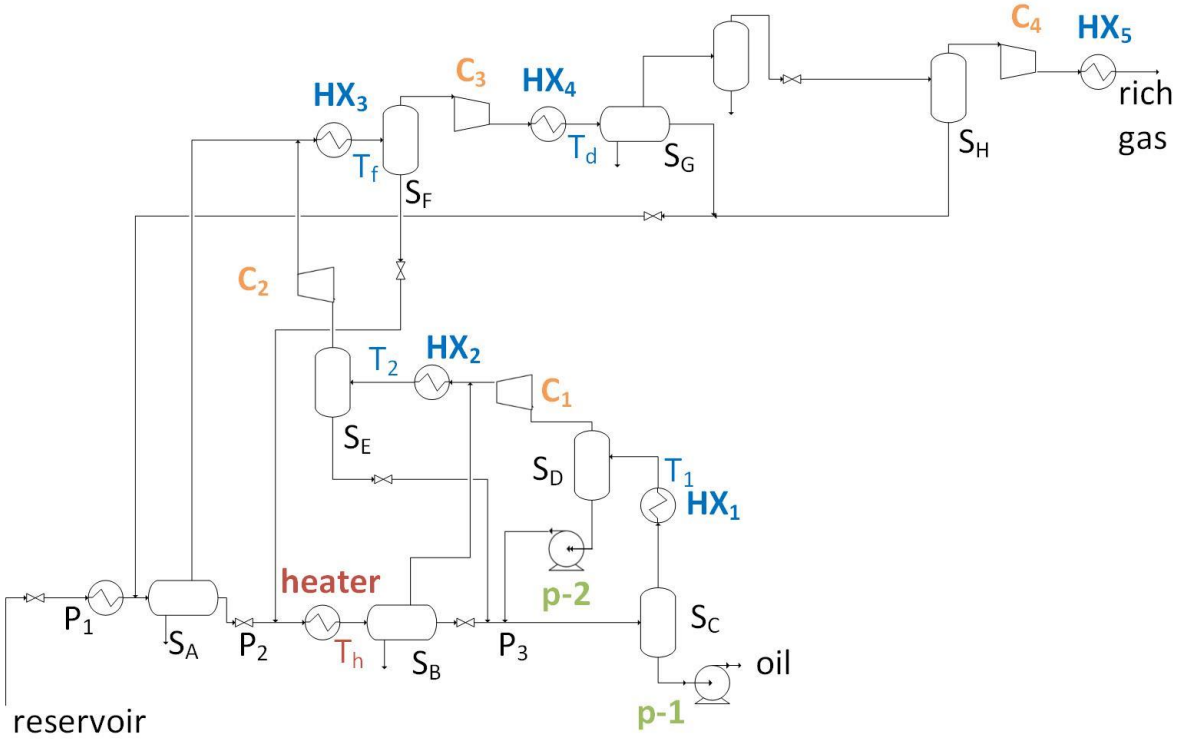

Figure 1: nomenclature for chapter 5, 6, 7 and 8

Condensate stabilization unit

- Levels of pressure: P_1, P_2, P_3
- Temperature after the heater: T_h
- Separators: S_A, S_B, S_C
- Pumps: p-1, p-2

Gas recompression train

- Coolers: HX_1, HX_2
- Temperature after coolers: T_1, T_2
- Separators: S_D, S_E
- Compressors: C_1, C_2

Gas processing

- Coolers: HX_3, HX_4, HX_5
- Temperature after coolers: T_f, T_d
- Gas scrubbers: S_F, S_G, S_H
- Compressors: C_3, C_4

List of figures

List of tables

List of equations

Introduction

Natural gas is an important source of energy when it is used as a fuel. It is also an important source of petrochemical feedstock. Between the raw material and the finished products, a lot of processes are used, both offshore and onshore, to ensure safety and good quality of the products.

The focus of this paper is on the offshore part where natural gas is treated to be able to be transported as a single phase and the oil is stabilized. Operating above the cricondenbar of the rich gas enables to ensure a safe transport. Concerning the oil, the stabilization processes limit the value of its true vapour pressure (TVP), a key criterion for its transport and storage.
These two specifications, cricondenbar of the rich gas and vapour pressure of the oil, are the main concerns of this work.

A typical offshore plant is modelled using the UniSim software. Once the specifications on the two products are reached, the model is used to optimise the plant. Optimisation is done using cricondenbar and TVP results. Three cases are studied: the maximisation of the gas production or the oil production and the minimisation of the total energy consumption of the plant. The variables which are considered to do these optimisations are the temperature and the pressure levels. The offshore plant containing recirculation loops, the choice of the location where the fluids are sent is also a parameter which is studied.
The combination of streams is also examined to reduce the energy consumption of the plant by using the heat released where a fluid is cooled to heat another fluid in the process which is called heat integration.
Optimisations are done in several steps. The first one is the parametric studies where the influence of process parameters (temperature, pressure) on different outputs (production rates, energy consumption…) are examined. Using these results, optimisations are done manually. Finally, the optimizer tool of the software is used to obtain better results.

This report is divided into two main sections: one theoretical part and another one more specific to an oil and gas offshore plant. The theoretical part contains the most relevant information for this work from literature review.
Chapter 1 introduces basic concepts in natural gas processing focusing more precisely on offshore plants. Chapter 2 and 3 are dedicated to the study of the specifications to meet on the plant: cricondenbar for the rich gas and vapour pressure for the crude oil. For both chapters, measurement and predictive techniques are introduced. Chapter 4 introduces common processes which are used to meet these specifications. Chapter 5 concentrates on the UniSim model of an oil and gas offshore plant. Inputs data are specified as well as the main relevant outputs. The aim of the two next chapters is to explain different ways to optimise the process with numerical results. Chapter 6 focuses on the maximisation of the production of the gas or the oil whereas chapter 7 is about the energy consumption minimisation. Finally, chapter 8 consists of two other studies: about the change of the reservoir composition and about the heat transfer during raw material transport toward the offshore plant.

Chapter 1 – Gas value chain

The aim of this chapter is to present the different steps from the raw natural gas to the finished products: from the well to the consumer. Main problems and specifications related to these steps are also introduced. The goal is to provide an overview of the gas value chain with a focus on offshore plants.

I. Raw natural gas

Natural gas comes from the decomposition of some plants and animal matter which are trapped in sediments of ancient lakes and oceans. Because of high pressure, geothermal heat and time this organic matter is turned into kerogen. Then, takes place the decomposition of kerogen into oil (hydrogen-rich kerogen) and gas (oxygen-rich kerogen) (Kidnay, 2011).

1. Classification

Different classifications are used to define natural gas depending on the type of source (conventional, unconventional) or component composition.

Conventional natural gas refers to the gas which is extracted from traditional oil and gas wells. Within this category, the distinction is made between natural gas which is found with crude oil in the same reservoir (associated gas) and gas without or little oil (nonassociated gas).
Unconventional natural gas is found in other resources. The main ones are tight gas sands, coal bed methane (CBM) and gas hydrates. Unconventional sources become more and more economically feasible because of higher gas prices and the development of new extraction techniques such as horizontal drilling and hydraulic fracturing technologies. Hence, the production from this category of gas is increasing (Kidnay, 2011).

Concerning the component characterization, a gas is said to be lean or rich depending on its liquids content. Rich gas refers to a gas with high liquids content since it is the most valuable in an economic point of view. Sulphur content below 4 ppm defines the gas as sweet whereas sour gas term is used for higher proportion of sulphur (Kidnay, 2011).

2. Hydrates

From the well to the offshore platform, natural gas is transported through pipelines. During this step, both the pressure and the temperature are reduced. The pressure reduction is the result of frictions between the fluid and the pipeline whereas the temperature reduction is the result of heat transfer between the hot gas and the sea. Since these two conditions are modified, the properties of natural gas are changed. In some conditions of pressure and temperature, gas hydrates can be formed.

Hydrate is a physical combination of water and another molecule producing a solid. Depending on the gas composition, its crystalline structure is different: type I (smaller molecules such as CH_4, C_2H_6), type II (larger molecules such as C_3H_8, i-C_4H_{10}, n-C_4H_{10}), type H (some isoparaffins and cyclohexanes larger than pentane). The structure highly influences the pressure and the temperature at which hydrates

may formed. Structure II is more stable than structure I. It results that for the same pressure, hydrates of structure II will be formed at a higher temperature (GPSA, 2004).

Since hydrates are solid, they can lead to plugging problems in the pipelines during the transport, and in the other equipment during the process. They must be avoided for safety and efficiency reasons.

There exist several ways to handle hydrates problem. A common one is the injection of chemical inhibitors at the wellhead. Monoethylene glycol (MEG) is commonly used. As a result, the separation of this inhibitor must be processed on the offshore plant. Regeneration can be done in another plant. Another way to avoid hydrates formation is to operate under the conditions of pressure and temperature where they cannot be formed. However, this possibility is not always possible in an industrial point of view. The third possibility is to dehydrate the gas before the transportation (Kidnay, 2011).
The choice of the method to prevent hydrates formation depends on which part of the process is considered. Between the well and the offshore plant, the only possibility is to inject a chemical inhibitor in the wellhead. Indeed, operating pressure and temperature cannot be changed because they result from physical phenomena.

II. Offshore oil and gas plant: main steps

In this section, the main steps of an offshore plant are introduced. The figure below illustrates a typical sequence of processes that produces rich gas and oil from raw natural gas. Specifications are established in contract negotiations. Hence, they are not the same in each country and are not definitive (Kidnay, 2011).

MEG injection, discussed previously, is also depicted on this figure.

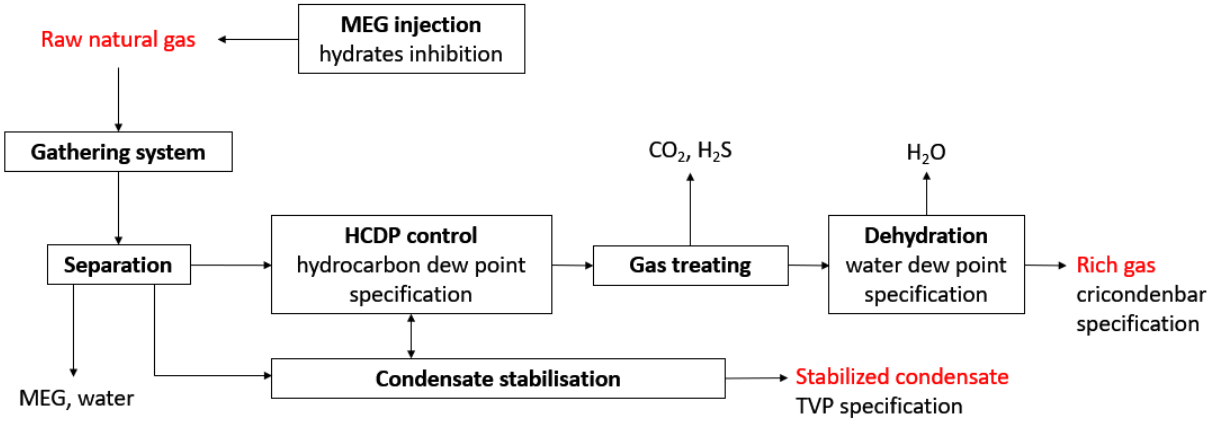

Figure 2: typical sequence of processes of an offshore plant

1. Gas treating

Gas treating is the step where acid gases CO_2 and H_2S are removed. This is necessary to meet their specifications and ensure equipment integrity (avoiding corrosion and plugging problems). Typical specifications are a maximal amount of 2 % (mole) for CO_2 in the rich gas and 2.5 ppmv for H_2S and COS (Gassco, 2018).

Depending on the composition of the raw material, different processes are used for acid gases removal. Chart exist to choose between different techniques according to the partial pressure of the acid gas in the inlet and in the outlet of the gas treating unit: chemical absorption, physical absorption, adsorption or membranes for example (Kidnay, 2011).

After being removed from the gas, CO_2 is vented or used as an injection fluid in enhanced oil recovery projects. Venting CO_2 to the atmosphere is only possible if the environmental regulations allow it (Kidnay, 2011). Nowadays, projects focus on carbon capture and storage (CCS) to mitigate climate change (Deflandre, 2019).
Concerning H_2S, different options are possible but the main one is its conversion into elemental sulphur which can be sold as an industrial chemical. This is the aim of sulphur recovery processes (Kidnay, 2011).

2. Dehydration

Water removal is essential to prevent hydrate formation as previously introduced.

Dehydration part takes place after the gas treating because water can be injected in the previous step. It is the case when amine-based solution is injected to remove H_2S for instance.

Water content is usually defined with its dew point. Typical value for the rich gas is 40 mg/Sm^3 (Gassco, 2018). Gas dehydration is commonly done using absorption phenomenon. Glycols such as triethylene glycol (TEG) is typically used. However, if an extreme dryness is required, adsorption on molecular sieves is chosen (Fredheim, Solbraa, 2018).

3. Hydrocarbon dew point control

There are two definitions of the hydrocarbon dew point (HCDP) specification: the cricondentherm, which is the highest temperature at which the fluid can be in multiple phase and the cricondenbar which is the highest pressure at which the fluid can be in multiple phase.
Common specifications are 40°C for the cricondentherm and 110 bar for the cricondenbar (Gassco, 2018).

HCDP specifications are identified in the following figure which represents the phase envelope of a rich gas. It is a pressure-temperature diagram showing the thermodynamic behaviour of the fluid. The dew point line and the bubble line are connected at the critical point.
It should be noticed that the cricondenbar can be higher than the critical pressure.

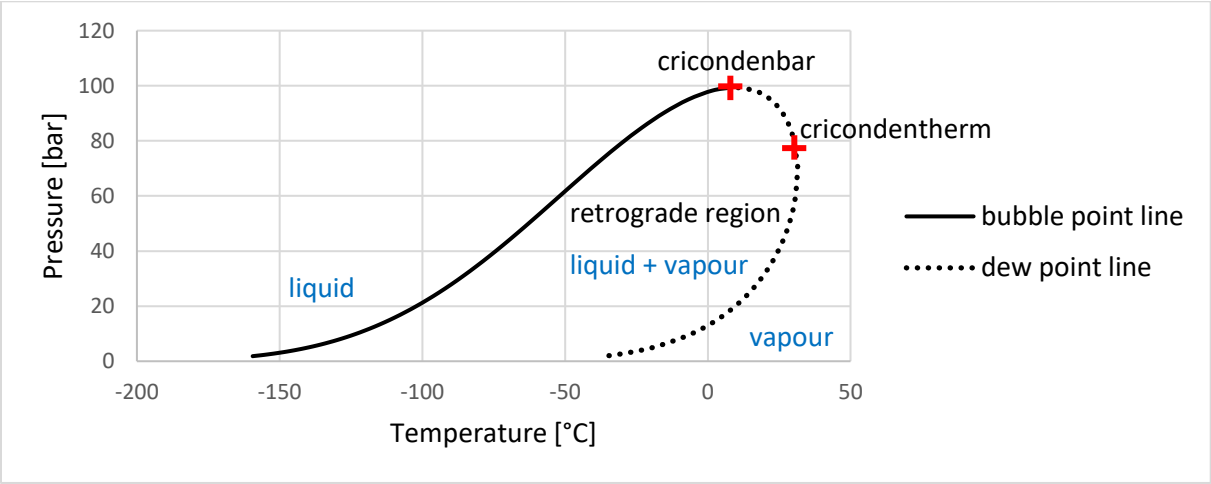

Figure 3: rich gas phase envelope (UniSim simulation)

The specification which is used in this work is the cricondenbar. Rich gas must be transported from the offshore plant to the onshore plant at a pressure above the cricondenbar so that hydrocarbons cannot condensate out of the gas.

Transporting the gas as a single phase protects equipment such as compressors since it avoids the destruction of the blades due to liquid droplets (Zhou et al., 2006). Moreover, it reduces the risk of decreased regularity and pipeline integrity (Skouras-Iliopoulos et al., 2014).

Cricondenbar specification must be reached in the entire transport system until the onshore plant. The inlet facilities of these onshore plants, such as water, H_2S and mercury removal systems, must also operate in the dense phase region (Skouras-Iliopoulos et al., 2014).

The layout of the phase envelope is very depending on the composition of the gas (Atilhan et al., 2011). Indeed, the retrograde region (the region of vapour-liquid equilibrium) is smaller for low hydrocarbon content that for high hydrocarbon content. Indeed, C_{6+} (hexane and higher hydrocarbons) fraction highly influences HCDP (Skouras-Iliopoulos et al., 2014). Hence, in order to control and respect the cricondenbar specification, hydrocarbon content is a key parameter.

4. Condensate stabilisation

A condensate stabilization unit is achieved to meet the crude oil specification. This is the volatility of the liquid mixture which is important. It is estimated through the vapour pressure. If the specification is not reached, vapour can be present and can lead to vapour lock, vaporisation loses, air pollution, unsafe storage and handling (Riazi et al., 2005).

There exist different ways to define the vapour pressure.
The true vapour pressure (TVP) is the pressure of a vapour in equilibrium with its condensed phase at a specific temperature (Riazi et al., 2005).
Reid vapour pressure (RVP) is the absolute pressure exerted by a mixture determined at 311 K and at a vapour to liquid ratio of 4. Note that the value of TVP measured at 311 K will be higher than RVP. Indeed, some sample vaporisation will usually occur in the RVP system (Riazi et al., 2005). Reid vapour pressure equivalent (RVPE) is also used in some correlations.
Finally, the vapour pressure of crude oil ($VPCR_x$) is the pressure exerted in an evacuated chamber at a vapour-liquid ratio x by conditioned or unconditioned crude oil where x varies from 0.02 to 4 (ASTM, 2016).

III. Further processes

This master's thesis is about offshore plants. Hence, there is no focus on the further processes. This section only introduces the main points to provide an overview of the global gas value chain.

1. Onshore processes

After being processed on offshore plant, rich gas is sent to onshore plants for further processing. It produces sales gas with specifications related to its composition and performance criteria. These are the combustion characteristics (Wobbe number, heating value, combustion emission products (Kidnay, 2011). Sales gas is then sent to the market (household, industry…).

Moreover, natural gas liquids (NGL), which correspond to C_{2+}, are usually extracted through the cryogenic expander process. After this step, fractionation allows to obtain pure petrochemicals: ethane, propane, n-butane, i-butane which can be sell to the customers (Fredheim, Solbraa, 2018).

Another possible product is liquefied natural gas (LNG). It corresponds to natural gas which has been made liquid. It is liquid at -163°C at atmospheric pressure. Different processes are in place to do it: cascade process or mixed refrigeration process for example (Pettersen, 2018).

2. Storage

2.1 Natural gas

Two types of gas storage exist depending on the quantity to store. On one hand, small capacity storage are aboveground, floating roof gas holders at ambient pressure. On the other hand, larger facilities which are prevalent are underground and operates at high pressure. It consists of depleted reservoirs, salt caverns or aquifers. The former is the most widespread because the geology of this reservoir is known and the techniques to inject or withdraw the gas are in place (Kidnay, 2011).

2.2 Crude oil

Crude oil can be stored in two different types of tank: fixed roof tank of constant volume or floating head tank. The liquid is usually stored very near to atmospheric pressure. The pressure of the tank must be higher than the TVP of crude oil in order to prevent loss of liquid during the storage (Kidnay, 2011).

Chapter 2 – Rich gas specification: cricondenbar

Cricondenbar specification of the rich gas is the specification relevant for this work and is the subject of this chapter. The first part is dedicated to the gas analysis. Results of this analysis are important for the prediction and measurement methods of the cricondenbar. These methods are introduced in the second and third part.

I. Gas analysis

1. Sampling

Results of gas analysis is dependent on the sampling technique and procedures. Hence, standards exist to ensure a good quality of the results and comparisons between different analyses. ISO 10715 states sampling guidelines for natural gas (ISO, 1997). This standard can only be used to study gas stream, not liquid stream or multiple flow.

To ensure representativeness of the gas sample, different parameters must be estimated. An important one is the sampling frequency and hence the number of samples which derive from it. It is necessary to have more than one sample because the composition of natural gas is not constant over the time and can vary even within the same day.

During transport or waiting time before the analysis, condensation can occur and revaporisation must be done to have a single gas phase. This is achieved by heating the sample for two hours (10°C above the source temperature or until 100°C if the temperature is unknown).

Special attention must be given to the choice and the preparation of the sampling system. In fact, some components can have strong sorption effects meaning that they will be adsorbed on the wall of the equipment distorting the composition analysis. This phenomenon can be reduced by surface treatment such as polishing techniques. Chemisorption can also occur between the sample and the material which can act as a catalyst (ISO, 1997).

2. Gas chromatography

After having a gas sample, gas chromatography can be done.

Gas chromatography determines the composition of the gas. It provides good inputs to the thermodynamic model used to estimate the phase envelope and the cricondenbar since it is strongly dependent on the composition (Rusten et al., 2008; Skouras-Iliopoulos, 2011).

ISO 6974 – 1 (ISO 2012) provides guidelines for the gas chromatographic analysis of natural gas and methods of data processing. This standard allows to measure H_2, He, O_2, N_2, CO_2 and hydrocarbons (individual components or as a group) from C_5 to C_{12} (ISO, 2006).

Chromatography separates the different components. After this step, they can be identified and quantified thanks to calibration data obtained in the same set of conditions. Quantification can be done with two methods: single or multiple operations. Single operation method is defined as the technique where all measured components are determined using a single sample injection and a single

detector whereas multiple operation method requires different systems to determine groups of components.

The notion of certified reference material (CMR) is introduced in this standard to define directly and indirectly measured components. On one hand, directly measured component is present as a certified component in the CMR and hence can be directly quantify using calibration data relating to this component. On the other hand, indirectly measured component must be quantify using a relative response factor. This factor is the ratio of the molar amount of one component to the molar amount of reference component giving an equal detector response.

ISO 6974-1 sets the procedure determining mole fractions of the components based on different steps: working range definition, requirements of the analytical method, selection of the equipment and working conditions, analysis of sample, calculation of component mole fractions. Additional steps must be required for example if there are indirect components (assign relative response factors).

3. C_{7+} characterization

As it was previously introduced, the layout of the phase envelope (so the cricondenbar) is very depend on the composition of the gas and especially on the heaviest components (Atilhan et al., 2011). In order to predict it in an accurate way, C_{7+} characterization is required (Rusten et al., 2008). It enables to reduce the number of individual components and the parameters used in the thermodynamic model for cricondenbar prediction (Skouras-Iliopoulos, 2011).

C_{7+} characterization consists of grouping the C_{7+} fraction into normal components (nC_7, nC_8…), pseudo components (C_7, C_8…) or by a PNA distribution. This last possibility groups the components depending on their type: paraffin, naphtene or aromatic (Rusten et al., 2008).

II. Cricondenbar prediction methods

1. Thermodynamic model

Cricondenbar of the rich gas can be identified knowing the phase envelope. It can be calculated using thermodynamic models based on equations of state (EoS). The two most common used in commercially available softwares are Peng-Robinson (PR) and Soave-Redlich-Kwong (SRK) (Gallagher, 2006). However, other EoS are developed and appeared to be more accurate in the prediction of the HCDP. Universal Mixing Rule – Peng Robinson UNIFAC (UMR-PRU) has been proven to be a good model for the prediction of the cricondenbar (Skouras-Iliopoulos et al., 2014; Skylogianni et al., 2016).

In order to develop more accurate thermodynamic models, experimental data for the phase envelope are necessary (Rusten et al., 2008). Indeed, the evaluation of a model is based on the comparison between predicted values and experimental values. Moreover, experimental measurements can be useful to identify the cause of problems in the process such as an off-spec gas (Rusten et al., 2008). The next section will introduce the main ways to obtain these experimental data for the phase envelope determination.

The improvement of EoS is also the result of more accurate density measurement (May et al., 2001). Indeed, knowing the precise density of natural gas improves the determination of the phase envelope.

2. Phase envelope prediction

Researches are done to determine models and algorithms to draw the phase envelopes from the EoS.

The work of Michelsen about the calculation of phase envelopes for multicomponent mixtures (Michelsen, 1980) is the basis of the recent developments to draw the entire phase envelope (Nikolaidis et al., 2016; Venkatarathnam, 2014). Phase equilibrium states that the component fugacity must be the same in each phase (equifugacity). EoS allows to estimate these parameters with respect to temperature, pressure and composition. SRK is used in Michelsen's approach but other EoS can be used. If C is the number of components in the mixture, C equations are solved simultaneously (equifugacity). Two more equations are also solved simultaneously: the specification equation and the condition that the sum of all mole fractions must be equal to one. Newton-Raphson iterations are used to solve the set of non-linear equations. Two factors are important in this approach: the choice of the specified variable and its initial estimation.

The bed spring method is a variation of Michelsen's algorithm. This method uses a "spring" that sets the slope value of the modified tangent plane distance in respect to the specification. This can be the pressure or the temperature (Nikolaidis et al., 2016).

The choice of the specified variable has a great importance for the calculation of the equilibrium point (Venkatarathnam, 2014). The density marching method (Venkatarathnam, 2014) allows to construct the phase envelope using the density of one of the phases as the ideal independent variable. Two steps are required to automatically obtain the phase envelope: calculation of the equilibrium point for a given vapour fraction at a specified density, then vary the density.

III. Cricondenbar measurement methods

Different techniques are used to directly measure the HCDP: visual equilibrium cell, microwave equipment or surface acoustic techniques for example (Atilhan et al., 2011). The measurements can be manual or automated.

1. Chilled mirror approach: a manual measurement

The chilled mirror approach is a manual visual dew point method to determine HCDP. The Bureau of Mines dew point apparatus is the most commonly accepted instrument to do it (Skouras-Iliopoulos et al., 2011). The principle of this technique is that a mirror is cooled at constant pressure until the condensation of natural gas occurs. Then, the operator identifies and notes this temperature corresponding to the HCDP temperature. The bubble point can also be identified by heating the mirror and checking when the last drop of liquid has disappeared meaning that natural gas is fully vaporized (Skouras-Iliopoulos et al., 2011).

The device is composed of two separated chambers: one containing the sample and the other one the refrigerant gas used to cool the mirror (Herring, 2010). The coolant is generally an expandable gas such as carbon dioxide (Skouras-Iliopoulos et al., 2011) or propane (Herring, 2010).

ASTM D1142 provides the procedure to use this apparatus (ASTM, 2012). Some key parameters are the control of the gas flow entering in the system and the rate of cooling and warming. These should be set in such a way that it approximates isothermal conditions as nearly as possible. Moreover, it states that the HCDP temperature value must be defined as the arithmetic average of the all estimated HCDP temperatures.

The main advantages of this technique are its simplicity, safety and it requires low capital investment (Herring, 2010). Even if ASTM D1142 provides a standard test method, it remains subjective since operator must identify the HCDP with its eyes. Hence, different values for the same sample can be obtained for different operators. It requires patience and training to use the system properly (Herring, 2010). Moreover, this measurement can be difficult because of glycol film which can be formed covering the mirror (Skouras-Iliopoulos et al., 2014). Note that glycol presence comes from the MEG injection to prevent hydrates formation.

2. Automatic measurements

In order to avoid subjectivity in the determination of HCDP, automatic techniques are developed. Automatic optical condensation is an example. The shiny property of hydrocarbon condensate is used. Cooling the gas will make hydrocarbons to condense producing a dew layer which can be seen as a mirror. The result is a strong image easily detectable (Herring, 2010). This method does not require an operator to visually identify the dew point.

Another possibility to determine HCDP is the use of an automated isochoric apparatus. The system presented by Jingjun Zhou et al. is composed of several elements including an isochoric cell in a vacuum chamber, an isothermal shield, a pressure measurement system, a heating and cooling system (Zhou et al., 2006). The key idea of determining the HCDP here is the change of the slope of an isochore as it passes the phase boundary (Atilhan et al., 2011).

Density measurements can also be used to estimate the dew point. Eric F. May et al. studied this method for binary and ternary mixtures using a dual-sinker densimeter (May et al., 2001). The device for density measurement is an automated magnetic suspension microbalance system. The measurement of the mass of the two sinkers allows to assess the density. The dew point is estimated at the conditions (P,T) where the density curves intersect.

As it was previously introduced, microwaves analysis can also be used to determine phase envelope of natural gas. This technique is presented by Michael D. Frørup et al. in their study (Frørup et al., 1989). The system is composed of four main parts: microwave source, resonance cavity, detector and circulator. The method consists of a reduction in pressure of the sample at a constant temperature. The consequence is a change in the quality factor of the reflected microwaves from the equilibrium cell. This factor is defined in the study as a measure of the energy stored and the energy dissipated in the electric and magnetic fields of the microwave circuit at the resonance frequency. When significant changes occur in the quality factor, dew point or bubble point is identified.

Another possibility is to use the speed of sound characteristic. It consists of a direct acoustic measurement in a medium and allows to determine the phase envelope if the density and the heat capacity of the gas are known (López et al.,2003).

IV. Online cricondenbar estimation: PhaseOpt technology

This section introduces the PhaseOpt technology developed by Statoil and Gassco. Most of the information are taken from their report *PhaseOpt - Online tool for hydrocarbon dew point monitoring* (Skouras-Iliopoulos et al., 2014).

The online cricondenbar estimation is necessary because of errors in the hydrocarbon dew point estimation by thermodynamic models which can lead to off-spec rich gas. To avoid this, safety margins in pressure are taken to ensure safe operation. Online measurements will lead to reduce these margins.

The reasons for the development of this technology called business drivers are efficient operations in gas plants, optimise pipeline capacity and achieve gas quality.

1. Tool description

As illustrated in the following figure, different sub-systems compose the PhaseOpt technology.

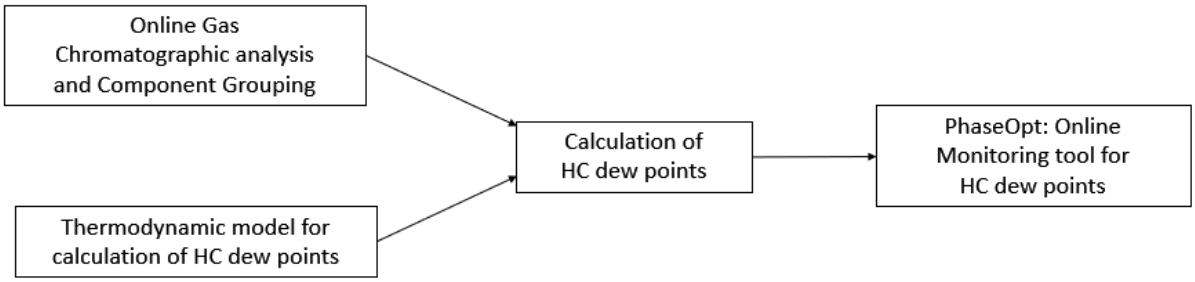

Figure 4: illustration of PhaseOpt technology (Skouras-Iliopoulos et al., 2014)

Firstly, a sample system is optimized to handle trace components analysis. Trace components that require attention are water, heavy hydrocarbons and glycols. They are present in the raw gas from the reservoir and are mostly removed by the offshore process, but some traces remain. Careful handling is necessary because adsorption of these molecules on the sampling system can occur and hence distort the results of the chromatography. To minimize this problem, PhaseOpt technology uses highly polished surfaces and silica treated materials. Eric F. May et al. study adsorption effects near the phase boundary at high pressures (May et al., 2001).

Since the HCDP is highly influenced by the heaviest hydrocarbons in the gas, the knowledge of the composition of the studied gas must be very accurate. This is the objective of the gas chromatography. In the case of PhaseOpt, the extended analysis of the gas provides detailed composition up to C_{12}.

With the previous information, the estimation of the HCDP can be done by thermodynamic model. The chosen model is UMR-PRU due to its accuracy for cricondenbar prediction of natural gas as previously mentioned (Skylogianni et al., 2016).

2. Tool qualification

In order to qualify this technology, different tests are done on two different fields. HCDP is directly measured in the field, in laboratory, predicted with SRK model and finally estimated with the PhaseOpt model. Direct measurements are done using the chilled mirror approach, previously introduced.

The results of Efstathios Skouras et al. show that the phase envelope and the cricondenbar of the gas sample are nearly the same which confirms the accuracy of PhaseOpt technology for online cricondenbar measurement.

Chapter 3 – Crude oil specification: vapour pressure

The specification on the oil, also called condensate, in the offshore process is based on the vapour pressure analysis. This specification is necessary to limit hydrocarbon emissions during the storage and the transport of the condensate (Mokhatab et al., 2015).

The table below indicates the standards used to determine this specification.

ASTM D2879-18 (ASTM, 2018)	Standard Test Method for Vapor Pressure-Temperature Relationship and Initial Decomposition Temperature of Liquids by Isoteniscope
ASTM D323-15a (ASTM, 2015)	Standard Test Method for Vapor Pressure of Petroleum Products (Reid Method)
ASTM D6377-16 (ASTM, 2016)	Standard Test Method for Determination of Vapor Pressure of Crude Oil: $VPCR_x$ (Expansion Method)

Table 1: standards for oil vapour pressure determination

I. Vapour pressure measurements

As introduced in the first chapter, different definitions exist concerning the vapour pressure. This section introduces some measurement methods depending on the definition which is considered.

1. True vapour pressure

The TVP can be directly measured using an isoteniscope as presented by the ASTM in its standard D2879-18 (ASTM, 2018). The method is suitable for crude oil having a TVP between 0.133 kPa and 101.3 kPa at the given temperature. The condition to use this method is that the mixture must not have a vapour pressure greater than 0.133 kPa at 50°C.

This technique consists of balancing the pressure due to the vapour of the sample against a known pressure of an inert gas.

Since the TVP measurement involves having a liquid sample, no air should be present. If present in the sample, it must be removed before the measure. Hence, it is not convenient for field or laboratory measures that require operating personnel (Campbell, 1992).

2. Reid vapour pressure

Contrary to TVP, RVP measurements can carry air. Standard cell must be used to determine RVP taking into account air partial pressure.

ASTM provides also a method to measure the RVP of a liquid and applicable to volatile crude oil: standard D323-15a (ASTM, 2015). The point 4.1 states the main idea of this technique: "*The liquid*

chamber of the vapor pressure apparatus is filled with the chilled sample and connected to the vapor chamber that has been heated to 37.8 °C in a bath. The assembled apparatus is immersed in a bath at 37.8 °C until a constant pressure is observed". This pressure is the RVP.

3. Vapour pressure of crude oil

An expansion method allows to estimate the VPCR for a specific vapour liquid ratio (index x) at a specific temperature T: standard D6377-16 (ASTM, 2016). This standard is used for samples with a vapour pressure between 25 kPa and 180 kPa at 37.8°C and for a vapour liquid ratio from 4 to 0.02. VPCR can be measured for a temperature between 0°C and 100°C.

A sample with a known volume is introduced into a small, cylindrical and evacuated chamber where a piston is present. This piston is moved until the volume gives the desired vapour to liquid ratio. Then, the temperature of the chamber is adjusted. When the equilibrium is reached the pressure is recorded as well as the temperature. The measured pressure is $VPCR_x$ (T).

This test method can be applied to online applications.

II. Vapour pressure predictions

1. Conversion from VPCR to RVPE

As introduced before, the standard ASTM D6377-16 (ASTM, 2016) provides the method to determine the vapour pressure of crude oil. The relative bias test method is also detailed. It consists of a correlation between VPCR measured at 37.8 °C for a vapour liquid ratio equal to 4 and the Reid vapour pressure equivalent (RVPE).

$$\mathrm{RVPE} = \mathrm{A} * \mathrm{VPCR}_4(37.8\ °\mathrm{C}) \tag{1}$$

RVPE	:	Reid vapour pressure equivalent	[kPa]
A	:	Coefficient $\mathrm{A} = 0.83$ for samples in pressurized floating piston cylinders $\mathrm{A} = 0.915$ for samples in nonpressurized 1-L sample containers	[-]
$\mathrm{VPCR}_4(37.8°\mathrm{C})$	:	Vapour pressure of crude oil for a vapour liquid ratio equal to 4 at 37.8°C	[kPa]

This correlation can only be used for crude oil with VPCR_x (37.8°C) between 34 kPa and 117 kPa.

ASTM D6377-16 clearly indicates that if this correlation is used, the result of the calculated RVPE must be compared to the value of RVP obtained by ASTM D323-15a. They should be the same.

2. Conversion from RVP to TVP

There is no direct prediction of TVP. This is the reason why correlations and algorithms are developed using the previous measurement or prediction of RVP.

3.1 Simple correlations

Mahmood Moshfeghian wrote an article about a model used to convert RVP to TVP and vice-versa for crude oil (Moshfeghian, 2016). This model is based on the equations given by API 2517.

The set of equations to convert RVP to TVP is presented below.

$$\begin{aligned} \mathrm{A} &= \mathrm{A}_1 - \mathrm{A}_2 * \ln(\mathrm{RVP}) \\ \mathrm{B} &= \mathrm{B}_1 - \mathrm{B}_2 * \ln(\mathrm{RVP}) \\ \mathrm{TVP} &= \exp\left(\mathrm{A} - \frac{\mathrm{B}}{\mathrm{T} + \mathrm{C}}\right) \end{aligned} \tag{2}$$

TVP	:	True Vapour Pressure	[kPa]
RVP	:	Reid Vapour Pressure	[kPa]
T	:	Temperature of crude oil	[°C]
A_1	:	SI parameter $\mathrm{A}_1 = 16.62$	
A_2	:	SI parameter $\mathrm{A}_2 = 0.9675$	
B_1	:	SI parameter $\mathrm{B}_1 = 5339$	
B_2	:	SI parameter $\mathrm{B}_2 = 675.7$	
C	:	SI parameter $\mathrm{C} = 273.15$	

This article provides also a set of equations to convert TVP into RVP.

$$\begin{gathered} A = A_1 - A_2 * \ln(TVP) - A_3 * (T + C) \\ B = B_1 - B_2 * \ln(TVP) - B_3 * (\ln(TVP))^2 \\ RVP = \exp\left(A - \frac{B}{T + C}\right) \end{gathered} \tag{3}$$

TVP	:	True Vapour Pressure	[kPa]
RVP	:	Reid Vapour Pressure	[kPa]
T	:	Temperature of crude oil	[°C]
A_1	:	SI parameter $A_1 = 13.1085$	
A_2	:	SI parameter $A_2 = -2.0857$	
A_3	:	SI parameter $A_3 = -0.0403$	
B_1	:	SI parameter $B_1 = 45.61$	
B_2	:	SI parameter $B_2 = -385.14$	
B_3	:	SI parameter $B_3 = -0.5028$	
C	:	SI parameter $C = 273.15$	

3.2 Algorithms

Another possibility to obtain TVP is to use a predictive tool knowing RVP and temperature. A. Bahadori developed such a model (Bahadori, 2014). It consists of an Arrhenius-type function combined with Vandermonde matrix. The studied systems are liquefied petroleum gases (LPG), natural gasolines and moto fuel components. This tool is suitable for a RVP above 35 kPa and a temperature between -20°C and 100°C. The advantages of this technique are its accuracy and clear numerical background.

Alireza Baghban et al. conducted a study to predict TVP from RVP and temperature as the previous one but based on another concept (Baghban et al., 2016). In this case, this is an adaptive neuro fuzzy inference system (ANFIS) algorithm which is presented. The systems of the study are the same as for the previous one: LPG, natural gasolines, motor fuel components, same conditions of temperature and pressure. The results obtained by this method are compared to the Bahadori correlation. They appear to be more accurate.

It should be noticed that these two methods are not presented for crude oil systems. Hence, further experiments must be conducted to see if the techniques can also be used for these systems.

Chapter 4 – Offshore oil and gas processes

The aim of this chapter is to introduce the usual offshore processes used to control the rich gas cricondenbar and the crude oil vapour pressure.

The figure below is a flow scheme of a typical offshore plant.

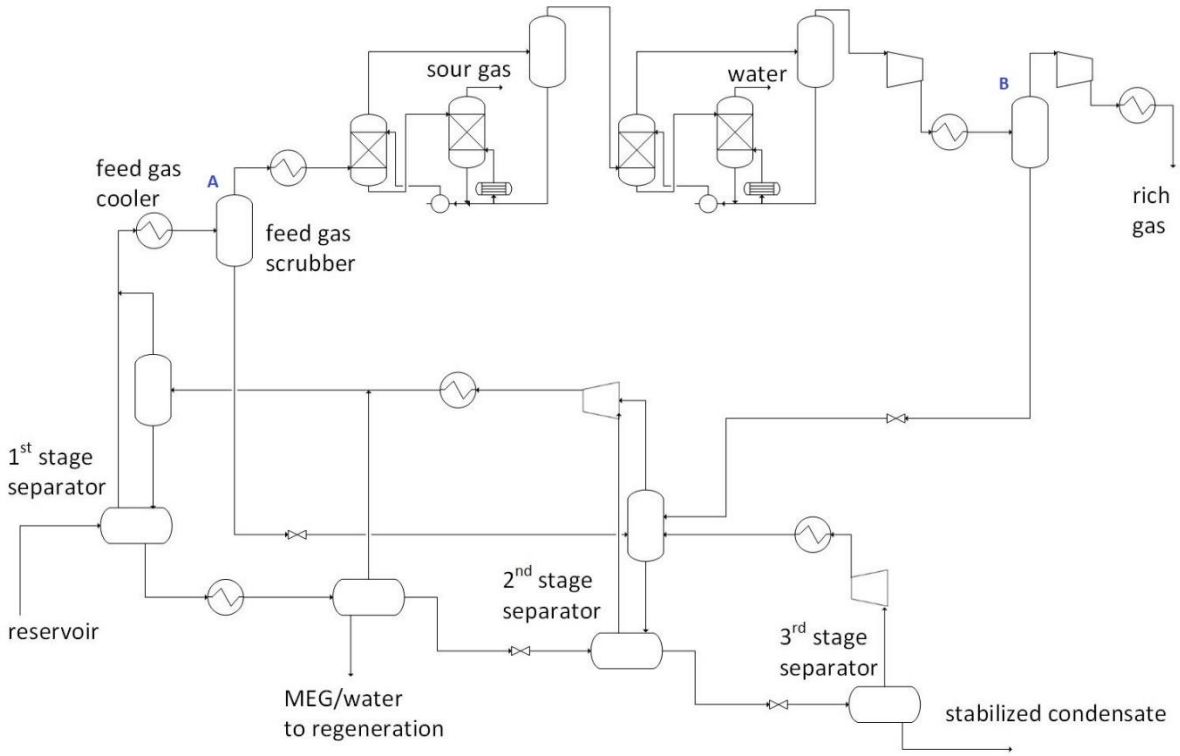

Figure 5: typical oil and gas offshore plant (Fredheim, Solbraa, 2018)

I. Rich gas cricondenbar control

As it was seen before, changing the composition of the gas changes the shape of the phase envelope and the value of the cricondenbar. Hence, removing hydrocarbons from the gas will reduce the cricondenbar and meet the gas specification. Different processes are used to reach this goal: cooling and separation, cooling and separation in combination with expansion, adsorption process or membrane process (Fredheim, Solbraa, 2018).

The figure below is a good representation of how the phase envelope is changed along the process. C_{3+} represents 57 % (mole basis) of the reservoir composition whereas its proportion in the rich gas is around 18 %.

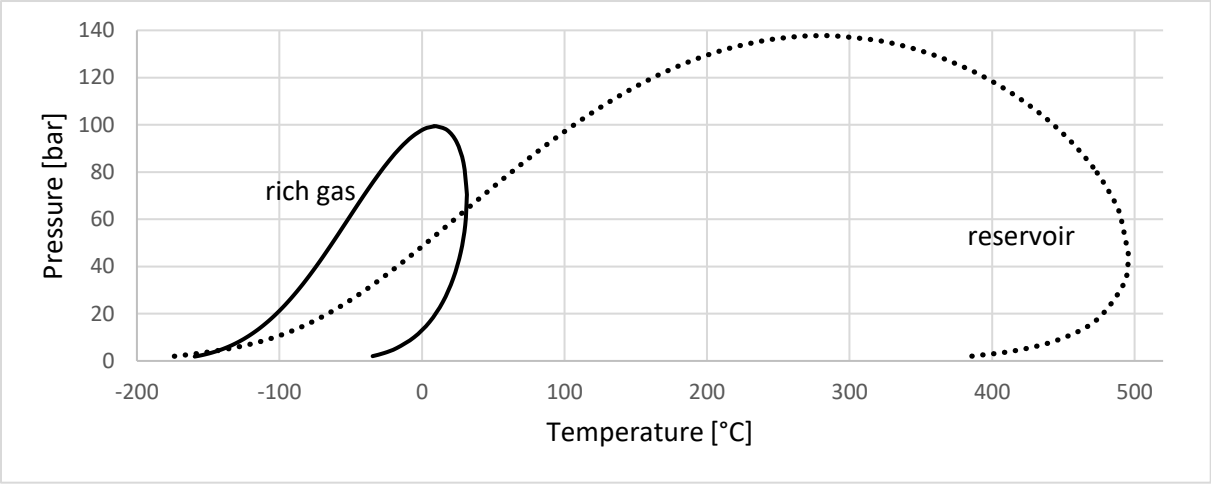

Figure 6: phase envelope and gas behaviour (UniSim simulation)

1. Cooling and separation

By cooling the gas, liquid is formed and can be removed. The liquid phase contains the heaviest hydrocarbons.

The feed gas scrubber is the last step where hydrocarbons are removed, this is where the cricondenbar can be controlled (point A on the *Figure 5*). The last scrubber in the process is used as a safety scrubber (point B on the *Figure 5*). Since in this part of the process the pressure is above the cricondenbar, no liquid should be present.

Several stages can be used to meet the specification as the figure below shows.

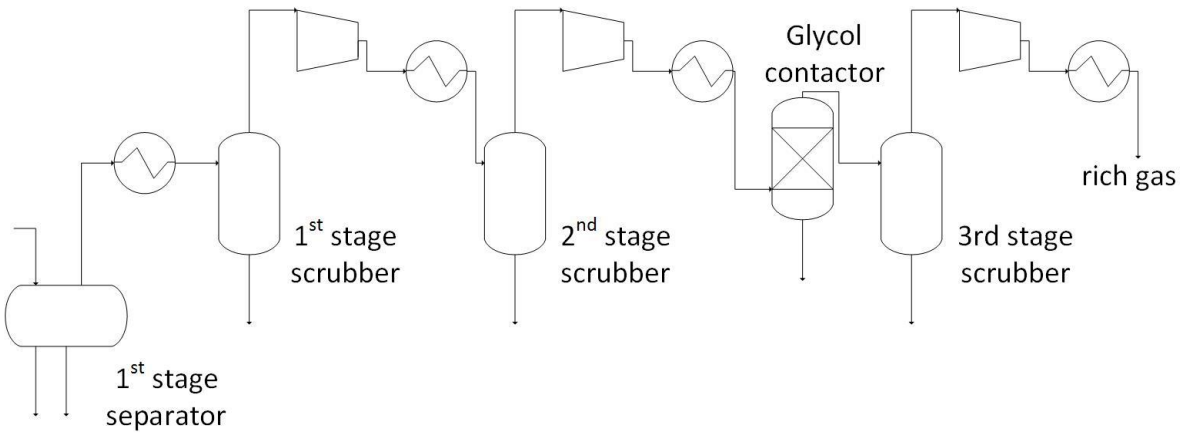

Figure 7: cooling and separation stages for cricondenbar control (Rusten et al., 2008)

Separation plays a key role in the efficiency of this type of process. Indeed, the liquid must be completely removed which require good scrubber technology (Rusten et al, 2008).

2. Cooling and separation in combination with expansion

The previous process can be combined with an expansion unit (adiabatic or Joule-Thomson valve, expander). It is used when the pressure difference with the cricondenbar is too high (Fredheim, Solbraa, 2018).

3. Adsorption process

Reaching the good value of the cricondenbar by reducing the hydrocarbon dew point can also be done by adsorption. One advantage of this technique is that the adsorbed hydrocarbons can be regenerated and hence, be used as valuable raw materials for the chemical industry (Berg et al., 2017). However, it is not relevant for an offshore process (Fredheim, Solbraa, 2018).

4. Membrane process

Membrane technology in natural gas field is almost used to remove carbon dioxide but is also used to reduce the hydrocarbon dew point in natural gas processing. Using membranes instead of cooling and separation process allows to reduce the global energy consumption (Baker, Lokhandwala, 2008; Neubauer et al., 2014).

ABB/MTR provides membranes that separate C_{3+} hydrocarbons from the gas to control the dew point. It consists of a spiral-wound module with perfluoro polymers silicone rubber. A flow scheme of this technology is drawn below. The feed gas passes through the membrane where the heaviest hydrocarbons are removed (permeate). They are compressed and cooled so that hydrocarbons are now in liquid phase. The non-condensing part is then injected in a second membrane module creating a recirculation loop around the condenser (Baker, Lokhandwala, 2008).

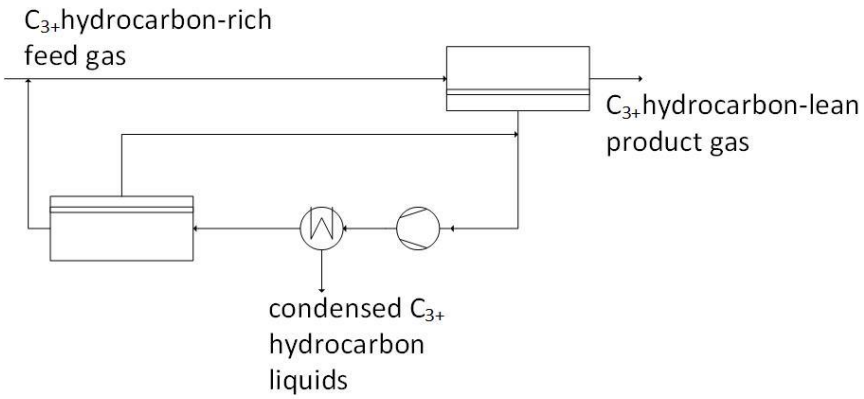

Figure 8: flow scheme of a membrane dew point control unit (Baker, Lokhandwala, 2008)

The choice of the type of membrane is based on the gas characteristics. Indeed, some of the components from the gas can degrade the membrane or reduce its efficiency by being collected on its surface (Baker, Lokhandwala, 2008).

The efficiency of membranes can be improved if there is liquid in the feed. This is what Katja Neubauer et al. show in their study about the separation of alkanes (Neubauer et al., 2014). Their conclusion is that MFI-type membranes can be used to separate liquefied parts of natural gas mixtures which occur during dew point adjustments.

As for the adsorption process, membrane technique for the reduction of heavy hydrocarbon content is not widely used on offshore plants (Fredheim, Solbraa, 2018).

II. Condensate stabilization unit

In order to limit the oil TVP, the lightest hydrocarbons must be removed from the condensate. This is the aim of the condensate stabilization unit.

The main information for this section are taken from *Handbook of natural gas transmission and processing: principles and practices (chapter 5)* (Mokhatab et al., 2015).

1. Cascade flash separation

This process consists of several flash separations of the lightest components. It is underlines on the following scheme.

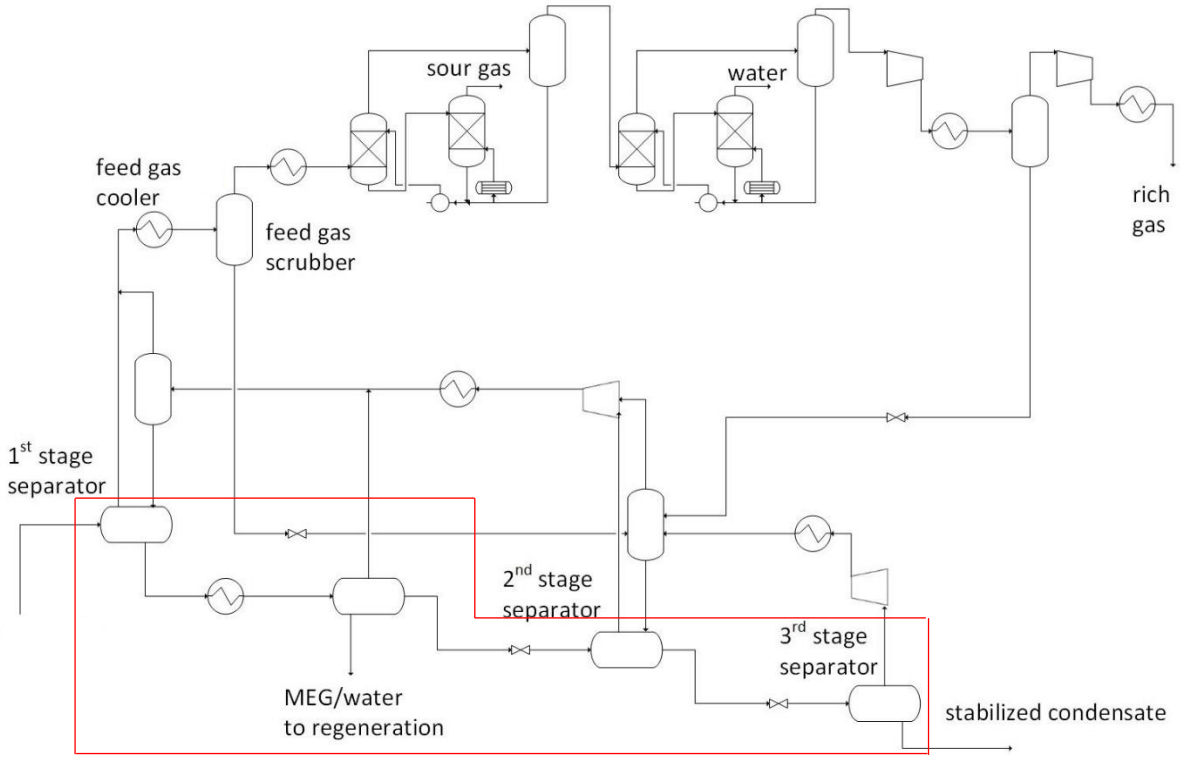

Figure 9: cascade flash separation for condensate stabilization (Fredheim, Solbraa, 2018)

The liquid from the first inlet separator is first heated and vapours containing the lightest hydrocarbons are formed. The three phases separator enables to separate the vapour phase, the mixture of MEG and water from the condensate.

Then, two stages of pressure reduction and separation are used. The reduction in pressure induces a flash releasing vapours of the lightest hydrocarbons. Note that the number of stages can vary from one plant to another. The pressure is reduced between the different flashes concentrating the condensate with the heaviest hydrocarbons. The choice of the pressure levels is a key parameter to meet the specification of crude oil but also to optimise the process. It can lead to energy saving in the other parts of the process.

The vapours from each stage are recompressed in the gas recompression stages and cooled down. Since it produces a multiple phase flow, separation units are used after these two steps. The vapour

phase is mixed with the vapour from the first inlet separator and sent to the gas processing unit for further processing. The liquid phase is sent back to the condensate stabilization unit.

Cascade flash separation is the most common process on offshore plants because of its simplicity and the compactness of the equipment. However, if the vapour pressure specification is too low, distillation separation process is required.

2. Distillation separation

The distillation process is more efficient than the cascade flash process. Since, it is mainly used in onshore plants, it will be only briefly discussed.

The system consists of a distillation column with or without reflux. Reflux enables to limit the loss of hydrocarbons in the vapour phase. Different options for the design of a such process exist: producing condensate only (figure below) or condensate and LPG.

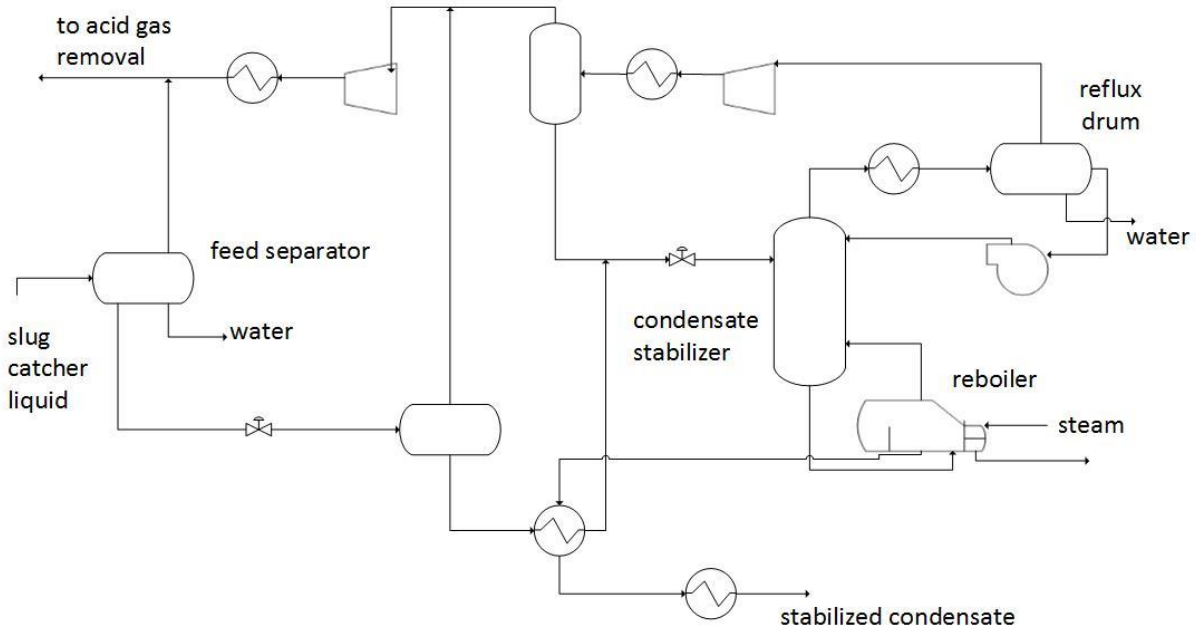

Figure 10: distillation separation for condensate stabilization (Mokhatab et al., 2015)

Chapter 5 – Simulation of an offshore oil and gas plant

This chapter presents a typical oil and gas offshore plant. It contains the description of the UniSim model with numerical inputs data, process parameters and results.

I. UniSim model of a typical offshore oil and gas plant

This section details the model of an offshore oil and gas processing plant set in the UniSim software. The specifications to meet are a TVP of crude oil smaller than 0.965 bar at 30°C and a rich gas cricondenbar smaller than 110 bar.

The thermodynamic model used for the simulation is SRK. However, it should keep in mind that using another EoS will have an impact on the results.

The following figure represents the plant as set in UniSim. Variables description can be found at the beginning of this report (section: *Nomenclature*).

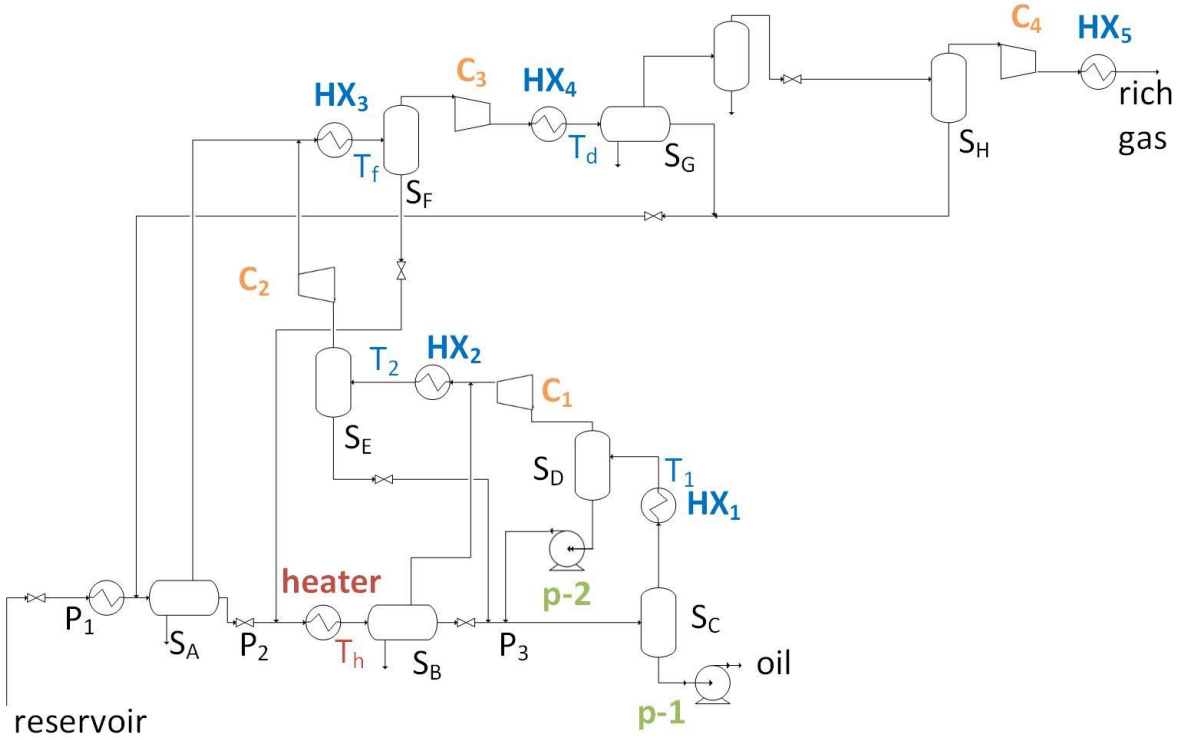

Figure 11: UniSim model of a typical offshore oil and gas plant

All the compressors in the process have an adiabatic efficiency of 75 %.

1. Reservoir conditions

The reservoir which is considered in this work is at 195.7 bar and 82.5 °C. The composition of the raw natural gas is given in appendix (*Appendix 1: natural gas composition*). The molar flow rate is set equal to 1 000 kmol/h.

2. Transport: from the well to the offshore plant

Pressure drop in the pipeline is modelled by a valve which brings the pressure to 16 bar (first level of pressure P_1). Heat transfer between natural gas and sea is performed by a heat exchanger bringing the temperature down to 70 °C. Since it is not a real heat exchanger, meaning that it is only set in the model to simulate a physical transfer, no pressure drop is considered.

3. Condensate stabilization unit and gas recompression train

A cascade flash separation with three levels of pressure is applied in this work: it is the condensate stabilization unit. The upper part where the gas is cooled and compressed is the gas recompression train which comprises two stages.

Because of the pressure reduction and heat transfer during the transport, some liquid is formed. The first inlet separation (S_A) enables to separate the three phases: gas, liquid and aqueous phase. Aqueous phase contains water which has condensed out of the gas as well as MEG if it was used for hydrate inhibition.

The liquid from the inlet separator is going through a valve where the pressure is reduced (second level of pressure P_2). A heater increases the temperature of the fluid before entering a three phases separator (S_B) where water is separated from the gas and the condensate. A pressure drop of 1.5 bar is considered in this heat exchanger.

The liquid from the second separator is sent to a valve for another pressure reduction (P_3). The resulting fluid is sent to a separator (S_C) where the liquid stream is the stabilized crude oil. The oil is then pumped to 13 bar and exported.
The gas from this third separator is cooled (HX_1). A pressure drop of 0.3 bar is considered. It creates a gas liquid mixture which is sent to a separator (S_D). On one hand, the liquid is pumped to the third level of pressure (P_3) and mixed with the liquid from the second separator (S_B). On the other hand, the gas is compressed and mixed with the vapour from S_B. The resulting mixture is cooled which makes hydrocarbons to condense. The pressure drop in this heat exchanger (HX_2) is set equal to 0.5 bar. After a separation in S_E, the liquid phase is depressurized and mixed with the liquid from the second separator. Finally, the gas is compressed and mixed with the feed gas from the inlet separator.

4. Gas processing

As it was previously introduced, the feed gas and the gas from the condensate stabilization unit are mixed together. Then, the fluid is cooled in HX_3 making some hydrocarbons to condense. The feed gas scrubber separates the vapour and the liquid phase. The liquid part is depressurized to the second level of pressure (P_2) and sent back the stabilization unit. The gas is compressed and cooled (HX_4)

before entering a three phases separator (S_G). Aqueous phase is removed. The liquid is depressurized to the first level of pressure (P_1) and sent back to the inlet separator.

After this separator, the dehydration is simulated. This done by using a component splitter in UniSim. A pressure loss of 7.7 bar during this step is modelled with a valve.

The following scrubber (S_H) is only used for safety reason avoiding liquid in the further compressor.

The final step is the recompression of the rich gas to 170.5 bar and a cooling to 30°C.

Note than all the coolers in the gas processing part (HX_3, HX_4 and HX_5) are modelled without any pressure drop.

II. Crude oil vapour pressure specification

1. Available properties in UniSim

In UniSim, the available properties for the stabilized oil include both RVP and TVP. The correlations used to estimate them are respectively: “Reid VP at 37.8 C” and “True VP”. These two correlations are the active ones by default in the software. The temperature reference for TVP can be chosen and is equal to 30°C in this work.

However, other correlations can be used for RVP: “API 5B1.1”, “API 5B1.2”, “ASTM D323-73/79”, “ASTM D323-82”, “ASTM D4953-91” and “ASTM D5191-91”. The reference temperature is 37.78 °C for all of them since this is at this temperature that RVP is defined. The UniSim user guide provides information about the different correlations (Honeywell, 2009).

“API 5B1.1” is applicable to gasoline and finished petroleum products but not for crude or oxygenated blends. Hence, it is irrelevant for this work.

“API 5B1.2” is suitable for condensate and crude oil systems which is the case of the stabilized oil. The result from this correlation is relevant for this work.

“ASTM D323-73/79” is almost the same as “Reid VP at 37.8 C”. The difference is the basis used: wet for the former and dry for the later.

Since oxygen is not present in the stream of interest, “ASTM D323-82”, “ASTM D4953-91” (gasoline-oxygenated blends) and “ASTM D5191-91” cannot be used.

2. Choice of the correlation of vapour pressure

For this work, the specification is defined for a value of TVP less than 0.965 bar at 30°C.

The recommended value of RVP is 0.760 bar. If the *Equation 2* is used to convert RVP into TVP, it results that TVP should be below 0.875 bar.
If the TVP specification is converted with *Equation 3*, the new specification is to have a RVP below 0.821 bar.

Since RVP is only given as a recommendation, TVP is used as the specification to meet. It should be below 0.965 bar at 30 °C. The correlation used is named “True VP” in UniSim, the only one available.

III. Parametric studies

In the offshore plant, different levels of pressure and temperature exist.

This section gives the results of the parametric studies which were carried out. It enables to see the influence of these parameters on specifications and on production rates. Variations are said significant if there are above 1 bar for the rich gas cricondenbar, 0.1 bar for the TVP of crude oil and 10 kmol/h for the production rates.

Thanks to these studies, the process parameters values required to meet both the rich gas cricondenbar and the oil TVP are identified.

The nomenclature used can be found in *Figure 1* and graphical results in appendix (*Appendix 2: parametric studies).*

1. Condensate stabilization unit

1.1 Second level of pressure P_2

In this section, the impact of the reduction of the second level of pressure in the condensate stabilization unit (P_2) is studied and explained. The study is done by varying the pressure from 14 bar to 4.5 bar.
Numerical results are obtained for P_3 equal to 2.56 bar, T_1, T_2, T_f, T_d to 30°C and T_h to 80°C.

Specifications

Pressure reduction makes ethane and propane to vaporise. Consequently, their proportion in oil decreases. Since less intermediate components are present in oil, TVP of crude oil is reduced. The result is a variation of 0.3 bar which is significant.

It should be noticed that in order to have a TVP below 0.965 bar, the pressure P_2 must be below 8.1 bar.

In the same time, ethane and propane proportions increase in the rich gas. It should lead to an increase of the cricondenbar. However, what is observed in a small increase until P_2 equal to 8.5 bar. After, it starts to decrease (*Figure 12*). Globally, cricondenbar decreases by 0.5 bar.
This decline can be explained by the fact that the i-pentane also decrease in rich gas decreasing the cricondenbar. It is observed in the following figure that the cricondenbar behaviour follows i-pentane behaviour.

In the considered range of pressure, cricondenbar is always below the specification of 110 bar.

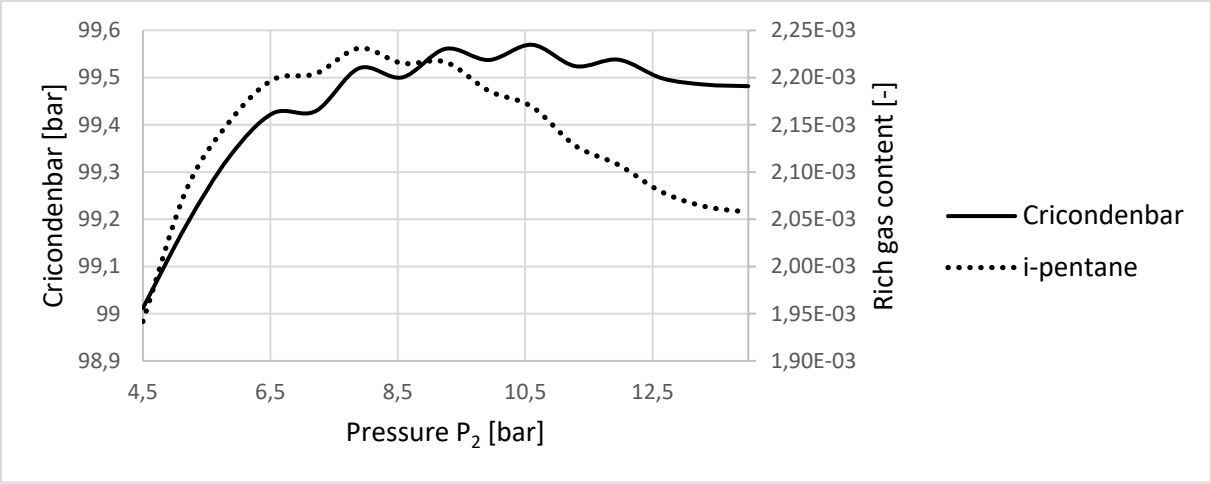

Figure 12: influence of P_2 on i-pentane content in rich gas and on cricondenbar

Production

A reduction of pressure leads to more vaporisation. The consequence is an increase of the gas molar flow and a decrease of liquid molar flow from following the three phases separator (S_B). It is also visible on the final products: increase of rich gas production and decrease of oil production. The variation of production is 7 kmol/h.

1.2 Third level of pressure P_3

The study of the reduction of the last level of pressure (P_3) is done by changing the pressure between 7 bar and 1 bar.
Numerical results are obtained for P_2 equal to 9.5 bar, T_1, T_2, T_f, T_d to 30°C and T_h to 80°C.

Specifications

The same conclusion than for P_2 can be drawn. Ethane and propane content in oil decreases with pressure reduction because of vaporisation. It explains the fact that TVP is reduced (by 3 bar).

The pressure should be reduced below 2.5 bar in order to respect the TVP specification.

Ethane and propane contents in rich gas increase. It should lead to an increase of cricondenbar. However, it is not what it observed. The cricondenbar is reduced (by 5 bar). Once again it could be explained by the behaviour of i-pentane whose proportion is reduced in rich gas.

Cricondenbar is always below 110 bar.

Production

Before pressure reduction the fluid is on the bubble point line. This reduction will bring the fluid into the two-phases area of the phase envelope creating vapour. It is observed in the model: the amount of vapour rises.

The flow entering the third separator S_C increases as the pressure decreases. Since the vapour fraction also increases, the production of vapour at the outlet of this separator rises also. As a result, the production of oil is reduced (by 60 kmol/h). Consequently, the production of rich gas is increased.

The increases of the input of S_C can be explained by studying the mix of streams: liquid from the inlet (first stage), second and third stage. They are all influenced by the change of pressure because of the recirculation loops. The flow rate of liquid from the second stage (from S_E) increases with the reduction of pressure. It is the most sensitive compared to the other streams. In fact, more recycles are created by the reduction of the third level of pressure.

1.3 Heater temperature T_h

The influence of the temperature at which the fluid is heated before the second stage of separation is studied for a range of temperature between 70°C and 150°C (T_h).
Numerical results are obtained for P_2 equal to 9.5 bar, P_3 to 2.56 bar, T_1, T_2, T_f, T_d to 30°C.

Specifications

Heating the fluid makes ethane and propane to vaporise reducing their content in oil. Consequently, oil TVP is reduced (by 0.8 bar).

It is necessary to the fluid until 82°C to respect the TVP specification.

In the same time, their content increases in rich gas. As before, cricondenbar behaviour is explained by i-pentane content in rich gas. It is reduced making the cricondenbar to decrease (by 3 bar).

Cricondenbar is always below 110 bar.

Production

Because of the increasing temperature, the production of gas increases and the one of oil decreases (by 20 kmol/h). At one point, the production of rich gas exceeds the production of oil.

2. Gas recompression train

2.1 First cooler temperature T_1

The case study of the reduction of the cooler temperature (T_1) in the first stage of the gas recompression train is done between 80°C and 10°C. The minimum temperature is dictated by the temperature at which hydrates may form.
Numerical results are obtained for P_2 equal to 9.5 bar, P_3 to 2.56 bar, T_2, T_f, T_d to 30°C and T_h to 80°C.

Specifications

Variations in ethane and propane proportion in oil are so small that the TVP is not influenced by the cooling temperature of the first stage of the recompression train.

It is not possible to find a value of T_1 which makes the TVP below the specification.

As for the oil, rich gas is not significantly influenced by T_1. It is observed on the cricondenbar value. There is a small increase when T_1 is reduced but the variation is not significant (0.07 bar).

Cricondenbar is always below 110 bar.

Production

Reducing the temperature after the cooler of the first stage leads to a small decrease of both oil and gas production (by 1 kmol/h). Theses productions decrease because more aqueous flows are removed from the first inlet separator (S_A) and the second one (S_B).

2.2 Second cooler temperature T_2

The temperature after the second stage cooler (T_2) is changed from 60°C to 5°C. The minimum temperature is dictated by the temperature at which hydrates may form.
Numerical results are obtained for P_2 equal to 9.5 bar, P_3 to 2.56 bar, T_1, T_f, T_d to 30°C and T_h to 80°C.

Specifications

When T_2 is reduced, ethane content increases in oil. Since it is a light component, it increases the oil TVP (by 0.05 bar).

As for T_1, it is not possible to find a value of temperature that brings the TVP below 0.965 bar.

There are two trends for the cricondenbar when T_2 is reduced. It is first increased (between 60°C and 35°C), then it decreases. This behaviour is explained by the i-pentane behaviour, as for the previous parameters. i-pentane flow increases until 35°C, then decreases.

For any value of T_2, the cricondenbar is below 110 bar.

Production

Reducing the cooler temperature decreases the amount of vapour in the stream so decreases the vapour flow rate in the separator S_E. It affects the gas processing part: less liquid is sent from the separator S_F to the second stage of stabilization unit. In the same time, less liquid from the separator S_G is sent to the inlet separator S_A.

Because of the reduction of temperature, more liquid is produced from S_E. This increase does not impact so much the production of oil because of the decrease of liquid flow rates previously

introduced. Indeed, only a small increase in oil production (5 kmol/h) is observed as well as a small decrease in gas production.

3. Gas processing

3.1 Feed gas cooler temperature T_f

The case study on the temperature after the feed gas cooler T_f was made between 60°C and 15°C. The lower value is set to be above the temperature at which hydrates can form.
Numerical results are obtained for P_2 equal to 9.5 bar, P_3 to 2.56 bar, T_1, T_2, T_d to 30°C and T_h to 80°C.

Specifications

Results show that the TVP is reduced by 0.01 bar when the temperature T_f is reduced from 60°C to 50°C. Below this temperature, oil TVP remains the same.

No value of T_f enables to obtain an oil TVP below the specification.

Globally, the cricondenbar of rich gas decreases (by 0.1 bar) with the decreasing temperature. However, what is observed is a maximum value around 30°C. i-pentane behaviour can explain the results of cricondenbar.

The rich gas cricondenbar is always below the specification.

Production

Two trends are observed for the production rates of rich gas and oil. In the first range of temperature, from 60°C to 30°C, oil production rises and rich gas production decreases. Below 30°C, the contrary is observed.

It can be noted that the change of shape of the curves takes place at the temperature at which the cricondenbar is maximal. It is also where the vapour content decreases in the feed of the gas scrubber and liquid production from S_F increases more drastically.

If the flow rate of liquid from S_G is studied (*Figure 13*), it is observable that in the beginning, it is not affected by the temperature reduction. Then, below 30°C, it decreases which has the consequence to increase the production of rich gas. However, the variations are not significant (less than 3 kmol/h).

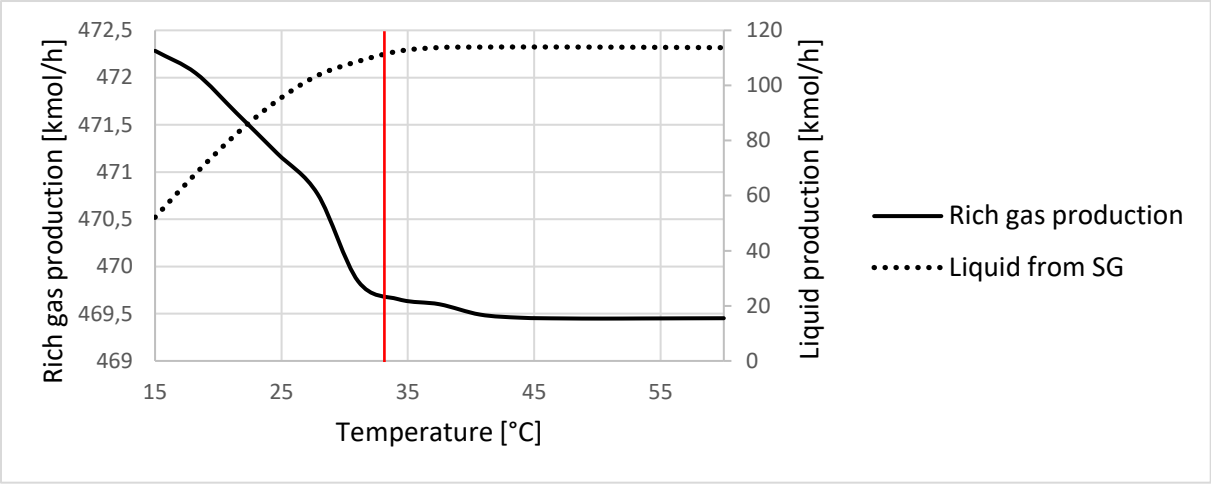

Figure 13: influence of T_f on liquid recycle and on rich gas production

3.2 Temperature before dehydration T_d

The influence of the temperature of the gas before the dehydration part (T_d) is studied between 100°C and 20°C. As before, the lower limit is the temperature of hydrates formation.
Numerical results are obtained for P_2 equal to 9.5 bar, P_3 to 2.56 bar, T_1, T_2, T_f to 30 °C and T_h to 80 °C.

Specifications

Oil TVP remains constant until 30°C, then increases (variation of 0.06 bar). It follows the behaviour of propane: its content in oil is constant and then increases.

There is no value of T_d that brings the oil TVP below the specification.

Concerning the cricondenbar, the contrary is observed: it remains constant until 30°C, then decreases (variation of 3 bar). Propane content decreases making the cricondenbar to decrease also.

Once again, the cricondenbar is always below 110 bar.

Production

Oil production rises (15 kmol/h) whereas rich gas production decreases. It is logical since more liquid is produced when the temperature is reduced.

IV. Base case model and results

Based on the different case studies introduced in the previous section, key parameters controlling the specifications and the production rates are identified.

On one hand, oil TVP is mainly influenced by the process parameters of the condensate stabilization unit: P_2, P_3 and T_h. On the other hand, the cricondenbar is affected by the choice of P_3 and T_h. Concerning the productions, they are also controlled by P_3 and T_h.

The table below gathers the process parameters that are set to meet the specifications on the rich gas and on the crude oil. It is referred as the base case model for in the following chapters.

Process parameters	**Condensate stabilization unit**	
	Second level of pressure P_2	9.50 bar
	Third level of pressure P_3	2.56 bar
	Heater temperature T_h	82°C
	Gas recompression stages	
	First stage cooler temperature T_1	30°C
	Second stage cooler temperature T_2	30 °C
	Gas processing	
	Feed gas cooler temperature T_f	30°C
	Cooler temperature before dehydration T_d	30°C
Results	Rich gas production	470 kmol/h
	Oil production	498 kmol/h
	Rich gas cricondenbar	98.85 bar
	Crude oil TVP at 30°C	0.9604 bar
	Total energy consumption [1]	2 898 kW
	Liquid mole fraction in the feed of S_F	1.5 %
	Liquid mole fraction in the feed of S_G	21 %
	Liquid mole fraction in the feed of S_H	1.0 %

Table 2: base case numerical results

S_F, S_G and S_H are gas scrubbers. It means that they are designed to handle gas with traces of liquid but not a huge amount of liquid. Hence, the liquid amount in the feed of these scrubbers is a parameter that must be checked with the other results of the simulations.

[1] The total energy consumption is the sum of all the energy consumed in the process: pumps, compressors and heater.

Chapter 6 – Oil and gas productions optimisation

At this point, the base case model of the oil and gas offshore plant enables to meet the required specifications: TVP and cricondenbar. In this chapter, these specifications are used to maximise the production of oil and gas separately.

The nomenclature is the same as in the previous chapter. It can be found in *Figure 1*.

I. Rich gas production maximisation

In the base case, the rich gas cricondenbar is below 100 bar meaning that there is a margin that can be used to maximise the production of gas.

1. Utilisation of parametric studies

The previous studies on the influence of different process parameters on production rates are used to optimise the production of gas (*Appendix 2: parametric studies on specifications and production rates*). The following table indicates how the process parameters should be changed if the goal is to increase the production rate of rich gas.

Condensate stabilization unit	
Second level of pressure P_2	↘
Third level of pressure P_3	↘
Heater temperature T_h	↗
Gas recompression stages	
First stage cooler temperature T_1	↗
Second stage cooler temperature T_2	↗
Gas processing	
Feed gas cooler temperature T_f	↘
Cooler temperature before dehydration T_d	↗

Table 3: evolution of process parameters to increase rich gas production

Since the effect of the cooler temperatures in the gas recompression train is not significant, T_1 and T_2 are not considered for the optimisation.

2. Optimisation

For the gas production optimisation, the optimizer tool in UniSim is used. The goal of this section is to introduce the utilization of this tool. Information are taken from the operation guide of the software (Honeywell, 2005).

There are five available modes in the optimizer. The original, the one by default, is chosen in this work.

The first step is the enter the variables of the problem with their lower and upper bonds. It should be noticed that this optimizer is a multivariable steady state optimizer meaning that it can optimise several variables in the same time.

The second step is to specify the objective function to optimise (minimize or maximise). In this case, this is the rich gas production which needs to be maximized.

Finally, constraints can be defined. In this work, the constraints are the two specifications, cricondenbar and TVP. The values must be below the 110 bar for the rich gas cricondenbar and 0.965 bar for the TVP of oil. It should be noted that the initial variables must be chosen in such a way that these constraints are met.

Different methods are used by this tool but only three over the five can handle inequality constraints which is the case of this work: the BOX method, the Sequential Quadratic Programming (SQP) method and the Fletcher Reeves Method. Details about the procedure of these methods can be found in the UniSim operation guide.

3. Results

Optimisation was done manually (using *Table 3*) in combination with the utilization of the optimizer tool. Only the final model which increases the rich gas production by 4 % is presented in the following table.

		Base case	Optimisation
Process parameters	**Condensate stabilisation unit**		
	Second level of pressure P_2	9.50 bar	5.33 bar
	Third level of pressure P_3	2.56 bar	1.50 bar
	Heater temperature T_h	82 °C	93 °C
	Gas recompression stages		
	First stage cooler temperature T_1	30 °C	30 °C
	Second stage cooler temperature T_2	30 °C	30 °C
	Gas processing		
	Feed gas cooler temperature T_f	30 °C	17 °C
	Cooler temperature before dehydration T_d	30 °C	50 °C
Results	**Rich gas production**	**470 kmol/h**	**514 kmol/h**
	Rich gas cricondenbar	98.85 bar	102.7 bar
	Crude oil TVP at 30°C	0.9604 bar	0.3823 bar
	Total energy consumption	2 898 kW	4 216 kW

Table 4: gas production optimisation results

By decreasing the two levels of pressure of the condensate stabilization unit and by increasing the heater temperature, more vapour is sent to the gas recompression stage (increase of 80 kmol/h [2]). Concerning the gas processing part, the temperature after the feed gas cooler (T_f) is reduced and the

[2] It corresponds to the sum of the molar flow from S_B and S_C.

temperature before the dehydration unit (T_d) is increased. These modifications on process parameters lead to a rise in gas production of 44 kmol/h (increase by 9 %).

3.1 Products analysis

Rich gas

The modification of the process parameters increases the production of each components in the rich gas (see *Appendix 3: rich gas production maximisation*).

Methane production is not influenced by this optimisation. Indeed, in the base case, the amount of methane in the end of the process (in the rich gas) represents more than 99 % of the initial amount (in the reservoir). Propane is the component which is the most responsible for the rise in rich gas production: its increase in production rate represents 46 % of the rich gas production rise. It is followed by n-Butane (24 %), i-Butane (13 %) and ethane (8.6 %).

The increase of the proportion of these components in the rich gas explains why the cricondenbar is higher than in the base case. The following figure represents the comparison between the phase envelopes.

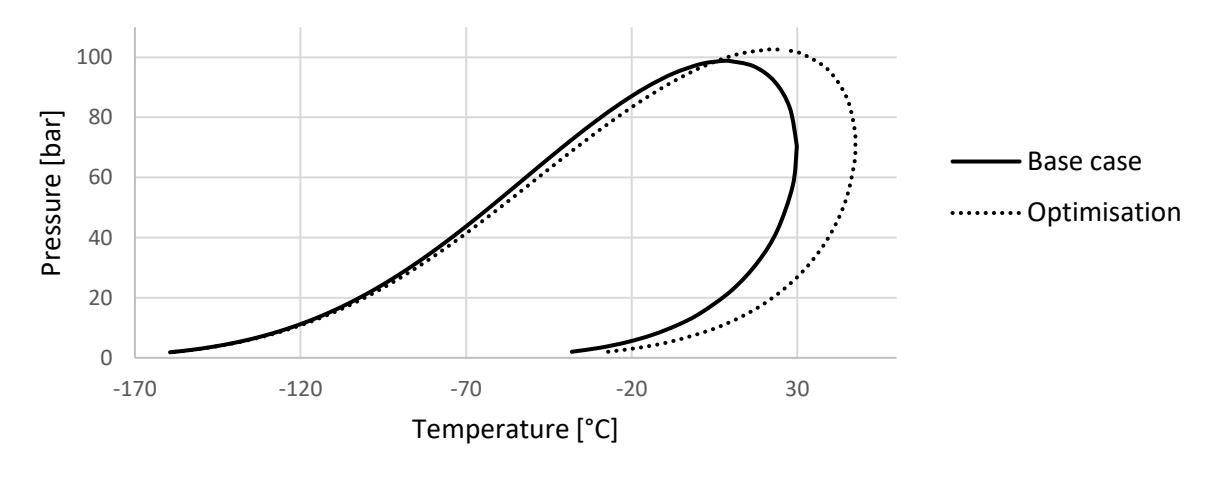

Figure 14: rich gas phase envelope for the gas production optimisation

Crude oil

In the same time, oil production decreases because of the decrease of ethane, propane and other components. As a result, the crude oil TVP is considerably reduced (by 60 %).

3.2 Energy consumption

Producing more gas leads to a rise in the total energy consumption (increase by 45 % compared to the base case). Each unit that requires energy is studied. Pumps are not affected by the changes of process parameters (responsible for less than 1 % of the increase of the total energy consumption). Compressors account for 9 % whereas the heater is responsible for more than 90 % of the rise in the total energy demand of the offshore plant.

The energy consumption in each unit is detailed in the following table.

Type	Unit	Energy consumption [kW]		Variation [kW]	
		Base case	Optimisation		
pumps	p-1	55.65	59.28	↗	3.631
	p-2	0.003	0.008	↗	0.005
	sum	55.66	59.29	↗	3.630
compressors	C_1	101.7	51.61	↘	50.05
	C_2	101.7	320.1	↗	218.4
	C_3	695.5	569.2	↘	126.3
	C_4	501.0	577.5	↗	76.46
	sum	1 400	1 518	↗	118.0
heater	heater	1 442	2 639	↗	1 196
total		2 898	4 216	↗	1 318

Table 5: effect of gas production increase on energy consumption

Heater energy consumption

The energy consumption of the heater is explained by two parameters: the flow going through the heat exchanger and the temperature difference between the inlet temperature and the outlet temperature. Optimisation increases the flow as well as the temperature difference.

The increase of flow in the heater is explained by several effects of the modified process parameters on the plant.
The new choice of T_d is so high that the fluid after the cooler HX_4 does not contain any liquid. As a result, there is no recirculation from the separator S_G (reduction by 131 kmol/h compared to the base case). Hence less flow enters the inlet separator (S_A) producing less vapour and liquid (variation by 58 kmol/h for the liquid).
In the same time, the temperature reduction of the feed gas cooler (T_f) produces more liquid which is recycled and sent back to stabilization unit (variation by 79 kmol/h).
The combination of these two streams, the inlet one and the recirculation from S_F, leads to a total increase by21 kmol/h inside the heat exchanger increasing its energy consumption.

Increasing the temperature after the heater increases the temperature difference (by 12°C) between the inlet and the outlet of the heat exchanger. Consequently, more energy is required to heat the condensate.

Compressors energy consumption

The reduction of P_2 and P_3 increases the pressure ratio in the second gas recompression stage. In the same time, there is more vaporisation due to the reduction of P_2 and the rise of heater temperature T_h. As a result, the flow going through the compressor C_2 increases (by 64 kmol/h). These two elements, pressure ratio and flow, explain why C_2 energy consumption increases.

Because of this vaporisation less liquid is sent to the last stage of the condensate stabilization unit. As a result, the flow entering the first compressor C_1 in the gas recompression stage decreases (by 31

kmol/h). Moreover, the pressure ratio is reduced. These two elements explain why the energy consumption of C_1 decreases with the new process parameters.

Concerning the gas processing part, T_f is reduced to 17°C increasing the recirculation from S_F and reducing the flow in the compressor C_3 (by 88 kmol/h) which has the consequence to reduce the energy consumption of C_3. T_d increases up to 50°C reducing the recirculation from S_G and so increases the flow of rich gas in C_4 (by 44 kmol/h) increasing its energy consumption.

Energy distribution

In the base case, energy consumption is distributed quite equally between the compressors work (mechanical energy) and the heater duty (thermal energy). However, the distribution is different in the gas production optimisation model as the following figure shows [3]. The new model requires more thermal energy.

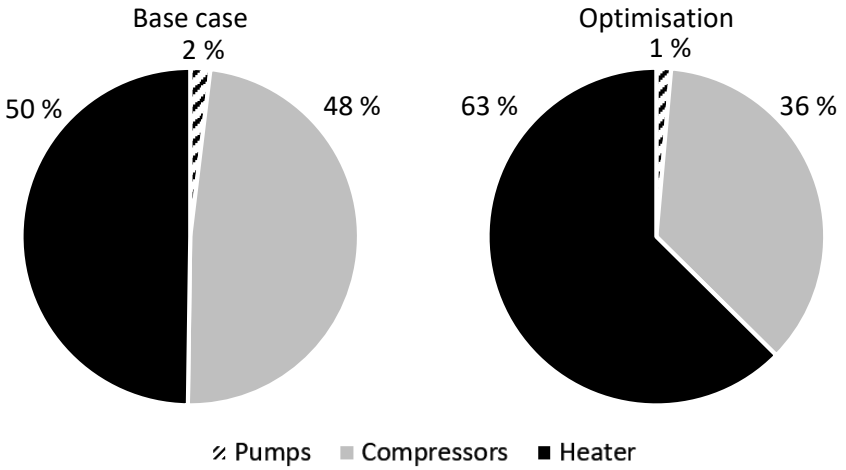

Figure 15: energy consumption distribution

3.3 Gas scrubbers

The choice of process parameters influences the proportion of gas and liquid entering the gas scrubbers as the following table shows.

	Base case	Optimisation
Feed gas scrubber S_F	1.50 %	14.6 %
Scrubber before dehydration S_G	21.1 %	0.00 %
Safety scrubber S_H	0.99 %	0.00 %

Table 6: liquid amount in feed to gas scrubber (mole basis) for gas production optimisation

[3] Note that the circle diameter does not represent the amount of energy consumption. For example, the compressors energy consumption increases between the base case model and the optimisation. However, its part in the total energy consumption decreases, this is this point which is illustrated.

On one hand, the inlet temperature T_f of the feed gas scrubber is reduced from 30°C to 17°C producing more liquid recirculation. On the other hand, the temperature before the dehydration unit was increased to 50°C. At this temperature, no liquid hydrocarbons can be found. As a result, no liquid enters the following scrubbers S_G and S_H, there is no recirculation from these two scrubbers.

II. Crude oil production maximisation

As for the gas production optimisation, the influence of process parameters on the oil production are identified thanks to the previous parametric studies (*Appendix 2: parametric studies on specifications and production rates).* The following table indicates how the process parameters should be changed if the goal is to increase the production rate of oil.

Condensate stabilization unit	
Second level of pressure P_2	↗
Third level of pressure P_3	↗
Heater temperature T_h	↘
Gas recompression stages	
First stage cooler temperature T_1	↗
Second stage cooler temperature T_2	↘
Gas processing	
Feed gas cooler temperature T_f	↗
Cooler temperature before dehydration T_d	↘

Table 7: evolution of process parameters to increase oil production

The maximisation of oil production is challenging since when the production is increased the TVP increases as it was seen in the previous parametric studies.

Since the TVP of crude oil in the base case is already high (0.9604 bar for a maximum value of 0.9650 bar), no optimisation of the oil production is possible. It would have been possible if the margin would have been larger.

Chapter 7 - Energy consumption minimisation

In the previous chapter, oil and gas specifications were used to maximise the production rates of the offshore plant. Another type of optimization is possible: minimize the total energy consumption of the plant. It includes pumps, compressors and heater energy consumption.

This chapter is built in such a way that it reflects the different steps achieved to obtain the final model.

I. Parametric studies

First of all, parametric studies are conducted to evaluate the influence of key process parameters on the energy consumption. It is used to determine the new values of these parameters.

Figure 1 indicates the nomenclature which is used. Results are summed up in appendix (*Appendix 4: energy consumption – parametric studies*).

In this section each unit is studied and results are explained. Pumps energy consumption is not significantly influenced by the change of the process parameters. So, this point is not discussed.

Compressors energy consumption rises if the pressure ratio and/or the flow increases. Concerning the heater, the energy demand is higher if the flow rises and/or if the temperature difference between the inlet and the outlet of the heat exchanger is increased.

1. Condensate stabilization unit

1.1 Second level of pressure P_2

The pressure in the second stage of the condensate stabilization unit (P_2) is reduced from 14 bar to 4.5 bar. Numerical results are obtained for P_3 equal to 2.56 bar, T_1, T_2, T_f, T_d to 30°C and T_h to 82°C.

The reduction of pressure leads to an increase in the total energy consumption of 1 748 kW (60 % [4]).

Compressors

Compressors are responsible for 21 % of the total increase of energy consumption.

The pressure reduction decreases the pressure ratio so the power of the first compressor in the gas recompression train (C_1). Concerning the second compressor (C_2), the pressure ratio rises as well as the energy consumption. It can be noticed that the energy consumption of the two compressors is the same for a pressure of 9.5 bar which is the value of P_2 in the base case.

[4] The percentage is related to the base case model (its energy consumption is 2 898 kW).

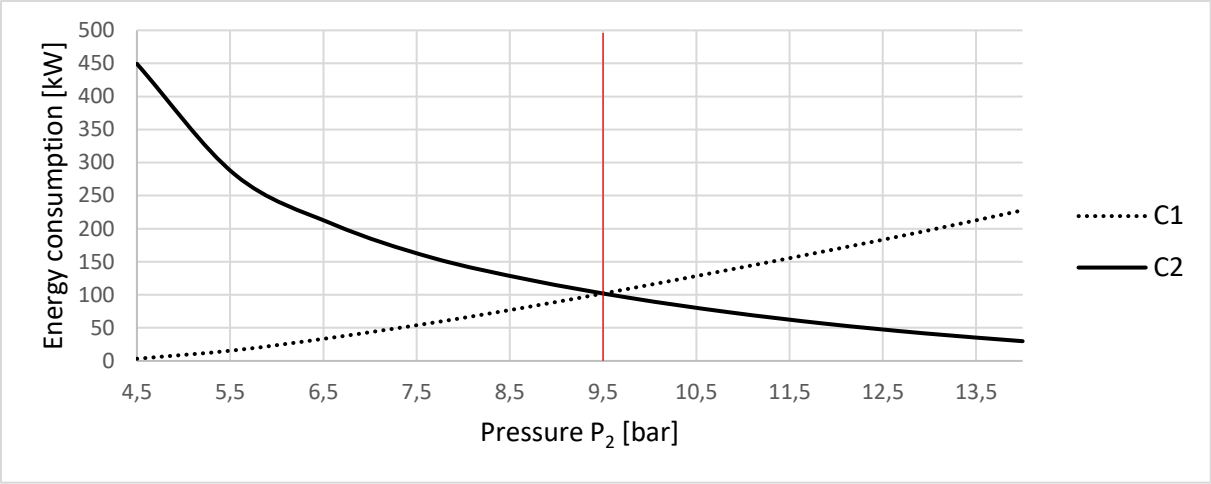

Figure 16: influence of P_2 on compressors energy consumption

Pressure ratios are not changed in the gas processing part (C_3 and C_4). Hence, energy consumption in this part is explained by the influence of the pressure reduction on the flow rates.
The reduction of P_2 produces more vapour. As a result, more flow (176 kmol/h) is going through C_3 which increases its power consumption. The gas is then cooled in HX_4 producing more liquid from the separator S_G. Since more liquid is recycled, the vapour flow entering the last compressor C_4 is not significantly increased (6 kmol/h). It explains the fact that the energy consumption of this compressor is not readily influenced by the reduction of P_2.

Heater

The rise in the total energy consumption is mainly due to the heater energy consumption (79 %).

The pressure reduction increases the heater power consumption. It is explained by the fact that the flow entering the heat exchanger rises (by 127 kmol/h). It is the result of the increase of liquid recirculation from S_F and S_G in the gas processing part.

Moreover, the inlet temperature decreases (by 11°C). It is logical since the recirculation are at a lower temperature than the fluid from the reservoir. Mixing a larger amount of cold streams reduces the temperature of the mixture entering the heater. Hence, the temperature difference before and after the heat exchanger is bigger. More energy is required to heat the fluid until 82°C.

1.2 Third level of pressure P_3

The pressure in the third stage of the condensate stabilization unit (P_3) is reduced from 7 bar to 1 bar. Numerical results are obtained for P_2 equal to 9.5 bar, T_1, T_2, T_f, T_d to 30°C and T_h to 82°C.

The total energy consumption increases by 2 591 kW (89 %) with this pressure reduction.

Compressors

In the case of P_3 reduction, the impact of compressors is bigger than for P_2 reduction. Indeed, they are responsible for 52 % of the total energy consumption rise.

The first stage of gas recompression is the most affected by the reduction of P_3. Indeed, the pressure ratio increases in C_1 as well as the flow (294 kmol/h) due to vaporisation.
The vaporisation also increases the flow rate in C_2 (240 kmol/h), C_3 (458 kmol/h) and in the last compressor C_4 but in a lower level (55 kmol/h).

The effect of P_3 reduction is less important for C_2, C_3 and C_4 than for C_1 because the pressure ratio is unchanged in these compressors.

Heater

Heater has a lower impact on the total energy consumption when P_3 is reduced (responsible for 46 % of the energy variation).

The flow going to the heater increases (by 179 kmol/h). It is explained by the fact that even if more vaporisation occurs, recirculation loops enable to send back more liquid into the condensate stabilization unit which increases the flow rate. The inlet temperature of this heater is reduced by the pressure reduction (by 10°C) increasing the energy required to heat the fluid.

1.3 Heater temperature T_h

The influence of the increase of T_h in the condensate stabilization unit is studied between 70°C and 150°C. Numerical results are obtained for P_2 equal to 9.5 bar, P_3 to 2.56 bar, T_1, T_2, T_f and T_d to 30°C.

This increase of heater temperature rises the energy consumption of the process by 9 458 kW (326 %).

Compressors

In this case, pressure ratios are unchanged. It explains why the rise in compressors power consumption is only responsible for 8 % of the total rise in energy consumption.

Increasing T_h produces more vapour from S_B. Hence, more flow (194 kmol/h) is going through the second stage of gas recompression (C_2). In the same time, liquid from S_E is sent back to the last stabilization stage increasing the flow in C_1 (234 kmol/h).

The increase of vapour production in the condensate stabilization unit rises the total vapour going to the gas processing part. More flow enters in C_3 (412 kmol/h). The last compressor C_4 is less influenced by the change of T_h since liquid is removed in S_G. Indeed, the flow increases only by 27 kmol/h in C_4.

Heater

Since T_h is increased, it is logical that the heater is responsible for 91 % of the total rise in energy demand of the plant.

The rise in energy consumption in the heater is explained by the rise of the flow going through it (169 kmol/h). It is the result of the recirculation: increase by 380 kmol/h for the recirculation from S_G and by 13 kmol/h from S_F.

It is also explained by the temperature levels. The feed gas is cooled down in HX_3 producing cold liquid which reduces the temperature of the mixture entering the heater (by 10°C). Moreover, the temperature at the outlet of the heater rises increasing the temperature difference between the inlet and the outlet of the heat exchanger.

2. Gas recompression train

2.1 First cooler temperature T_1

The temperature after the first stage cooler (T_1) is reduced from 70°C to 10°C. Numerical results are obtained for P_2 equal to 9.5 bar, P_3 to 2.56 bar, T_2, T_f, T_d to 30°C and T_h to 82°C.

The reduction of T_1 reduces the total energy consumption of the plant by 48 kW (1.7 %).

Compressors

The choice of T_1 influences mainly the compressors work. Indeed, their energy demand decreases is responsible for nearly 100 % of the total energy consumption decrease.

The temperature reduction in the first stage of gas recompression train produces more liquid, so less vapour enters the first compressor C_1 (20 kmol/h). This reduction of flow reverberates on the liquid flow from S_E in the second stage. It explains why the flows remains the same in the next part of the process. Consequently, C_2, C_3 and C_4 energy consumption are not affected by T_1.

Heater

T_1 reduction has no effect on the heater energy consumption. Indeed, the flow entering the heat exchanger and its inlet temperature are not significantly modified.

2.2 Second cooler temperature T_2

The temperature after the second stage cooler (T_2) is reduced from 60°C to 5°C. Numerical results are obtained for P_2 equal to 9.5 bar, P_3 to 2.56 bar, T_1, T_f, T_d to 30°C and T_h to 82°C.

The total energy consumption of the offshore plant decreases by 491 kW (17 %).

Compressors

Contrary to the effect of T_1 reduction, compressors energy consumption reduction is only responsible for 31 % of the total energy demand reduction.

The pressure ratios are not influenced by the reduction of temperature. Hence each compressor energy consumption is explained by the influence of the reduction of T_2 on the flow rates.

The reduction of T_2 produces more liquid from S_E which is sent to the third stage of the condensate stabilization unit. Hence more vapour (12 kmol/h) enters in C_1.
In the same time, less vapour is sent to the second compressors C_2 (65 kmol/h) and so to the gas processing part. Consequently, the energy consumption of C_3 is also reduced by the reduction of flow (by 109 kmol/h).

Concerning the last compression before transport (C_4), the energy consumption is not significantly changed by the reduction of T_2. Indeed, the flow rate is unchanged because of the recirculation loops.

Heater

Heater duty reduction is responsible for 68 % of the total energy consumption decrease.

Reducing the temperature T_2 leads to a reduction of the vapour flow sent to the gas processing part. Consequently, less liquid is recycled from S_F which reduces the flow entering the heater (by 61 kmol/h). Moreover, the inlet temperature increases (by 3°C) which reduces the temperature difference in the heat exchanger. These two elements, flow and temperature, explain the reduction of the heater energy consumption.

3. Gas processing

3.1 Feed gas cooler temperature T_f

The study of the reduction of temperature after the feed gas cooler is done by varying T_f between 60°C and 15°C. Numerical results are obtained for P_2 equal to 9.5 bar, P_3 to 2.56 bar, T_1, T_2, T_d to 30°C and T_h to 82°C.

The reduction of temperature decreases the total energy consumption by 266 kW (9 %).

Compressors

Compressors are responsible for 84 % of the decrease in energy demand.

If the temperature of the feed gas is reduced, more liquid is produced so less vapour is sent to the further compressor C_3 (77 kmol/h).

The next compressor does not follow the same tendency. In fact, vapour production increases in S_G which conducts to more flow in C_4 (2.6 kmol/h). Hence, its energy consumption increases a little bit.

Less liquid is recycled from S_G which reduces the flow in the condensate stabilization unit and in the gas recompression stages. The flow in C_1 decreases by 8.8 kmol/h and by 8.5 kmol/h in C_2 reducing their energy consumption.

Heater

The energy consumption of the heater decreases with T_f reduction and is responsible for 16 % of the total energy consumption decrease.

As it was previously introduced, the flow rate in the condensate stabilization unit is reduced. Less amount of fluid needs to be heated (decrease of 3.7 kmol/h).

3.2 Temperature before dehydration T_d

The reduction of the temperature of the fluid before the dehydration part (T_d) is studied from 100°C to 20°C. Numerical results are obtained for P_2 equal to 9.5 bar, P_3 to 2.56 bar, T_1, T_2, T_f to 30°C and T_h to 82°C.

Reducing T_d leads to an increase of the total energy consumption by 1 275 kW (44 %).

Compressors

Compressors are not significantly influenced by the change of T_d. Their increase in energy consumption represents 16 % of the total energy demand rise of the plant.

T_d reduction increases the flow of the recirculation from S_G (by 354 kmol/h). Hence, there is a larger quantity of fluid to be compressed in the gas recompression train (52 kmol/h for C_1 and 107 kmol/h for C_2).

The increase of flow reverberates on the input of the first compressor in the gas processing part (C_3). The flow is increases by 317 kmol/h.

Concerning the last stage, it was introduced that more liquid is produced from S_G. As a result, less vapour (43 kmol/h) enters the compressor C_4 reducing its energy consumption.

Heater

The energy required to heat the condensate in the stabilization unit is increased by the reduction of T_d. It accounts for 84 % of the total increase of energy consumption.

The recirculation from S_G increases which makes the flow in the heater to increase (by 138 kmol/h). Moreover, the liquid which is recycled is colder than the fluid from the reservoir. Hence, when the two are mixed together, the inlet temperature of the heater decreases (by 10°C). As a result, it requires more energy to heat the stream up to 82°C.

4. Conclusion

The following table gathers the information previously introduced. The range of values in which the studies were performed and their effect on the total energy consumption are presented.

Process parameters			**Energy consumption variation [kW]**		
Study	Range	Variation			
↘ P_2	From 14 bar to 4.5 bar	ΔP_2 = 9.5 bar	↗	1 748	(60 %)
↘ P_3	From 7 bar to 1 bar	ΔP_3 = 7 bar	↗	2 591	(89 %)
↗ T_h	From 70°C to 150 °C	ΔT_h = 80°C	↗	9 458	(326 %)
↘ T_1	From 70°C to 10°C	ΔT_1 = 60°C	↘	48	(1.7 %)
↘ T_2	From 60°C to 5°C	ΔT_2 = 55°C	↘	491	(17 %)
↘ T_f	From 60°C to 15°C	ΔT_f = 45°C	↘	266	(9 %)
↘ T_d	From 100°C to 20°C	ΔT_d = 80°C	↗	1 275	(44 %)

Table 8: influence of process parameters on energy consumption

As mentioned at the beginning of this chapter, pumps are not influenced by the variation of the process parameters that are studied. Depending on the parameter of interest, the total energy consumption evolution is driven mainly by the compressors work (mechanical energy) or by the heater duty (thermal energy). The following figure is a graphical representation of the results. It can be commented using *Table 8* as follow. It the pressure P_2 is reduced from 14 bar to 4.5 bar, compressors are responsible for 21 % of the total increase of energy consumption.

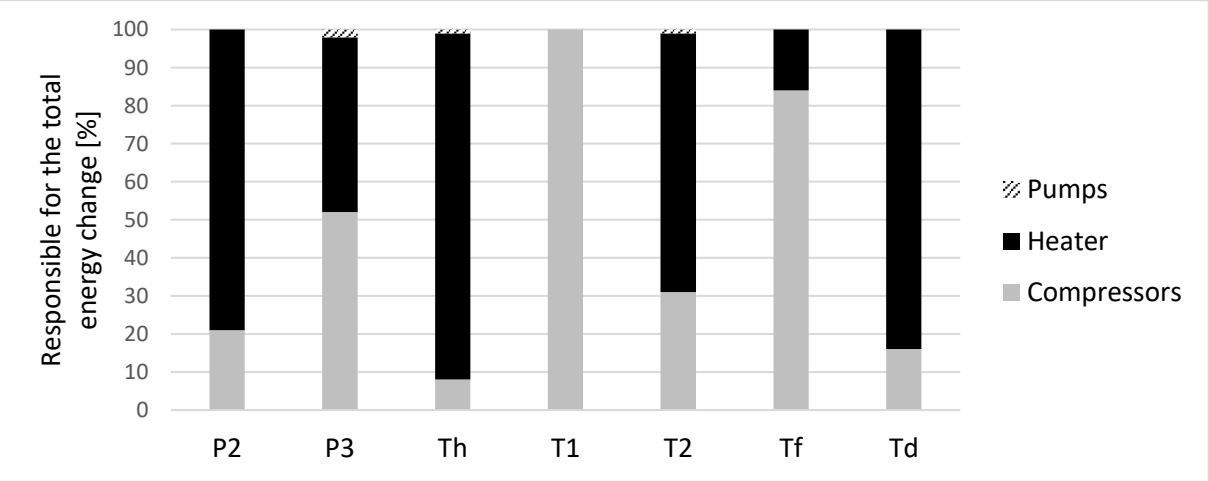

Figure 17: units responsible for the energy change

II. Optimized process parameters

1. Utilisation of parametric studies

The previous parametric studies enable to see how the process parameters should be changed to optimise the total energy consumption of the oil and gas offshore plant. Using these results (*Table 8* and *Appendix 4: energy consumption – parametric studies),* the range of possible values for these parameters can be identified.

Table 8 indicates that the pressures of the condensate stabilization unit should be increased (P_2 and P_3) whereas the temperature after the heater should be reduced (T_h). However, if pressures are too high and/or if the temperature is too low, crude oil TVP can be off-spec.

Concerning the gas recompression train, T_1 and T_2 should be reduced to minimize the total energy consumption. Results show that there is no problem of specification for T_1. Hence, the minimum value is the temperature at which hydrates may form. However, it is different for T_2. If T_2 is too low, TVP will be off-spec.

The temperature after the feed gas cooler (T_f) must also be reduced. The minimum temperature is dictated by the hydrate formation temperature.

Finally, minimizing the total energy demand of the plant requires to increase the temperature before the dehydration unit (T_d). However, this value should not be too high to meet the TVP specification.

The following table is a recap of the lower and upper bounds for each process parameter. “TVP” means that the value of the parameter is chosen to meet the correct TVP. “hydrates” means that the minimum temperature is the temperature at which hydrates may form and “energy” means that the bound is defined to minimize the energy consumption.

Process parameter	Lower bond	Upper bound
P_2	energy	TVP
P_3	energy	TVP
T_h	TVP	energy
T_1	TVP [5]	energy
T_2	TVP	energy
T_f	hydrates	TVP
T_d	TVP	TVP

Table 9: lower and upper bounds for process parameters optimisation

[5] The previous parametric studies on T_1 was made from 70°C to 10°C. The hydrate temperature formation is always below 0°C. So, the parametric study was done another time from 10°C to 0°C. It reveals that the lower bound is not the hydrate temperature but is dictated by the crude oil TVP.

Numerical results of the bounds are presented in *Table 10*. The other parameters are also indicated. Indeed, if the other parameters are changed, it leads to a modification of the bounds of the process parameter of interest.

Process parameter	If the other parameters are
4.5 bar < P_2 < 9.59 bar	P_3 = 2.56 bar; $T_1 = T_2 = T_f = T_d$ = 30°C; T_h = 82°C
1 bar < P_3 < 2.56 bar	P_2 = 9.5 bar; $T_1 = T_2 = T_f = T_d$ = 30°C; T_h = 82°C
81.9°C < T_h < 150°C	P_2 = 9.5 bar; P_3 = 2.56 bar; $T_1 = T_2 = T_f = T_d$ = 30°C
3.3°C < T_1 < 70°C	P_2 = 9.5 bar; P_3 = 2.56 bar; $T_2 = T_f = T_d$ = 30°C; T_h = 82°C
26.9°C < T_2 < 60°C	P_2 = 9.5 bar; P_3 = 2.56 bar; $T_1 = T_f = T_d$ = 30°C; T_h = 82°C
11°C < T_f < 45.3°C	P_2 = 9.5 bar; P_3 = 2.56 bar; $T_1 = T_2 = T_d$ = 30°C; T_h = 82°C
26°C < T_d < 36°C	P_2 = 9.5 bar; P_3 = 2.56 bar; $T_1 = T_2 = T_f$ = 30°C; T_h = 82°C

Table 10: range of process parameters to meet the specifications

The main conclusion is that optimisation should be done by finding a compromise between minimizing the energy consumption of the plant and meeting the specifications.

2. Optimisation

The energy consumption optimisation is made using the previous case studies and using the optimizer tool in UniSim software introduced in the previous chapter.

Intermediate results are presented to explain the progress of the optimisation.

The following table restates how the process parameters should evolve in order to reduce the total energy consumption of the plant.

Condensate stabilization unit	
Second level of pressure P_2	↗
Third level of pressure P_3	↗
Heater temperature T_h	↘
Gas recompression stages	
First stage cooler temperature T_1	↘
Second stage cooler temperature T_2	↘
Gas processing	
Feed gas cooler temperature T_f	↘
Cooler temperature before dehydration T_d	↗

Table 11: evolution of process parameters to reduce the total energy consumption

First, it is noticed from the parametric studies that all the process parameters have not the same impact on the energy consumption of the plant. Consequently, only the most relevant are used for the first optimisation: P_2, P_3, T_h and T_d. T_1, T_2 and T_f are kept equal to 30°C as for the base case model. This optimisation is done by the optimizer tool.

The results of this optimisation are presented in *Table 12*: part (b). As expected, the heater temperature (T_h) decreases and the temperature before dehydration (T_d) increases.
However, the two levels of pressure of the condensate stabilization unit are reduced instead of being increased. It is due to the TVP specification. As introduced before, TVP dictates the upper bound of P_2 and P_3. Since, other parameters are changed (P_2, P_3, T_h and T_d), the upper bounds differ from the values of *Table 10*. For example, if T_h is equal to 70°C, T_d to 50°C and P_2 to 9.5 bar, the maximum value of P_3 is 1.98 bar. If T_h is equal to 70°C, T_d to 50°C and P_3 to 1.95 bar, the maximum value of P_2 is 10.3 bar.

	P_2 [bar]	**P_3 [bar]**	**T_h [°C]**	**T_d [°C]**	**Cricondenbar [bar]**	**Oil TVP [bar]**	**Energy consumption [kW]**	**Energy saving [6]**
(a) [7]	9.5	2.56	82	30	98.85	0.9604	2 898	-
(b)	9.41	1.95	70	50	106.1	0.9453	1 523	47.4 %

Table 12: first step for energy optimisation

The results of this first optimisation indicates that there is still a margin for the TVP meaning that it can be increased to minimize the total energy consumption of the plant. At this point different possibilities exist. They are introduced in the next sub-sections.

2.1 Possibility A: optimisation with only P_2, P_3, T_h and T_d

One possibility is to change one parameter between P_2, P_3, T_h and T_d. The influence of these changes on TVP specification and on energy consumption are graphically represented in appendix (*Appendix 5: energy consumption minimisation).* The results from these studies are that P_2 can be increased up to 10.3 bar, P_3 to 1.98 bar, T_h can be reduced until 69.1°C. These three parameters are dictated by TVP value. Concerning T_d, 50°C is already the optimal value. It corresponds to the minimum of the total energy consumption of the plant. TVP is not a constraint in this case.
Results are introduced in the following table. Part (a) is the results of the base case model and part (b) of the first optimisation. Part (c), (d) and (e) correspond to the new optimisations. In bold are the process parameters that have been changed compared to the first optimisation.

	P_2 [bar]	**P_3 [bar]**	**T_h [°C]**	**T_d [°C]**	**Cricondenbar [bar]**	**Oil TVP [bar]**	**Energy consumption [kW]**	**Energy saving**
(a)	9.5	2.56	82	30	98.85	0.9604	2 898	-
(b)	9.41	1.95	70	50	106.1	0.9453	1 523	47.4 %
(c)	**10.3**	1.95	70	50	105.9	0.9622	1 507	48.0 %
(d)	9.41	**1.98**	70	50	106.1	0.9596	1 518	47.6 %
(e)	9.41	1.95	**69.1**	50	106.1	0.9628	1 450	50.0 %

Table 13: second step of energy optimisation (possibility A)

[6] It refers to the amount of energy which is saved compared to the base case energy demand. It corresponds to the sum of the pumps, heater and compressors energy consumption.
[7] Part (a) corresponds to the base case model.

Among P_2, P_3, T_h and T_d, results show that this is T_h which is the most relevant for energy consumption optimisation. It confirms what was found in the previous parametric studies (*Table 8*).

The upper bonds for P_2 and P_3 are re-evaluated with the new value of T_h (69.1°C). The maximum value for P_2 is now 9.43 bar. There is no difference for P_3. Setting P_2 equal to 9.43 bar instead of 9.41 bar does not lead to a significant change. Results are presented in the following table, part (f).

	P_2 [bar]	P_3 [bar]	T_h [°C]	T_d [°C]	Cricondenbar [bar]	Oil TVP [bar]	Energy consumption [kW]	Energy saving
(a)	9.5	2.56	82	30	98.85	0.9604	2 898	-
(b)	9.41	1.95	70	50	106.1	0.9453	1 523	47.4 %
(c)	10.3	1.95	70	50	105.9	0.9622	1 507	48.0 %
(d)	9.41	1.98	70	50	106.1	0.9596	1 518	47.6 %
(e)	9.41	1.95	69.1	50	106.1	0.9628	1 450	50.0 %
(f)	9.43	1.95	69.1	50	106.1	0.9632	1 449	50.0 %

Table 14: third step for energy optimisation (possibility A)

2.2 Possibility B: introduce T_1, T_2 and T_f

The second possibility to optimise the first optimisation is to focus on the parameters that were not considered at the beginning. It means that P_2 is set equal to 9.41 bar, P_3 to 1.95 bar, T_h to 70°C and T_d to 50°C. Only T_1, T_2 and T_f are considered for the rest of the optimisation. Results from the optimizer tool are introduced in the following table: part (g).

As indicated before (*Table 11*), these temperatures should be reduced to minimize the total energy consumption of the process. This is what is observed.

	T_1 [°C]	T_2 [°C]	T_f [°C]	Cricondenbar [bar]	Oil TVP [bar]	Energy consumption [kW]	Energy saving
(b)	30	30	30	106.1	0.9453	1 523	47.4 %
(g)	26	25	13	102.4	0.9461	1 510	47.9 %

Table 15: second step for energy optimisation (possibility B)

As for the possibility A, it remains a margin for the crude oil TVP. Hence, the same procedure is achieved as before: one temperature between the three is reduced keeping the others constant. It corresponds to part (h), (i) and (j) in *Table 16*.

The choice of the temperature T_2 is based on TVP analysis, below this temperature, TVP is off-spec. T_f is set to be above hydrate formation temperature. The choice of these lower bounds were already presented in *Table 9*.

However, it is different for T_1. The lower bond is not dictated by the TVP of crude oil but by the hydrate formation temperature and the freezing temperature. Since the process parameters are different from the base case, TVP is no longer a problem for the choice of T_1.

	T_1 [°C]	T_2 [°C]	T_f [°C]	Cricondenbar [bar]	Oil TVP [bar]	Energy consumption [kW]	Energy saving
(b)	30	30	30	106.1	0.9453	1 523	47.4 %
(g)	26	25	13	102.4	0.9461	1 510	47.9 %
(h)	**5**	25	13	102.5	0.9466	1 499	48.3 %
(i)	26	**8.3**	13	101.6	0.9631	1 489	48.6 %
(j)	26	25	**11**	101.8	0.9461	1 519	47.6 %

Table 16: third step for energy optimisation (possibility B)

The change of the cooler temperature in the second stage of gas recompression (T_2) is the most relevant parameter for the energy optimisation between T_1, T_2 and T_f. It confirms the results from the parametric studies (*Table 8*).

2.3 Optimized model

The optimized model is chosen to be the one with the minimum total energy consumption. Process parameters and results are presented in the following table. With these parameters the total energy consumption (pumps, heater and compressors) is reduced by 50 % compared to the base case.

			Base case	Optimisation
Process parameters	Condensate stabilization unit	**P_2**	9.50 bar	9.43 bar
		P_3	2.56 bar	1.95 bar
		T_h	82°C	69.1°C
	Gas recompression stages	**T_1**	30°C	30°C
		T_2	30°C	30°C
	Gas processing	**T_f**	30°C	30°C
		T_d	30°C	50°C
Specifications	Cricondenbar		98.85 bar	106.1 bar
	TVP @30°C		0.9604 bar	0.9632 bar
Energy consumption			2 898 kW	1 449 kW
Production	Rich gas		470 kmol/h	489 kmol/h
	Oil		498 kmol/h	475 kmol//h

Table 17: energy optimisation results

3. Results analysis

The aim of the section is to compare in more detail the optimized model and the base case. *Figure 1* and its nomenclature is used to explain the results.

3.1 Energy consumption

The following table gather the distribution of the energy consumption of the plant between the different units.

Type	Unit	Energy consumption [kW]		Variation [kW]	
		Base case	Optimisation		
pumps	p-1	55.65	57.39	↗	1.740
	p-2	0.003	0.002	↘	0.001
	sum	55.66	57.39	↗	1.730
compressors	C_1	101.7	114.1	↗	12.40
	C_2	101.7	77.92	↘	23.78
	C_3	695.5	582.8	↘	112.7
	C_4	501.0	567.9	↗	66.90
	sum	1 400	1 343	↘	57.00
heater	heater	1 442	48.91	↘	1 393
total		2 898	1 449	↘	1 449

Table 18: comparison between the base case and the optimized model

Heater energy consumption

Results show that the heater energy consumption reduction is responsible for 96 % of the total energy consumption reduction.

Since the temperature before the dehydration unit T_d is increased from 30°C in the base case to 50°C in the optimized model, less liquid is recycled from S_G (reduction by 129 kmol/h). It explains why the flow is reduced by 58 kmol/h in the heater.

The reduction of this recirculation, which is colder than the inlet stream, increases the inlet temperature of the condensate in the heater (rise by 3.5°C). Moreover, optimisation reduces the outlet temperature of the heater (from 82°C to 69.1°C). As a result, the temperature difference between the inlet and the outlet temperature of the fluid in the heater is considerably reduced: from 16°C to less than 1°C.

The reduction of flow and temperature difference in the heater explain why its energy consumption is significantly reduced (by 96 %).

Compressors energy consumption

The effect of the new process parameters on compressors energy consumption is smaller. Only 4 % of the total energy demand decrease is due to the compressors.

As introduced above, recirculation reduces the flow in the condensate stabilization unit. It is observable for the compressors in the gas recompression stages (decreases by 11 kmol/h for C_1 and by 39 kmol/h for C_2). However, because the pressure ratio increases in C_1 (due to the decrease of P_3), the energy consumption of C_1 increases. The decrease of flow is not enough to make its consumption to decrease. Concerning C_2, the pressure ratio is almost unchanged (the pressure P_2 is only reduced from 9.5 bar to 9.43 bar). The decrease of its energy consumption is due to the flow reduction.

The energy consumption in the two compressors of the gas processing part, C_3 and C_4, is only explained by the evolution of flow rate since the pressure ratio are unchanged in the optimized model. Recirculation from S_G is reduced (by 129 kmol/h) as it was previously explained. Hence, less flow enters the inlet separator S_A, producing less vapour (variation of 72 kmol/h) and less liquid. This liquid is then processed in the condensate stabilization unit. Because its flow is reduced and also because the two

levels of pressure P_2 and P_3 are reduced, this unit produces less vapour (reduction by 39 kmol/h). This vapour from the compressor C_2 is then mixed with the initial vapour from S_A. As a result of the reduction of these two flows, the flow going to C_3 is considerably reduced (by 110 kmol/h) which explains the reduction of its energy consumption.
As already mentioned, the flow in the inlet of the gas processing part is reduced by 110 kmol/h and the recirculation from S_G is reduced by 129 kmol/h. As a result, the flow entering in the last compressor C_4 increases by 19 kmol/h which rises its energy consumption.

Energy distribution

Energy optimisation was made by minimizing the total energy consumption of the plant. However, it should be noticed that two types of energy are required: mechanical energy for the pumps of the compressors and thermal energy for the heater.

In the base case, energy consumption is distributed quite equally between the compressors work and the heater duty. However, the distribution is completely different for the optimized model. Indeed, almost all the energy consumption of the oil and gas offshore plant is due to the compressor work. The following figure illustrates this point [8].

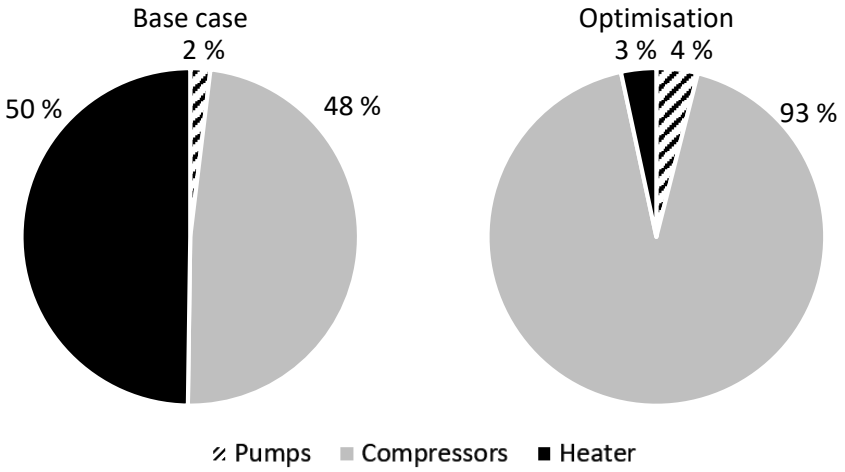

Figure 18: energy consumption distribution between units

It should be noticed that the energy distribution differs from one optimisation to another. Graphical representation as above can found in appendix (*Appendix 6: energy consumption distribution*) for each studied case from (a) to (j).

What is shown is that the same tendency is observed for each optimisation: the compressors work is the main responsible for energy consumption. It represents between 85 % and 93 % of the total energy consumption of the plant.

[8] Note that the circle diameter do not represent the amount of energy consumption. For example, the compressors energy consumption decreases between the base case model and the optimisation. However, its part in the total energy consumption increases, this is this point which is illustrated by the *Figure 18*.

3.2 Products analysis

Rich gas

As it was introduced in the energy consumption section, there is more flow going through the last compressor. It means that with the new process parameters, the production of rich gas is increased by 19 kmol/h. The components that are the main responsible for this rise are: propane (28 % [9]), i-butane (15 %), n-butane (32 %) but also i-pentane, n-pentane and n-hexane.

Because the rich gas contains more hydrocarbons compared to the base case, the area of its phase envelope is bigger and the cricondenbar is higher. The comparison is represented in the following figure.

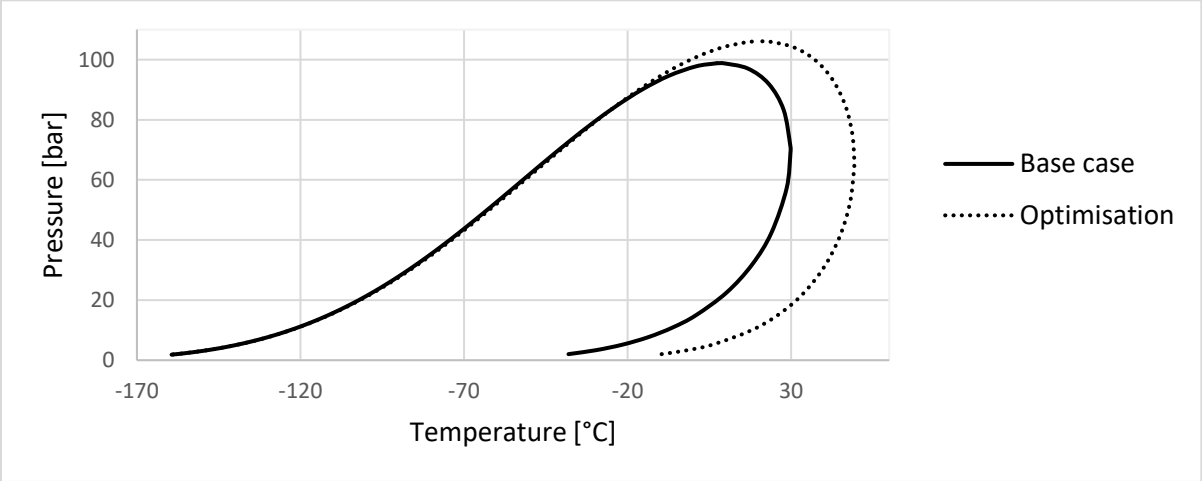

Figure 19: rich gas phase envelope in the energy optimisation model

Crude oil

The variation of process parameters increases the production of rich gas so decreases the production of crude oil. It should be noticed that, whereas the production of oil is above the one of the gas in the base case, the contrary is observed in the optimized model.

Concerning the specification, crude oil TVP is increased by the optimisation. It can be explained by the fact that intermediate components such as propane, i-butane, n-butane are reduced in the oil whereas the production of methane and ethane, the lightest hydrocarbon components, increases. This increase is due to the fact that the heater temperature T_h is reduced.

[9] The percentages represent the contribution of the component to the total rise of rich gas production. For example, it means that the increase of propane production in rich gas is responsible for 28 % of the rise of rich gas production.

3.3 Gas scrubbers

The amount of liquid entering the different gas scrubbers are also noted. Results are presented in the following table.

	Base case	Optimisation
Feed gas scrubber S_F	1.50 %	1.63 %
Scrubber before dehydration S_G	21.1 %	0.06 %
Safety scrubber S_H	0.99 %	0.32 %

Table 19: liquid amount in feed to gas scrubber (mole basis) for energy optimisation

The optimisation of energy consumption impacts mainly the scrubber before the dehydration unit (S_G). Indeed, since the temperature before this scrubber T_d is increased (from 30°C to 50°C), the proportion of liquid decreases in S_G as well as in the following scrubber S_H but in a lesser extent.

Concerning the feed gas scrubber S_F, it is the small changes of the phase envelope which can explain the change of the liquid amount.

4. Heat integration

As introduced before, energy consumption is distributed between two categories: mechanical energy and thermal energy. The latter can be reduced with heat integration.

The goal of heat integration is to use the energy released by the hot fluids when they are cooled to heat another fluid.

Heat integration is applied to the optimized model which minimizes the total energy consumption. It means that P_2 is equal to 9.43 bar, P_3 to 1.95 bar, T_h to 69.1°C, T_1, T_2 and T_f to 30°C and finally T_d is equal to 50°C.

The methodology to build the new process is explained in detail in this section.

4.1 Step1: identify the hot and cold streams

Hot streams refer to the streams that need to be cooled down whereas the cold stream is the one that requires energy to be heated.

These streams are identified in the following figure representing the offshore plant.

Note that the fluid going through the first cooler is not considered in the heat integration. Indeed, this cooler is used to model the heat transfer between the extracted natural gas and the sea during its transport toward the offshore plant. It is not a “real” heat exchanger. Hence, this fluid cannot be used to heat the condensate in the offshore platform.

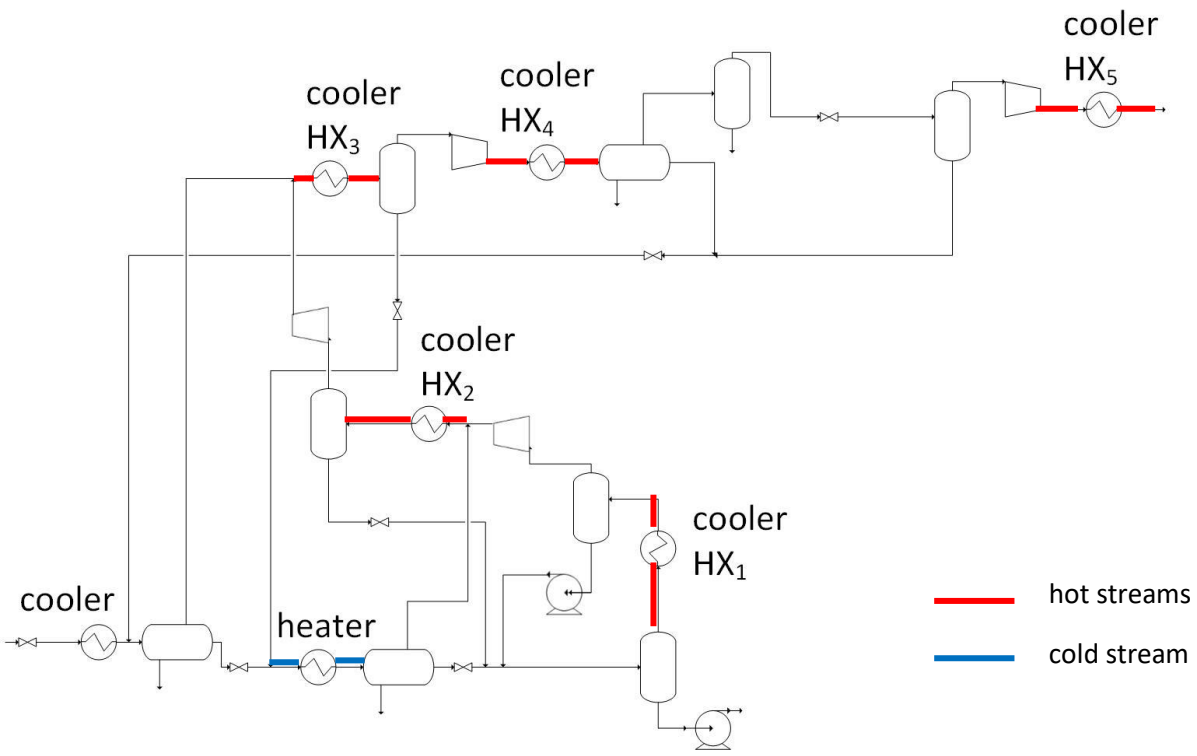

Figure 20: heat integration

4.2 Step 2: levels of temperature

For each stream, previously identified, the levels of temperature (inlet and outlet of the heat exchanger) are identified and represented in the following figure.

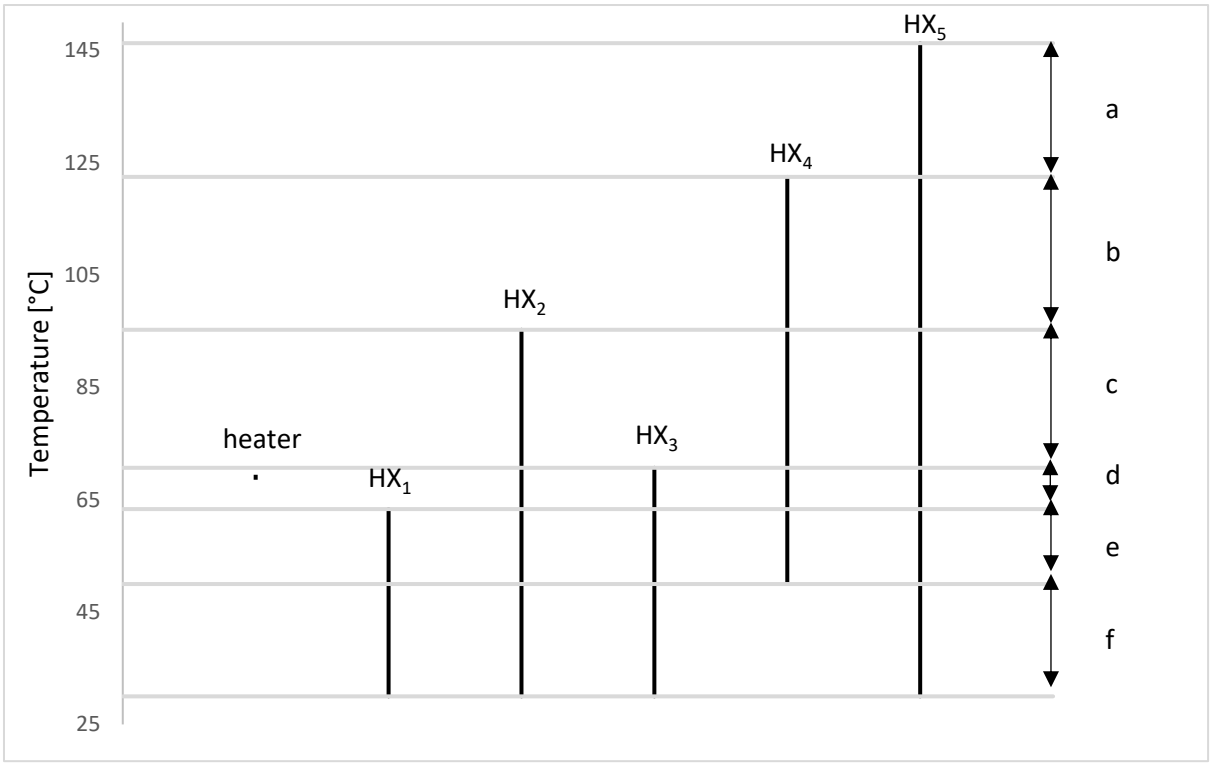

Figure 21: levels of temperature for the optimized model

The next step is to draw the ($\dot{Q}$, T) diagram. It represents the energy released or required related to the levels of temperature.
It is a straight line for the cold stream. However, it is not the case for the hot streams. Indeed, the five hot streams are combined to draw a unique curve: it is called the hot composite curve. This curve is composed of different parts depending on the levels of temperature: a, b, c, d, e and f, identified on the previous figure.

4.3 Step 3: energy consumption

The values of the heat duty exchanged in each heat exchanger are taken from the UniSim simulation ($\dot{Q}$). With the levels of temperature, the heat flow per unit of temperature ($\dot{m} * \overline{C_p}$) can be calculated.

$$\dot{m} * \overline{C_p} = \frac{\dot{Q}}{T_{out} - T_{in}} \tag{4}$$

$\dot{m} * \overline{Cp}$	:	Duty per unit of temperature	[kW/°C]
$\dot{Q}$	:	Duty	[kW]
T_{out}	:	Temperature after the heat exchanger	[°C]
T_{in}	:	Temperature before the heat exchanger	[°C]

	$\dot{Q}$ [kW]	T_{in} [°C]	T_{out} [°C]	$\dot{m} * \overline{C_p}$ [kW/K]
heater	48.92	68.93	69.1	283
HX_1	149.2	63.35	30.0	4.47
HX_2	211.9	95.27	30.0	3.25
HX_3	402.4	70.70	30.0	9.89
HX_4	658.4	122.5	50.0	9.08
HX_5	1 357	146.3	30.0	11.7

Table 20: power consumption in heat exchangers in the optimised model

Knowing $\dot{m} * \overline{C_p}$ and the range of temperature for each part of the hot composite curve, the duty that can be exchanged in each part is computed.

$$\dot{Q} = \dot{m} * \overline{C_p} * \Delta T \quad (5)$$

$\dot{Q}$	:	Duty	[kW]
$\dot{m} * \overline{Cp}$	:	Duty per unit of temperature	[kW/°C]
ΔT	:	Temperature difference	[°C]

		$\dot{m} * \overline{C_p}$ to consider	$\dot{Q}$ [KW]
Cold stream		$(\dot{m} * \overline{C_p})_{heater}$	48.92
Hot streams	a	$(\dot{m} * \overline{C_p})_{HX5}$	277.7
	b	$(\dot{m} * \overline{C_p})_{HX4} + (\dot{m} * \overline{C_p})_{HX5}$	564.7
	c	$(\dot{m} * \overline{C_p})_{HX2} + (\dot{m} * \overline{C_p})_{HX4} + (\dot{m} * \overline{C_p})_{HX5}$	589.6
	d	$(\dot{m} * \overline{C_p})_{HX2} + (\dot{m} * \overline{C_p})_{HX3} + (\dot{m} * \overline{C_p})_{HX4} + (\dot{m} * \overline{C_p})_{HX5}$	832.6
	e	$(\dot{m} * \overline{C_p})_{HX1} + (\dot{m} * \overline{C_p})_{HX2} + (\dot{m} * \overline{C_p})_{HX3} + (\dot{m} * \overline{C_p})_{HX4} + (\dot{m} * \overline{C_p})_{HX5}$	1 561
	f	$(\dot{m} * \overline{C_p})_{HX1} + (\dot{m} * \overline{C_p})_{HX2} + (\dot{m} * \overline{C_p})_{HX3} + (\dot{m} * \overline{C_p})_{HX5}$	585.4

Table 21: power consumption in each part of the composite curves in the optimised model

4.4 Step 4: pinch analysis

Knowing the heat duty and the levels of temperature, the hot composite curve and the cold curve can be drawn.

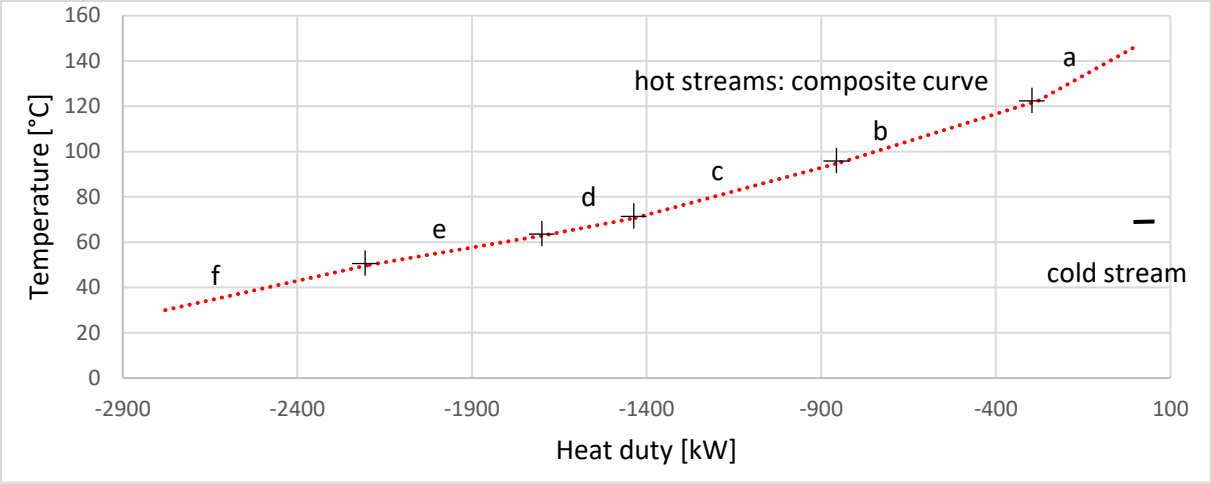

Figure 22: composite curves for the optimized model

Then, the cold stream needs to be horizontally translated to the left until the pinch is reached. The pinch is the minimum temperature difference between the hot stream and the cold stream. It is set equal to 10 K.

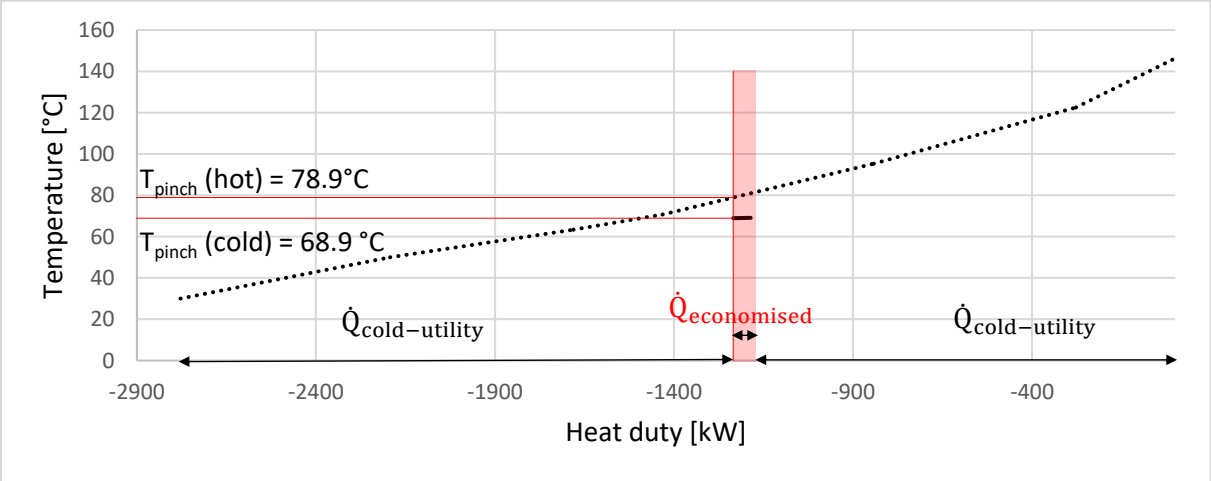

Figure 23: pinch identification for the optimized model

The amount of energy that can be economized ($\dot{Q}_{economised}$) if cold fluids and hot stream are combined can be identified. It corresponds to the area where the two curves overlap.

In this case, the economized energy is the energy required by the heater. It means that all the required energy to heat the fluid is given by the hot streams. Hence, no hot utility is required.

However, cold utilities are required to cool down the remaining hot streams ($\dot{Q}_{cold-utility}$).

4.5 Step 5: new network of heat exchangers

Due to temperature levels, only three hot streams can be used to bring energy to the fluid which needs to be heated: fluids from HX_2, HX_4 and HX_5.

The heat duty that can be given to the cold stream must be recalculated. Indeed, there must not be a cross of temperature in the heat exchanger: there must always have a temperature difference between the hot fluid and the cold one above or equal to the pinch. It means that the outlet temperature of the hot stream is not the one from *Table 20* but is equal to $T_{pinch}(hot)$.

$$\dot{Q}_{HX} = (\dot{m} * \overline{C_p})_{HX} * \left(T_{in,HX} - T_{pinch}(hot)\right) \quad (6)$$

$\dot{Q}_{HX}$	:	Duty	[kW]
$(\dot{m} * \overline{C_p})_{HX}$	:	Duty per unit of temperature	[kW/°C]
$T_{pinch}(hot)$	:	Outlet temperature of the hot stream $T_{pinch}(hot) = 78.9\ °C$	[°C]
$T_{in,HX}$	:	Inlet temperature of the hot stream	[°C]

The available heat duty is calculated for each possible fluid: from HX_2, HX_4 and HX_6. Results are introduced in the following table.

	HX_2	**HX_4**	**HX_5**
$\dot{Q}_{HX}$ [kW]	53.1	396	786

Table 22: available heat duty to heat the fluid in the optimized model

Numerical results show that the available energy for each fluid is above the required energy by the heater (48.92 kW). Hence, only one hot stream is necessary to heat the cold stream. The choice of which fluid is used does not impact the energy consumption of the process.

Rich gas, going through HX_5, is chosen as the hot stream.

Since only a part of the available energy is used to heat the fluid, the outlet temperature of the hot stream is not 78.9°C but needs to be recalculated.

$$T_{out,hot} = T_{in,hot} - \frac{\dot{Q}_{heater}}{(\dot{m} * \overline{C_p})_{HX5}} \quad (7)$$

$T_{out,hot}$	:	Outlet temperature of the hot stream $T_{out,hot} = 142°C$	[°C]
$T_{in,hot}$	:	Inlet temperature of the hot stream $T_{in,hot} = 146°C$	[°C]
$\dot{Q}_{heater}$	:	Heat duty required by the cold stream $\dot{Q}_{heater} = 48.92\ kW$	[kW]
$(\dot{m} * \overline{C_p})_{HX5}$	:	Duty per unit of temperature $(\dot{m} * \overline{C_p})_{HX5} = 11.7\ kW/°C$	[kW/°C]

The figure below represents the new oil and gas plant with heat integration leading to the minimisation of the total energy consumption.

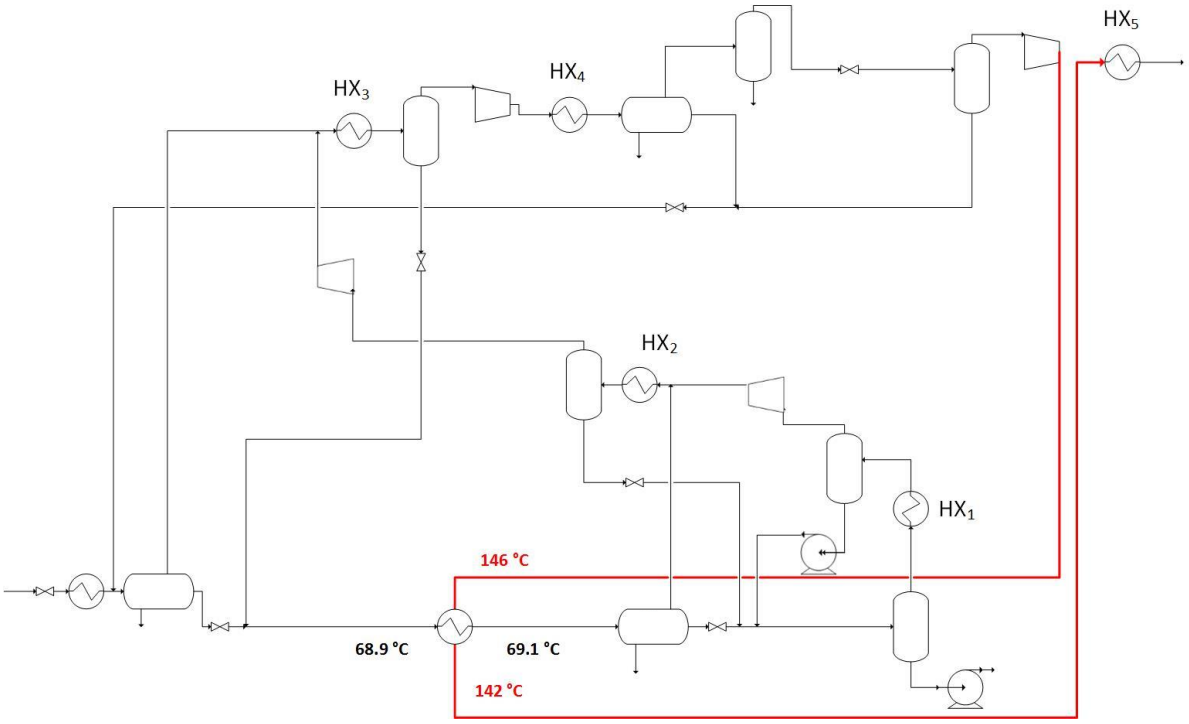

Figure 24: new network of heat exchangers

4.6 Conclusion

Heat integration of the optimized process enables to save 49 kW compared to the optimized model without heat integration. With this modification, all the energy consumption is due to pumps and compressor.

Since, the heater energy consumption represents only 3 % of the total energy consumption of the plant in the optimized model, heat integration has not a huge effect on the total energy demand.
However, as it was previously introduced, the energy consumption in the base case model is equally distributed between heater and compressors. Hence, a larger amount of energy is saved if heat integration methodology is applied to the base case. Results in appendix (*Appendix 7: heat integration of the base case model*) enable to answer the question if the minimum total energy consumption of the plant is obtained by doing heat integration on the base case model or on the optimized process parameters model.

1 159 kW are economised with heat integration in the base case model. However, it is not enough to obtain a better solution than with heat integration of the optimized model. Moreover, the construction of the new network of heat exchangers imposes to add three more heat exchangers if heat integration is done in the base case model, which increases the capital cost of the oil and gas offshore plant.

The following table sums up the relevant results.

	Base case	**Optimisation**
$\dot{Q}_{economised}$	1 159 kW	49 kW
$\dot{Q}_{hot-utility}$	284 kW	0 kW
Total energy consumption	1 739 kW (- 40 % [10])	1 400 kW (- 3.4 % [10])
Heat exchangers	+ 3	+ 0

Table 23: comparison of heat integration between the base case model and the optimized one

[10] Compared to the same case without heat integration.

III. Recirculation studies

Along the process four streams of liquid are recycled. R_1 and R_2 correspond to the liquid produced by the two stages of cooling of the feed gas in the gas processing part. R_3 and R_4 refer to the recirculation streams from the cooling before the recompressions of the gas.

All these recirculation are sent back to the condensate stabilization unit. In this section, the influence of the stage in which they are sent (first, second or third stage) on the total energy consumption and on specifications is studied.

Numerical values are obtained with the process parameters from the base case meaning P_2 is equal to 9.5 bar, P_3 to 2.56 bar, T_1, T_2,T_f, T_d = 30°C and T_h equal to 82°C.

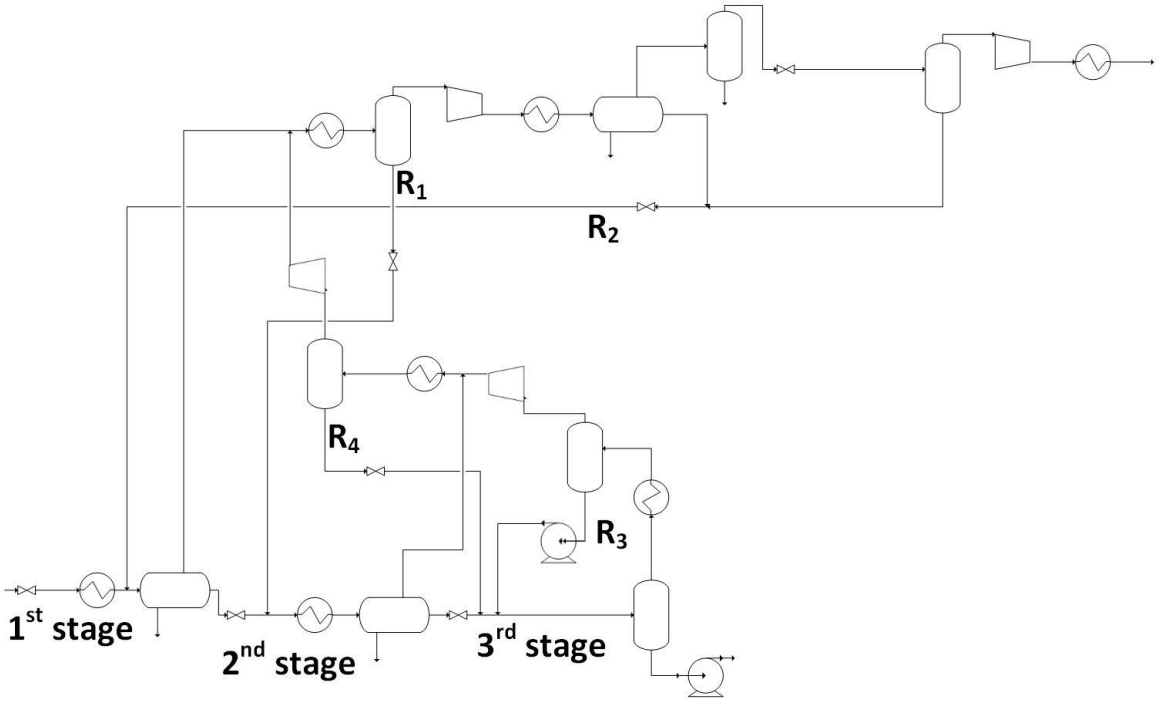

Figure 25: nomenclature for recirculation studies (base case recirculation)

In a first time, each recirculation is sent to another stage than the stage in the base case. For example, the energy consumption and the specification are evaluated for R_1 going to the 1st stage or to the 3rd stage keeping the other recirculation as in the base case.

The results are introduced in appendix (*Appendix 8: recirculation studies).* The main conclusion from these results is that even if the total energy consumption is reduced by changing the location where the recycled liquid is sent, the specification on TVP of oil is not met. As a result, process parameters must be changed.

Not all the different cases of recirculation are studied, since they are too many. Because, the results in appendix 8 show that the recirculation R_1 sent to the first stage of the condensate stabilization unit leads to the minimum of energy consumption, this this case which is studied in this work.

As in the previous studies, rich gas cricondenbar is never a problem. Hence, this specification is not discussed in this section.

1. New process parameters

The minimum value for the total energy consumption is 2 750 kW. It is reached when R_1 is sent to the first stage of the condensate stabilization unit instead of the second stage. The goal of this section is to check if it is possible to obtain a crude oil TVP below the specification of 0.965 bar by changing the process parameters.

Graphical results can be found in appendix (*Appendix 9: new process parameters for the recirculation studies).*

1.1 Condensate stabilization unit

Heater temperature T_h

To remove the lightest hydrocarbons from the oil and hence reduce the TVP to meet the specification, the temperature after the heater can be increased. It must be above 85.7°C to meet the specifications if the other parameters are the base case ones [11] (*Figure 61*). However, it increases the energy consumption compared to the base case.

Second level of pressure P_2

A value of P_2 cannot be found to meet the TVP specification [12]. So, the study of this parameter is made with T_h equal to 85.7°C. In this case, a pressure of 9.5 bar is the maximum value to meet the specification (*Figure 62*). It also corresponds to the minimum of energy consumption.

Third level of pressure P_3

The pressure should be reduced to limit the vaporisation. By keeping the process parameters as defined in the base case model [13], the maximum third level of pressure to meet the TVP specification is 2.40 bar (*Figure 63*).

1.2 Gas recompression train

First cooler temperature T_1

The choice of T_1 is not relevant if the other parameters are the same as in the base case [14]. Indeed, oil TVP is always off-spec. If T_h is equal to 85.7°C, T_1 must be chosen between 11°C and 22°C (*Figure 64*) to meet the TVP specification. The lowest value of T_1 gives the lowest value of energy consumption.

[11] P_2 = 9.5 bar, P_3 = 2.56 bar, $T_1 = T_2 = T_f = T_d$ = 30°C
[12] P_3 = 2.56 bar, T_h = 82°C, $T_1 = T_2 = T_f = T_d$ = 30°C
[13] P_2 = 9.5 bar, T_h = 82°C, $T_1 = T_2 = T_f = T_d$ = 30°C
[14] P_2 = 9.5 bar, P_3 = 2.56 bar, T_h = 82°C, $T_2 = T_f = T_d$ = 30°C

Second cooler temperature T_2

With the base case parameters [15], oil TVP is never met for any value of T_2. However, if the heater temperature (T_h) is selected equal to 85.7°C, the specification is within the good range of value and the energy consumption of the process can even be minimized if T_2 is reduced (*Figure 65*). The minimum value of T_2 is dictated by the hydrate formation temperature (6°C).

1.3 Gas processing

Feed gas cooler temperature T_f

As for the temperature T_2, crude oil TVP is never met if the process parameters other than T_f are the same as in the base case model [16]. If the heater temperature is fixed to 85.7°C, TVP is always met (*Figure 66*). In this case, reducing T_f reduces the energy consumption of the plant. The minimum value for the feed gas cooler temperature is dictated by the hydrate formation temperature (11°C).

Temperature before dehydration T_d

If the other parameters are the base case parameters [17], the impact of T_d on TVP is no significant and do not allow to obtain a value below the specification of 0.965 bar. However, if the heater temperature is increased to 85.7°C, results of parametric studies show that T_d must be set to 32.5°C to minimize the energy consumption meeting the TVP specification (*Figure 67*).

2. Optimisation

Process parameters can be chosen to meet the specifications when the recirculation from the feed gas scrubber R_1 is sent to the inlet separator. This section evaluates how the energy consumption of the plant (pumps, compressors, heater) can be reduced by changing the process parameters values.

The evolution of process parameters to reduce the energy consumption of the plant is the same as for the case where R_1 is sent to the second stage of the condensate stabilization unit (*Table 11*).

3. Results

Optimisation is done using the previous studies and the optimizer tool of UniSim. Results are presented in the following table.

[15] P_2 = 9.5 bar, P_3 = 2.56 bar, T_h = 82°C, $T_1 = T_f = T_d$ = 30°C
[16] P_2 = 9.5 bar, P_3 = 2.56 bar, T_h = 82°C, $T_1 = T_2 = T_d$ = 30°C
[17] P_2 = 9.5 bar, P_3 = 2.56 bar, T_h = 82°C, $T_1 = T_2 = T_f$ = 30°C

			Base case	Optimisation
Process parameters	Condensate stabilization unit	**P_2**	9.50 bar	8 bar
		P_3	2.56 bar	2.56 bar
		T_h	82°C	82.5°C
	Gas recompression stages	**T_1**	30°C	14°C
		T_2	30°C	8°C
	Gas processing	**T_f**	30°C	12°C
		T_d	30°C	33°C
Specifications	Cricondenbar		98.85 bar	99.90 bar
	TVP @30°C		0.9604 bar	0.9629 bar
Energy consumption			2 898 kW	2 450 kW
Production	Rich gas		470 kmol/h	475 kmol/h
	Oil		498 kmol/h	488 kmol//h

Table 24: optimisation with change on recirculation loop

3.1 Energy consumption

If the liquid R_1 is sent to the first stage of the condensate stabilization unit with the above process parameters, the total energy consumption can be reduced by 15 % compared to the base case. Details can be found in the following table.

Type	Unit	Energy consumption [kW]		Variation [kW]	
		Base case	Optimisation		
pumps	p-1	55.65	55.53	↘	0.118
	p-2	0.003	0.005	↗	0.002
	sum	55.66	55.54	↘	0.116
compressors	C_1	101.7	55.57	↘	46.70
	C_2	101.7	95.15	↘	6.519
	C_3	695.5	546.8	↘	148.7
	C_4	501.0	511.5	↗	10.53
	sum	1 400	1 209	↘	190.8
heater	heater	1 442	1 185	↘	257.1
total		2 898	2 450	↘	448.0

Table 25: effect of recirculation optimisation on energy consumption

Heater energy consumption

The reduction of the heater energy consumption is responsible for 57 % of the total decrease.

The temperature difference between the inlet and the outlet of the heater is not significantly changed from the base case model. As a result, only the modification of flow rate explains the decrease of energy consumption.

Reducing the temperature after the coolers in the gas recompression stages (T_1 and T_2) decreases the amount of vapour entering the gas processing part. In addition, the temperature before the

dehydration unit is increased. Consequently, less liquid flow is recycled from S_G. Since R_2 is sent to the condensate stabilization unit, it reduced the flow in the heater (by 50 kmol/h).

Compressors energy consumption

43 % of the total energy demand decrease is due to the compressors work.

The most affected compressor is the first one the gas processing unit: C_3. As mentioned above, the flow rate is reduced (by 149 kmol/h) decreasing C_3 energy consumption. In the last compressor, a small increase of flow (10 kmol/h) explains the rise in its energy consumption.

Concerning the gas recompression train, flow is also reduced in C_1 (by 46 kmol/h) and C_2 (by 6.5 kmol/h) but in a lower level than in C_3.

Energy distribution

The repartition between the different types of energy is not influenced by the recirculation optimisation as shown by the following figure. Thermal and mechanical energy are equally distributed.

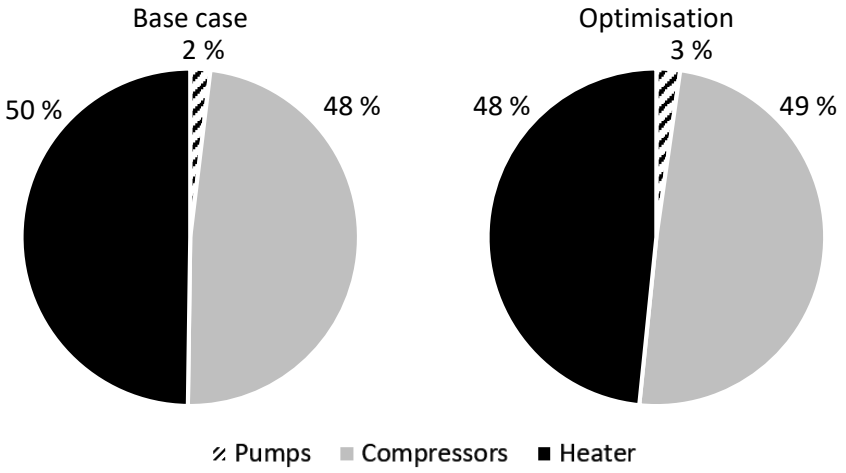

Figure 26: energy distribution for the recirculation optimisation

3.2 Products analysis

Rich gas

As mentioned above, the flow increases in the last compression stage which means an increase in rich gas production. The main components responsible for this rise are propane (45 %), n-butane (30 %) and i-Butane (16 %). Their proportion also increases a little bit which leads to a small increase of the cricondenbar.

Crude oil

Oil production is reduced by the optimisation since more intermediate components (propane, n-butane, i-butane) are sent to the gas. However, TVP increases. It could be explained by the increase of methane and ethane production in the oil (variation less than 1 kmol/h).

3.3 Gas scrubbers

As for the other studies, the amount of liquid entering the gas scrubbers are noted and presented in the following table.

	Base case	Optimisation
Feed gas scrubber S_F	1.50 %	3.40 %
Scrubber before dehydration S_G	21.1 %	3.25 %
Safety scrubber S_H	0.99 %	1.00 %

Table 26: liquid amount in feed to gas scrubber (mole basis) for recirculation optimisation

The temperature after the feed gas scrubber T_f is reduced which increases the amount of liquid in S_F. The temperature before the dehydration unit is increased which reduces the liquid in the inlet of S_G. Concerning the safety scrubber, the is no significant change.

4. Heat integration

Heat integration of this new model enables to save 773 kW. As a result, the total energy consumption is 1 677 kW. Sending R_1 to the first stage of the condensate stabilization unit with optimal process parameters combined with heat integration reduces the energy consumption of the base case model by 42 %.

Intermediate results are presented in appendix as well as the new network of heat exchangers (*Appendix 10: heat integration of the optimised recirculation model*).

5. Conclusion

The study of the recirculation R_1 sent to the first stage of the condensate stabilization unit shows that it is not possible to reduce the energy consumption of the plant more than in the case of the optimized process parameters.

Chapter 8 – Further studies

This last chapter brings additional information about the oil and gas offshore plant and components behaviour. It includes the effect of changing the composition of the natural gas and the effect of heat transfer during its transport toward the offshore plant.

I. New natural gas composition

The aim of this section is to study the impact of the change of the raw natural gas composition. The motivation of this new study is based on the fact that for the previous natural gas (NG1) the rich gas cricondenbar was never a problem. Hence it was not used for the different optimisations.

1. Comparison with the previous natural gas composition

The offshore plant is the same as for the other natural gas (*Figure 11*) and the process parameters are set as in the base case model. It means that for the condensate stabilization unit the second level of pressure (P_2) is equal to 9.50 bar, the third one (P_3) to 2.56 bar and the heater temperature T_h to 82°C. The temperature after the coolers are equal to 30°C (T_1, T_2, T_f and T_d). The flow rate of raw natural gas is still equal to 1 000 kmol/h.

The oil TVP specification is the same as before, 0.965 bar. However, the rich gas cricondenbar specification is reduced to 105 bar for this new natural gas.

The new composition of natural gas (NG2) is presented in appendix (*Appendix 11: NG2 composition*). The following figure shows the comparison between NG1 and NG2 composition.

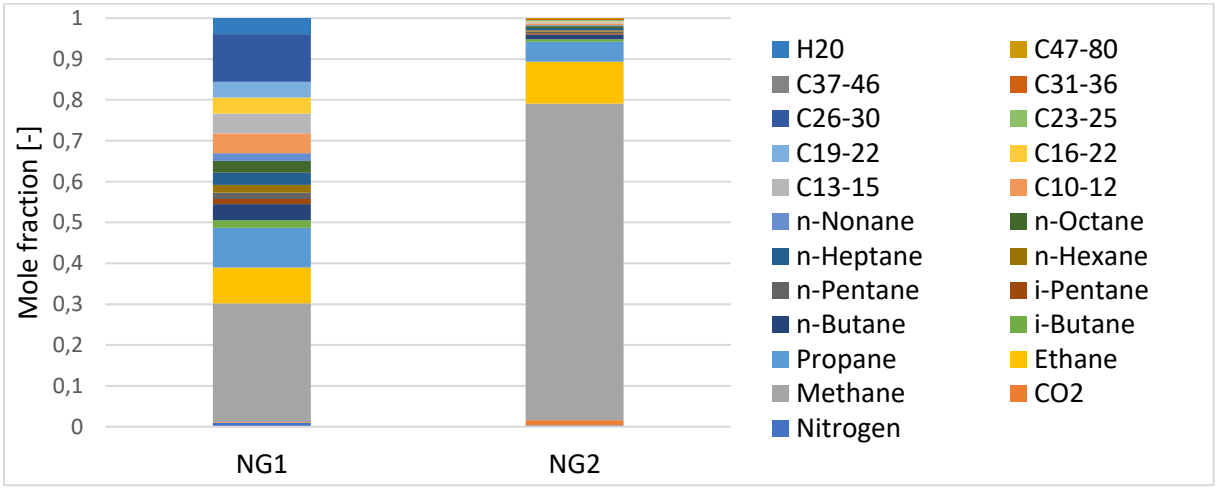

Figure 27: reservoir composition comparison

The new natural gas is richer in methane and ethane. Since they are light hydrocarbons, the increase of their content in the reservoir increases the production of rich gas (by 497 kmol/h). Whereas for NG1, the production of gas and oil were approximately the same, rich gas production is predominant for NG2 (more than 95 % of the raw natural gas is converted into rich gas).

The following table introduces the main results of the simulation. It shows that by changing the composition of the gas keeping the same process parameters [18], TVP specification of crude oil is not met.

	NG1	NG2
Gas production [kmol/h]	470	967
Oil production [kmol/h]	498	33
Rich gas cricondenbar [bar]	98.85	102.5
Oil TVP @30°C [bar]	0.9604	1.288

Table 27: results comparison between NG1 and NG2

2. Parametric studies

In this section, the influence of process parameters on the specifications are studied.

Note that for each parameter study, the other parameters are the ones of the base case model [18]. Figures representing the following points can be found in appendix (*Appendix 12: parametric studies with NG2 composition*).

2.1 Condensate stabilization unit

The minimum heater temperature (T_h) to meet the good TVP is 100.3°C (*Figure 72*).
It is not possible to find a value of P_2 that meets the TVP (*Figure 73*). However, it is different for P_3. Indeed, it must be selected below 2 bar to have an oil TVP in the good range of values (*Figure 74*).

In any case, changing a parameter of the condensate stabilization unit influences the cricondenbar. It remains around 102.5 bar.

2.2 Gas recompression train

TVP is not affected by the values of the temperature after the coolers in the gas recompression stages (T_1 and T_2). It is never below 0.965 bar (*Figure 75* and *Figure 76*).

As for the condensate stabilization unit, rich gas cricondenbar is always around 102.5 bar.

[18] With process parameters from the base case model: P_2 = 9.5 bar, P_3 = 2.56 bar, T_h = 82°C, $T_1 = T_2 = T_f = T_d$ = 30°C

2.3 Gas processing

In the gas processing part, T_f and T_d cannot be selected to obtain a TVP within the good range of value if the other parameters are the same as in the base case model (*Figure 77* and *Figure 78*).

However, these two parameters influence the cricondenbar. It is reduced when the temperatures are reduced. A too high T_d leads to an off-spec rich gas.

2.4 Conclusion

On one hand, these studies show that the oil TVP is significantly influenced by T_h, P_3 and less significantly by T_f. On the other hand, rich gas cricondenbar is dictated by T_f and T_d.

These studies enable to conclude that even with a natural gas with a larger proportion of light hydrocarbons, cricondenbar is never a problem. Indeed, in all the simulations which were carried out, when the oil TVP is met, cricondenbar is automatically met. As a result, cricondenbar specification cannot be used for optimisation.

3. More restrictive cricondenbar specification

In order to identify if the cricondenbar can be used for the optimisation of the plant, the specification is reduced to 100 bar. It should be noted that it can also be the result of a margin taken when sizing the plant.

Previous parametric studies indicate that the process parameters which dictates the value of the cricondenbar are T_f and T_d. These two need to be reduced to reduce the cricondenbar (see appendix *A12.3 Gas processing*). The feed gas cooler temperature must be below 12.5°C [19] (*Figure 77*) or the temperature before dehydration below 25°C [20] (*Figure 78*).

Process parameters must also be changed to meet the correct oil TVP. Graphical results can be found in appendix (*Appendix 13: cricondenbar specification of 100 bar*). The following sub-sections present these results.

3.1 Cricondenbar controlled by T_f

If T_f is equal to 12.5°C, cricondenbar is met but not the TVP. As introduced before, T_h, P_3 influence the value of TVP. Hence, parametric studies on these two parameters are carried out with the new value of T_f. In this case the minimum heater temperature is 94°C to meet the TVP [21] (*Figure 79*) and the maximum pressure P_3 is 2.17 bar [22] (*Figure 80*).

[19] P_2 = 9.5 bar, P_3 = 2.56 bar, T_h = 82°C, $T_1 = T_2 = T_d$ = 30°C
[20] P_2 = 9.5 bar, P_3 = 2.56 bar, T_h = 82°C, $T_1 = T_2 = T_f$ = 30°C
[21] P_2 = 9.5 bar, P_3 = 2.56 bar, $T_1 = T_2 = T_d$ = 30°C, T_f = 12.5°C
[22] P_2 = 9.5 bar, T_h = 82°C, $T_1 = T_2 = T_d$ = 30°C, T_f = 12.5°C

3.2 Cricondenbar controlled by T_d

Another possibility to control the rich gas cricondenbar is to change the value of the temperature before the dehydration unit. If T_d is set equal to 25°C, TVP of oil is off-spec. In this case, T_h must be above 99.1°C [23] (*Figure 81*) or P_3 below 2.04 bar [24] (*Figure 82*). Changing T_f does not bring the oil within the good range of TVP values.

3.3 Cricondenbar controlled by T_f and T_d

The last possibility to control the cricondenbar is to reduce both T_f and T_d. Different couples of temperatures can be obtained.

3.4 Conclusion

Optimisation with a natural gas richer in light hydrocarbons and with a low value of cricondenbar specification can be done in two distinct steps. The first one is to obtain a correct cricondenbar. If it is too high, T_f and/or T_d can be reduced. Then, if the oil TVP is not correct, adjustments on the relevant parameters can be achieved: increase T_h, reduce P_3 and/or reduce T_f (*Figure 77*).

[23] P_2 = 9.5 bar, P_3 = 2.56 bar, $T_1 = T_2 = T_f$ = 30°C, T_d = 25°C
[24] P_2 = 9.5 bar, T_h = 82°C, $T_1 = T_2 = T_f$ = 30°C, T_d = 25°C

II. Influence of heat transfer during transport

As mentioned in the chapter 5, heat transfer occurs between the hot extracted natural gas and the sea before arriving to the offshore plant. As a result, the gas arriving in the plant is colder. This section studies the influence of this temperature. Indeed, it mays vary depending on the weather conditions, pipelines materials or pipeline integrity for example.

1. Specifications

Process parameters must be changed if the heat transfer is too important. Indeed, the following figure indicates that if the temperature of natural gas arriving at the inlet of the offshore plant is too low, oil TVP is off-spec.

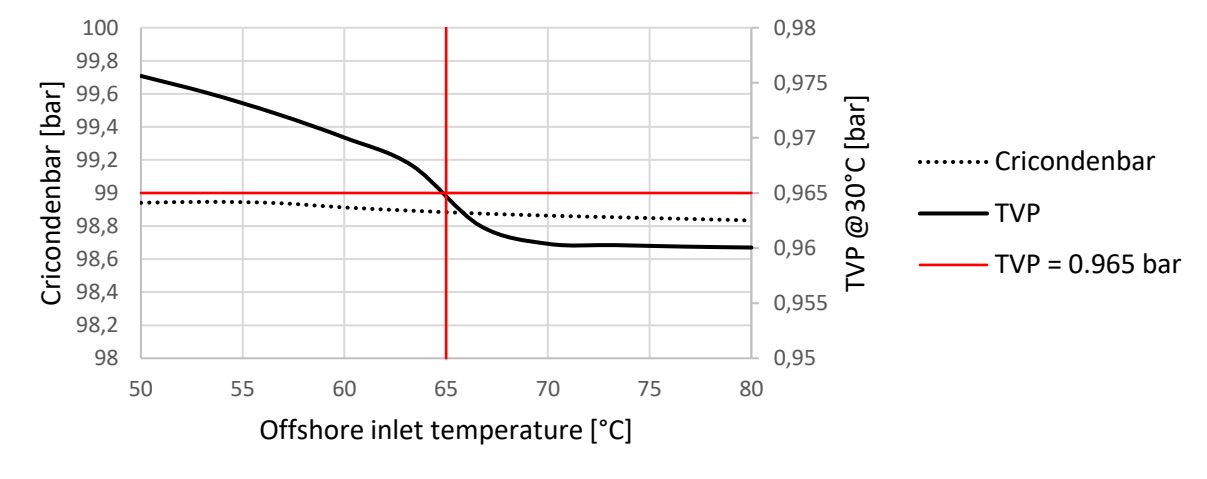

Figure 28: influence of offshore inlet temperature on specifications [25]

1.1 Rich gas

As shown in the previous figure, cricondenbar is not significantly affected by this temperature. It is explained by the fact that the production of rich gas and the distribution of its components is not affected by the heat transfer.

1.2 Crude oil

A variation of 0.016 bar is observed for the TVP.

The reduction of the inlet temperature increases the production of light hydrocarbons in the oil (ethane by 0.3 kmol/h and propane by 1.2 kmol/h) which increases the TVP.

[25] With process parameters from the base case model: P_2 = 9.5 bar, P_3 = 2.56 bar, T_h = 82°C, $T_1 = T_2 = T_f = T_d$ = 30°C

2. Energy consumption

The energy consumption of the offshore plant is also studied. The energy demand is highly influenced by heat transfer as the following figure shows.

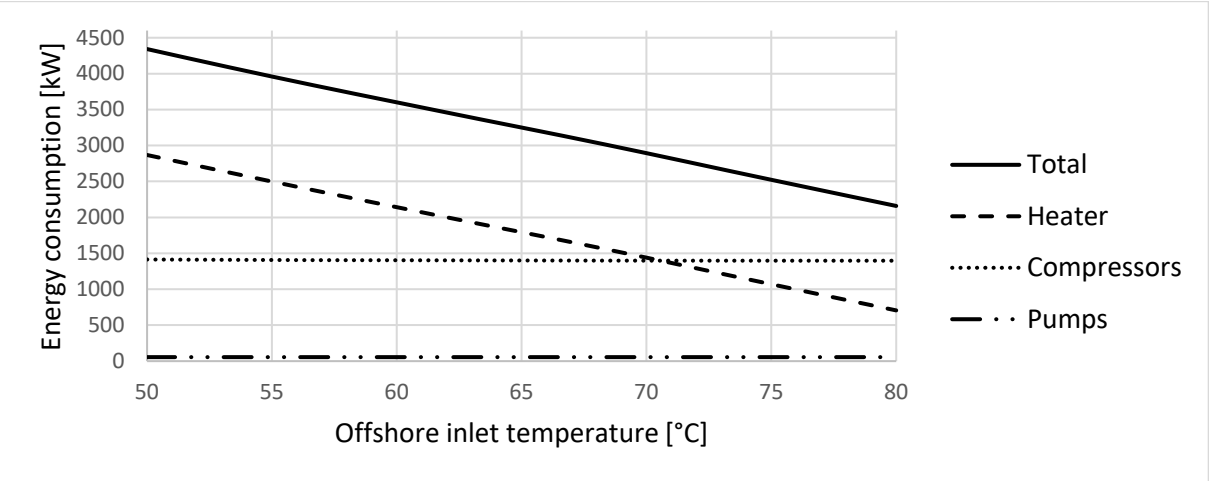

Figure 29: influence of the offshore inlet temperature on energy consumption

More the heat transfer is important, more energy is required in the process. This increase of energy demand is due to the heater of the condensate stabilization unit.

Indeed, the inlet temperature of the fluid is lower which increases the temperature difference with the outlet of the heat exchanger (by 18°C). In the same time, the liquid flow is more important (by 30 kmol/h). These two elements explain the increase of heater energy consumption.

Conclusion

Based on literature review, personal background and Equinor inputs data, a typical oil and gas offshore plant was simulated in the UniSim software. With the given specifications of 110 bar for the cricondenbar and 0.965 bar for the oil TVP at 30°C, pressure and temperature levels were determined.

Different optimisations were carried out: maximisation of the rich gas production, maximisation of the oil production and minimization of the total energy consumption of the plant.

By changing the pressure and temperature parameters in the plant enables to increase the production of gas by 4 %. However, it should be noticed that there is still a margin in the cricondenbar specification and in the oil TVP. Hence, a better optimisation could be found.

Optimisation of the oil production is not conducted in this work due to the high value of TVP in the base case model. Indeed, the increase of oil production leads to an increase in oil TVP.

The last optimisation concerns the energy consumption of the plant. The total energy demand is minimized (sum of the pumps, compressors and heater energy consumption). A reduction by 52 % is observed.
In this case, the temperature before the dehydration unit is increased to 50°C. However, the dehydration part is not simulated in this work. It means that a component splitter is used to model the dehydration instead of the industrial process such as the absorption of water by a glycol solution. This unit should be simulated in order to evaluate if its initial sizing must be changed or not to meet the required water dew point.

Concerning the heat transfer between the natural gas and the sea before the inlet offshore plant, the results show that it should be minimised to avoid an oil TVP off-spec. The choice of materials to build the pipelines can play a key role in this part. Indeed, minimizing the heat transfer minimises also the energy consumption of the plant.

Finally, the results must be taken carefully since there are obtained from simulations. Indeed, they are predicted by a unique thermodynamic model: SRK. However, the choice of thermodynamic model can affect the results. Consequently, a margin should be taken when sizing the different equipment of the process.

Further developments can be to integrate the PhaseOpt technology and direct measurements of fluids properties into a simulation software. Consequently, results of the simulation will be more precise, and the margin taken for the equipment sizing could be reduced. Reducing he margin will reduce the size so the cost of the different equipment.

References

ASTM. (2012). ASTM D1142-95 Standard Test Method for Water Vapor Content of Gaseous Fuels by Measurement of Dew-Point Temperature. In. West Conshohocken, PA.

ASTM. (2015). ASTM D323-15a Standard Test Method for Vapor Pressure of Petroleum Products (Reid Method). In. West Conshohocken, PA.

ASTM. (2016). ASTM D6377-16 Standard Test Method for Determination of Vapor Pressure of Crude Oil: VPCRx (Expansion Method). In. West Conshohocken, PA.

ASTM. (2018). ASTM D2879-18 Standard Test Method for Vapor Pressure-Temperature Relationship and Initial Decomposition Temperature of Liquids by Isoteniscope. In. West Conshohocken, PA.

Atilhan M., A. S., Ejaz S., Cristancho D., Hall K. R. (2011). PρT Behavior of a Lean Synthetic Natural Gas Mixture Using Magnetic Suspension Densimeters and an Isochoric Apparatus: Part I. *Journal of Chemical & Engineering Data, 56*(2), 212-221. doi:10.1021/je100676j

Baghban A., Bahadori M., Ahmad Z., Kashiwao T., Bahadori A.. (2016). Modeling of true vapor pressure of petroleum products using ANFIS algorithm. *Petroleum Science and Technology, 34*(10), 933-939. doi:10.1080/10916466.2016.1170843

Baker R. W., Lokhandwala K. (2008). Natural gas processing with membranes: An overview. *Ind. Eng. Chem. Res., 47(7)*, 2109-2121. doi:10.1021/ie071083w

Berg F., Pasel C., Luckas M., Eckardt T., Bathen D. (2017). Adsorption of Cyclic Hydrocarbons on Silica Alumina Gels in Natural Gas Processing. *Chemie Ingenieur Technik, 89*(7), 935-943. doi:10.1002/cite.201600183

Campbell J. M. (1992). *Gas conditioning and processing : 1 : The basic principles* (7th ed. Vol. 1). Norman, Okla: Campbell Petroleum Series.

Deflandre J.-P. (2019). *Carbon Capture and Storage - Introduction*. MOOC energy transition. IFP school.

Fredheim A., Solbraa E. (2018). *TEP 4185 - Natural Gas Technology. Part 1: Gas Processing*. Department of Energy and Process Engineering. NTNU - Norwegian University of Science and Technology.

Frørup M. D., Jepsen J. T., Fredenslund A., Rasmussen P. (1989). High pressure dew and bubble points from microwave measurements. *Fluid Phase Equilibria, 52*(C), 229-235. doi:10.1016/0378-3812(89)80329-2

Gallagher J. E. (2006). *Natural Gas Measurement Handbook*. Burlington: Elsevier Science.

Gassco (2018). Terms and conditions for transportation of gas in Gassled.

GPSA (2004). *Engineering data book : published as a service to the gas processing and related process industries* : Sections 16-26 (12th ed., SI version. ed. Vol. 2). Tulsa, Okla: Gas Processors Suppliers Association.

Herring J. (2010). Hydrocarbon dew point is a critical consideration for pipeline operations.(Best Measurement Practices). *Pipeline & Gas Journal, 237*(7), 48.

Honeywell (2005). UniSim Design - Operations Guide.

Honeywell (2009). UniSim Design - User Guide.

ISO (1997). ISO 10715:1997 Natural gas - Sampling guidelines. In.

ISO (2006). ISO 23874:2006 Natural gas - Gas chromatographic requirements for hydrocarbon dew point calculation. In.

ISO (2012). ISO 6974-1: 2012 Natural Gas - Determination of composition and associated uncertainty by gas chromatography. Part 1: General guidelines and calculation of compostion. In.

Kidnay A. J. (2011). *Fundamentals of natural gas processing* (2nd ed.). Boca Raton, Fla: CRC/Taylor & Francis.

López E. R., Daridon J. L., Baylaucq A., Fernández J. (2003). Thermophysical Properties of Two Poly(alkylene glycol) Derivative Lubricants from High Pressure Acoustic Measurements. *Journal of Chemical & Engineering Data, 48*(5), 1208-1213. doi:10.1021/je034036t

May E., Miller R. C., Shan Z. (2001). Densities and dew points of vapor mixtures of methane plus propane and methane plus propane plus hexane using a dual-sinker densimeter. *J. Chem. Eng. Data, 46*(5), 1160-1166. doi:10.1021/je010050z

Michelsen M. L. (1980). Calculation of phase envelopes and critical points for multicomponent mixtures. *Fluid Phase Equilibria, 4*(1-2), 1-10. doi:10.1016/0378-3812(80)80001-X

Mokhatab S., Poe W. A., Mak J. Y. (2015). Chapter 5 - Condensate Production. In S. Mokhatab, W. A. Poe, & J. Y. Mak (Eds.), *Handbook of Natural Gas Transmission and Processing* (Third Edition) (pp. 169-180). Boston: Gulf Professional Publishing.

Moshfeghian M. (2016). Correlations for Conversion between True and Reid Vapor Pressures (TVP and RVP). Retrieved from http://www.jmcampbell.com/tip-of-the-month/2016/02/correlations-for-conversion-between-true-and-reid-vapor-pressures-tvp-and-rvp/

Neubauer K., Dragomirova R., Stöhr M., Mothes R., Lubenau U., Paschek D., Wohlrab, S. (2014). Combination of membrane separation and gas condensation for advanced natural gas conditioning. *Journal of Membrane Science, 453*, 100-107. doi:10.1016/j.memsci.2013.10.060

Nikolaidis I. K., Economou I. G., Boulougouris G. C., Peristeras L. D. (2016). Calculation of the phase envelope of multicomponent mixtures with the bead spring method. In (Vol. 62, pp. 868-879).

Pettersen J. (2018). *TEP 4185 - Natural Gas Technology. Part 2: LNG*. Department of Energy and Process Engineering. NTNU - Norwegian University of Science and Technology.

Riazi M. R., Albahri T. A., Alqattan A. H. (2005). Prediction of Reid Vapor Pressure of Petroleum Fuels. *Petroleum Science and Technology, 23*(1), 75-86. doi:10.1081/LFT-20009686225

Rusten B., Gjertsen L. H., Solbraa E., Kirkerød T., Haugum T., Puntervold S. (2008). *Determination of the phase envelope - crucial for process design and problem solving*. Paper presented at the GPA Annual Conference, Texas.

Skouras-Iliopoulos, E. (2011). *Inputs to GL025 - Analysis and Calculations of Hydrocarbon Dew Point*.

Skouras-Iliopoulos E., Solbraa E., Vegard Løkken T., Aaserud C., AS Gassco. (2014). PhaseOpt–Online tool for hydrocarbon dew point monitoring.

Skylogianni E., Novak N., Louli V., Pappa G., Boukouvalas C., Skouras, S., . . . Voutsas E. (2016). Measurement and prediction of dew points of six natural gases. *Fluid Phase Equilibria, 424*, 8-15. doi:10.1016/j.fluid.2015.08.025

Venkatarathnam G. (2014). Density Marching Method for Calculating Phase Envelopes. *Industrial & Engineering Chemistry Research, 53*(9), 3723-3730. doi:10.1021/ie403633d

Zhou J., Patil P., Ejaz S., Atilhan M., Holste J. C., Hall K. R. (2006). (p, V m, T) and phase equilibrium measurements for a natural gas-like mixture using an automated isochoric apparatus. *The Journal of Chemical Thermodynamics, 38*(11), 1489-1494. doi:10.1016/j.jct.2005.12.011

Appendices

Appendix 1: natural gas composition

Component	Mole fraction
Nitrogen	0.0097
CO_2	0.0015
Methane	0.2911
Ethane	0.0873
Propane	0.0970
i-Butane	0.0194
n-Butane	0.0388
i-Pentane	0.0126
n-Pentane	0.0155
n-Hexane	0.0194
n-Heptane	0.0291
n-Octane	0.0291
n-Nonane	0.0194
$n\text{-}C_{12}$	0.0485
$n\text{-}C_{15}$	0.0485
$n\text{-}C_{18}$	0.0388
$n\text{-}C_{22}$	0.0388
$n\text{-}C_{27}$	0.0291
$n\text{-}C_{30}$	0.0873
H_20	0.0388

Table 28: reservoir composition (NG_1)

Appendix 2: parametric studies on specifications and production rates

A2.1 Condensate stabilization unit: second level of pressure P_2

With P_3 = 2.56 bar, $T_1 = T_2 = T_f = T_d$ = 30°C, T_h = 80°C.

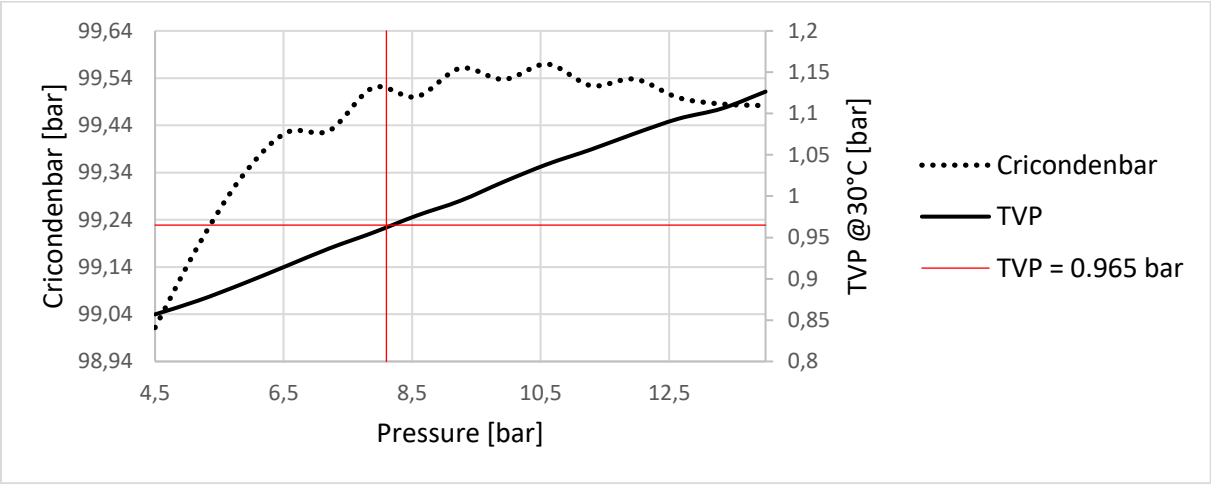

Figure 30: influence of the P_2 on specifications

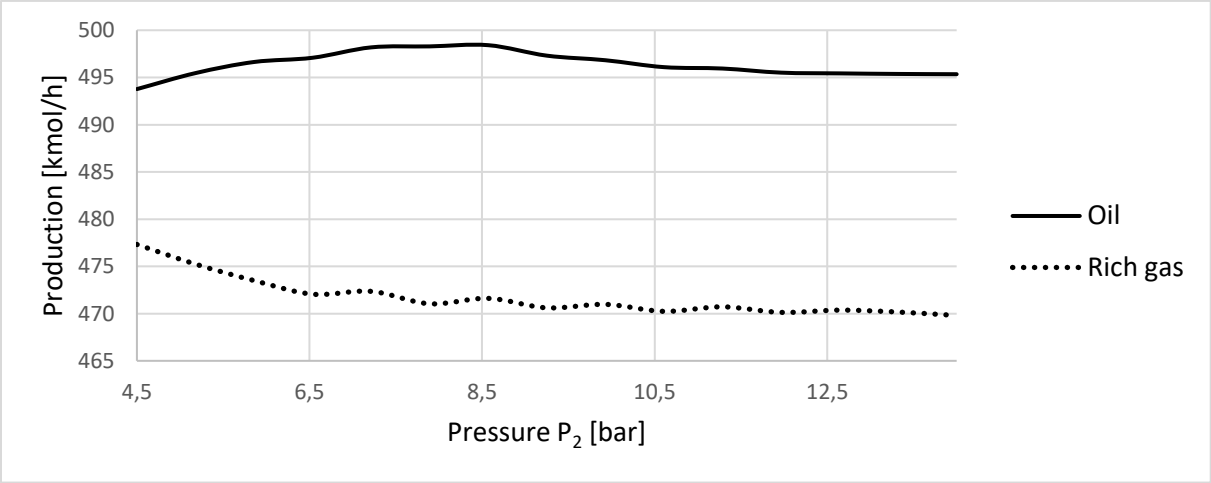

Figure 31: influence of P_2 on production rates

A2.2 Condensate stabilization unit: third level of pressure P_3

With P_2 = 9.5 bar, $T_1 = T_2 = T_f = T_d$ = 30°C, T_h = 80°C.

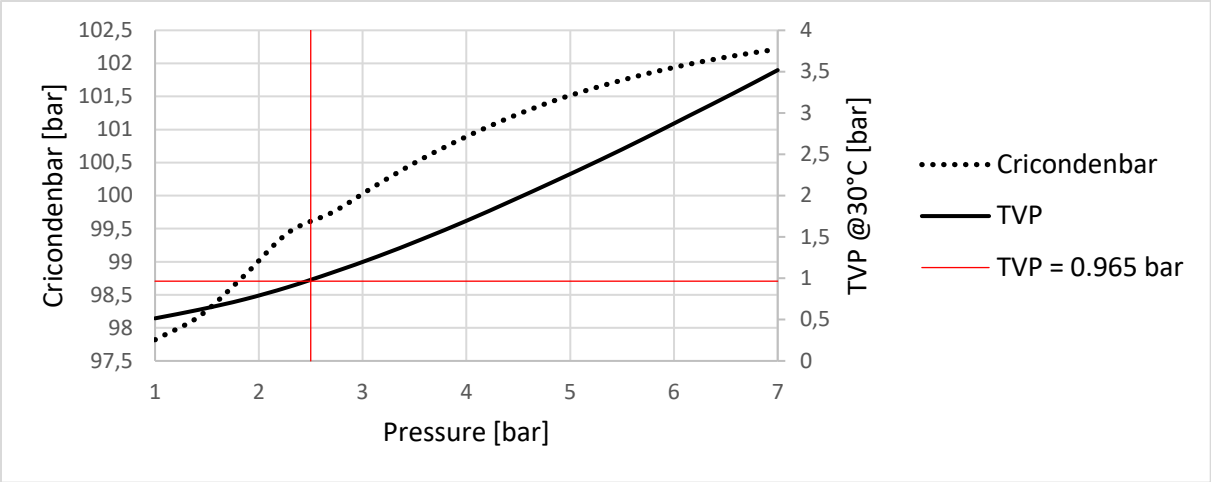

Figure 32: influence of P_3 on specifications

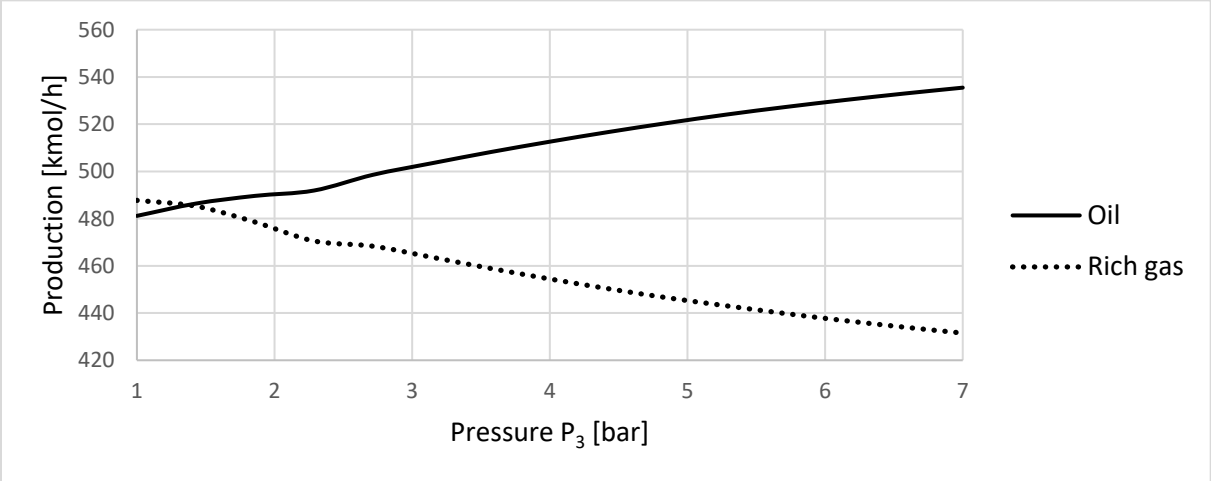

Figure 33: influence of P_3 on production rates

A2.3 Condensate stabilization unit: heater temperature T_h

With P_2 = 9.5 bar, P_3 = 2.56 bar, $T_1 = T_2 = T_f = T_d$ = 30°C.

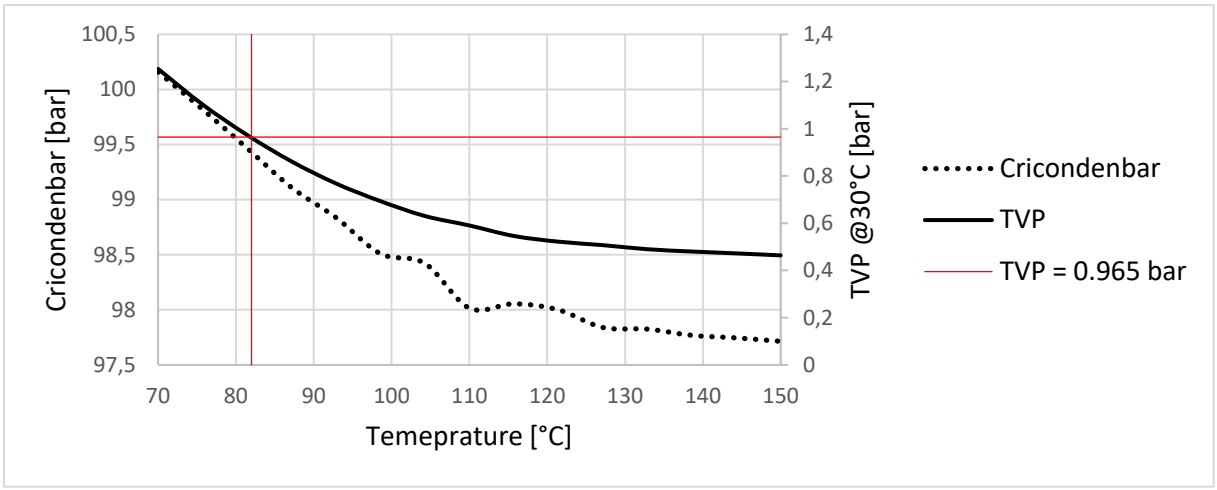

Figure 34: influence of T_h on specifications

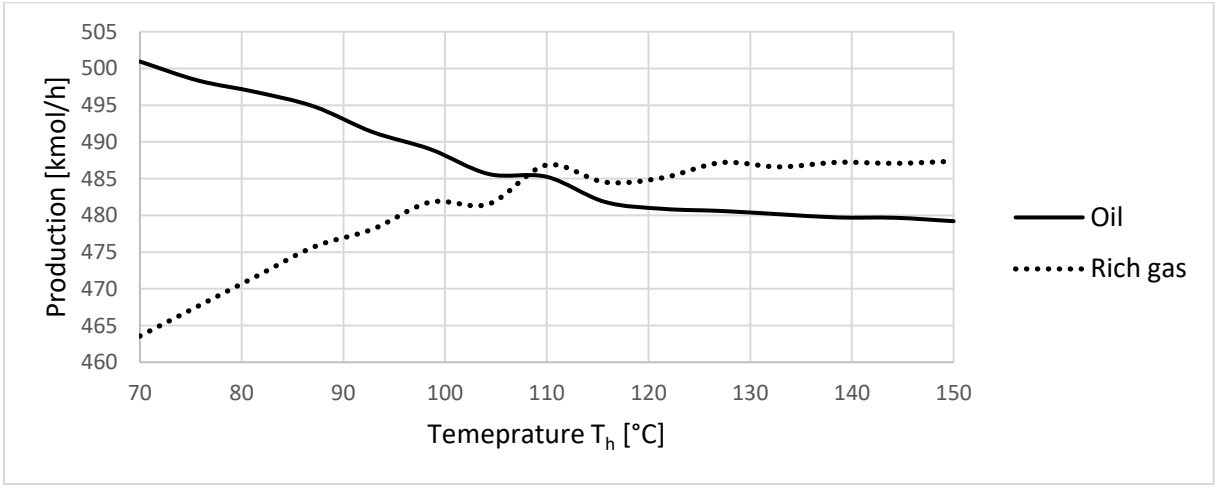

Figure 35: influence of T_h on production rates

A2.4 Gas recompression train: first cooler temperature T_1

With P_2 = 9.5 bar, P_3 = 2.56 bar, $T_2 = T_f = T_d$ = 30°C, T_h = 80°C.

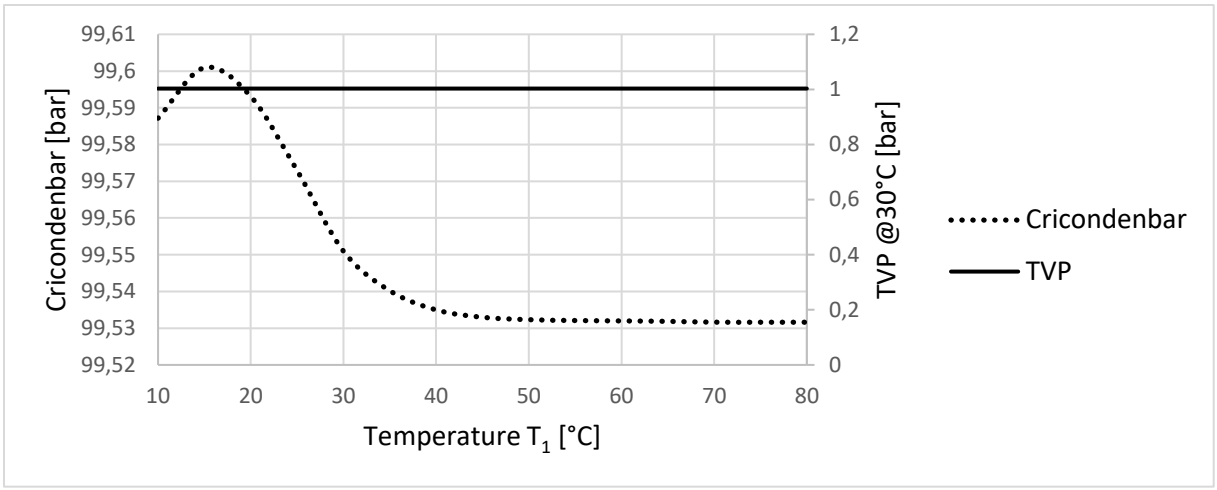

Figure 36: influence of T_1 on specifications

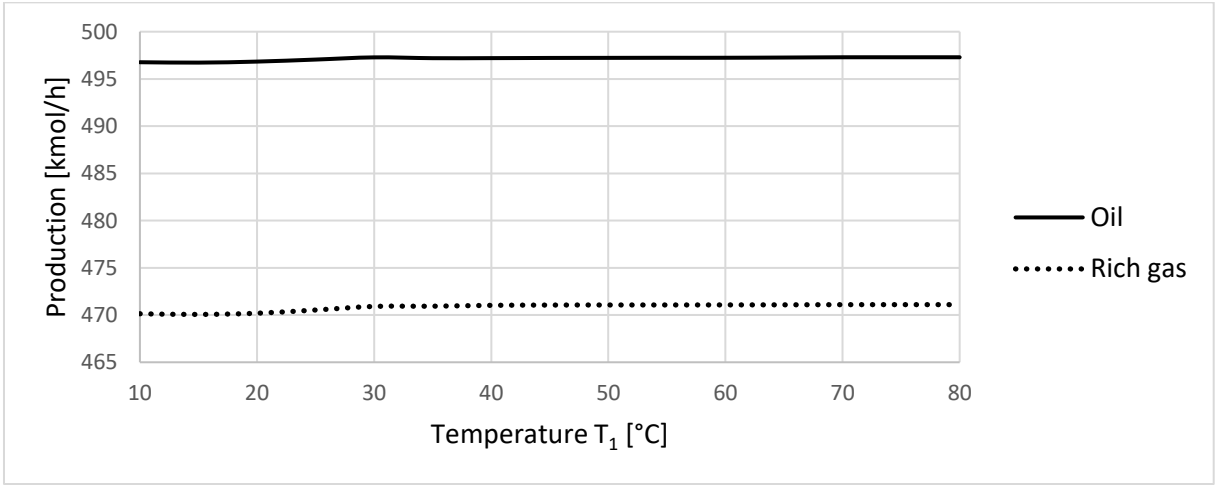

Figure 37: influence of T_1 on production rates

A2.5 Gas recompression train: second cooler temperature T_2

With P_2 = 9.5 bar, P_3 = 2.56 bar, $T_1 = T_f = T_d$ = 30°C, T_h = 80°C.

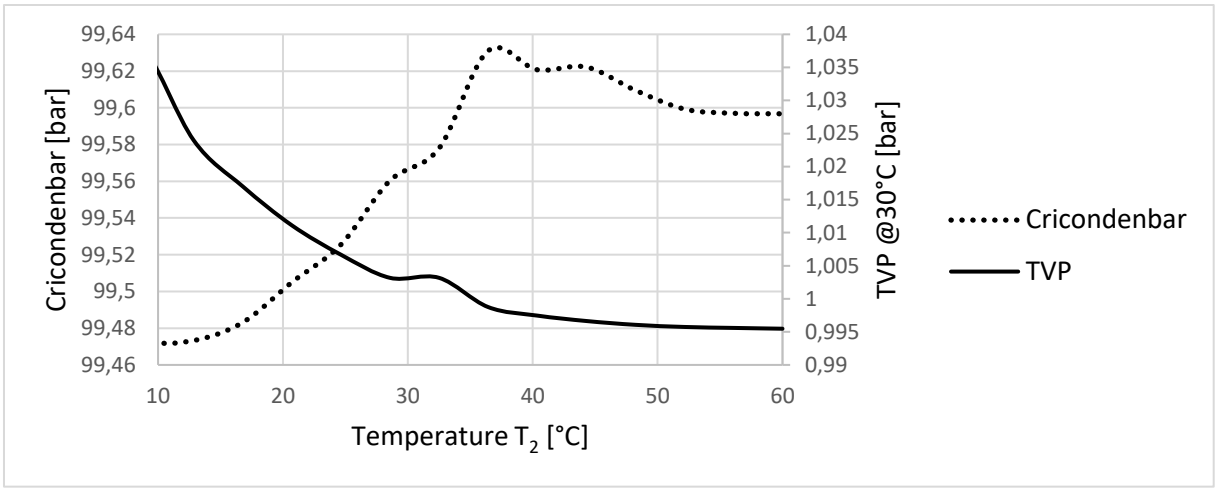

Figure 38: influence of T_2 on specifications

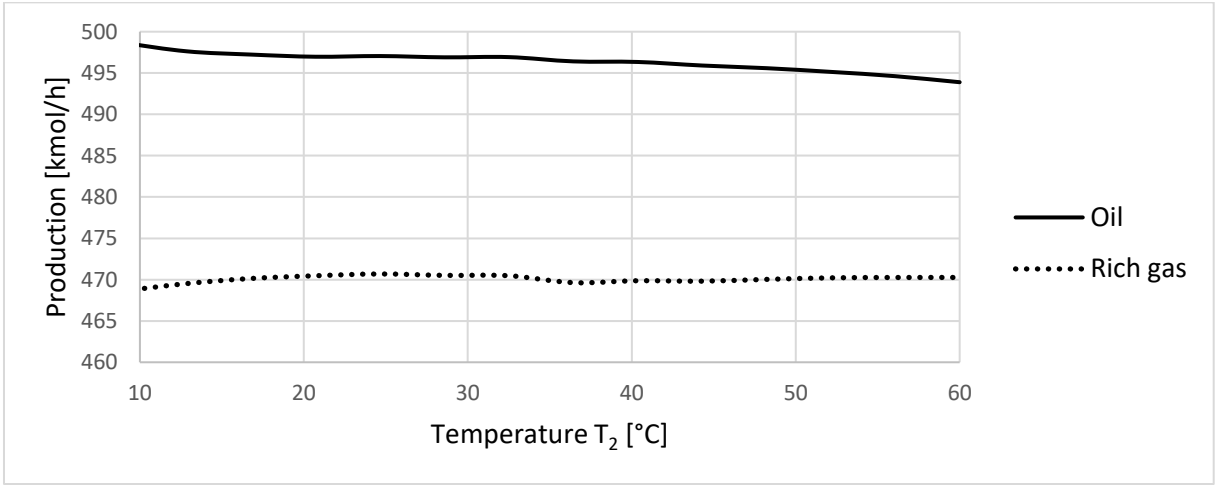

Figure 39: influence of T_2 on production rates

A2.6 Gas processing: feed gas cooler temperature T_f

With P_2 = 9.5 bar, P_3 = 2.56 bar, $T_1 = T_2 = T_d$ = 30°C, T_h = 80°C.

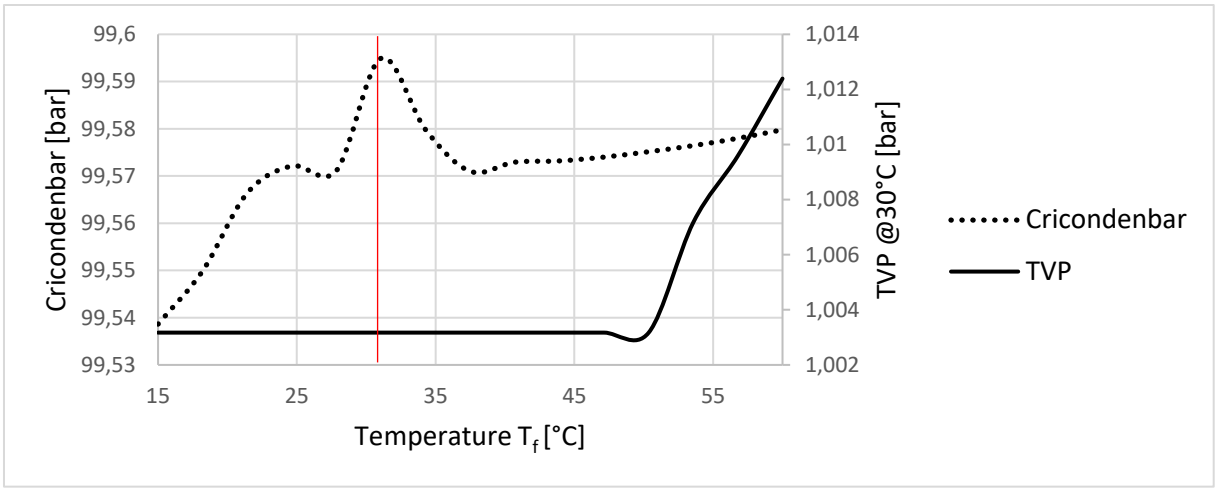

Figure 40: influence of T_f on specifications

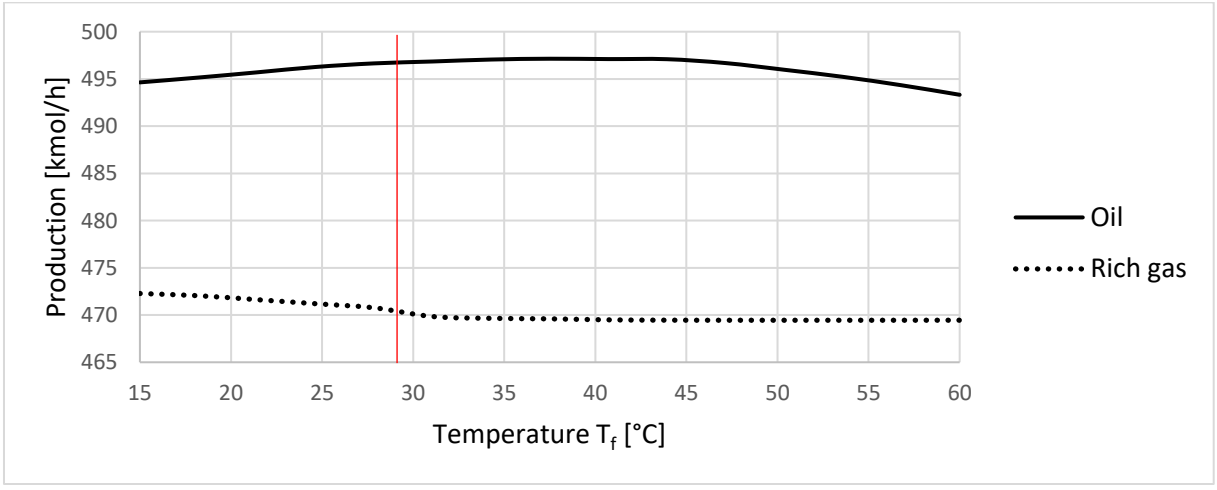

Figure 41: influence of T_f on production rates

A2.7 Gas processing: temperature before dehydration T_d

With P_2 = 9.5 bar, P_3 = 2.56 bar, $T_1 = T_2 = T_f$ = 30°C, T_h = 80°C.

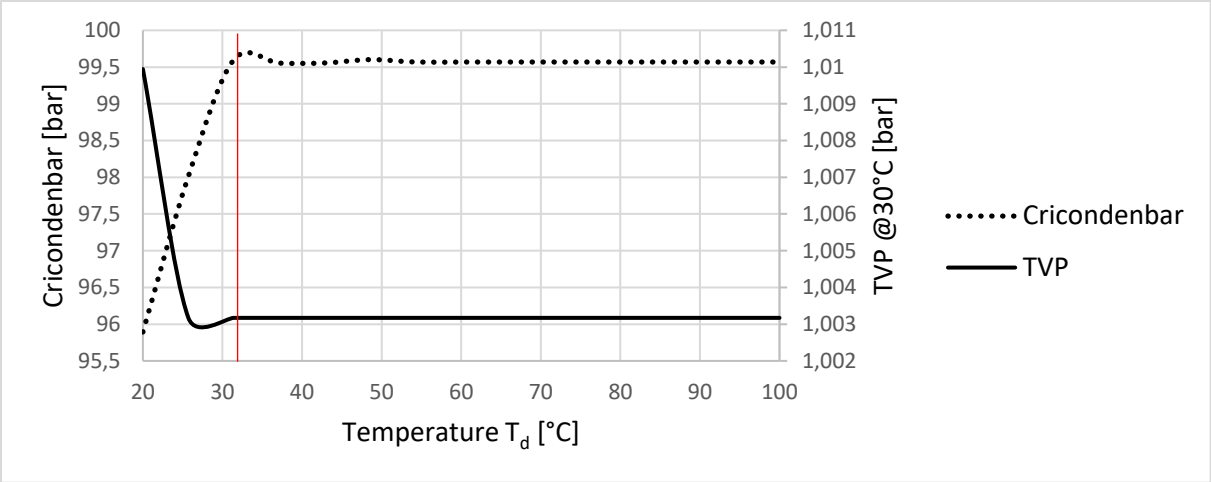

Figure 42: influence of T_d on specifications

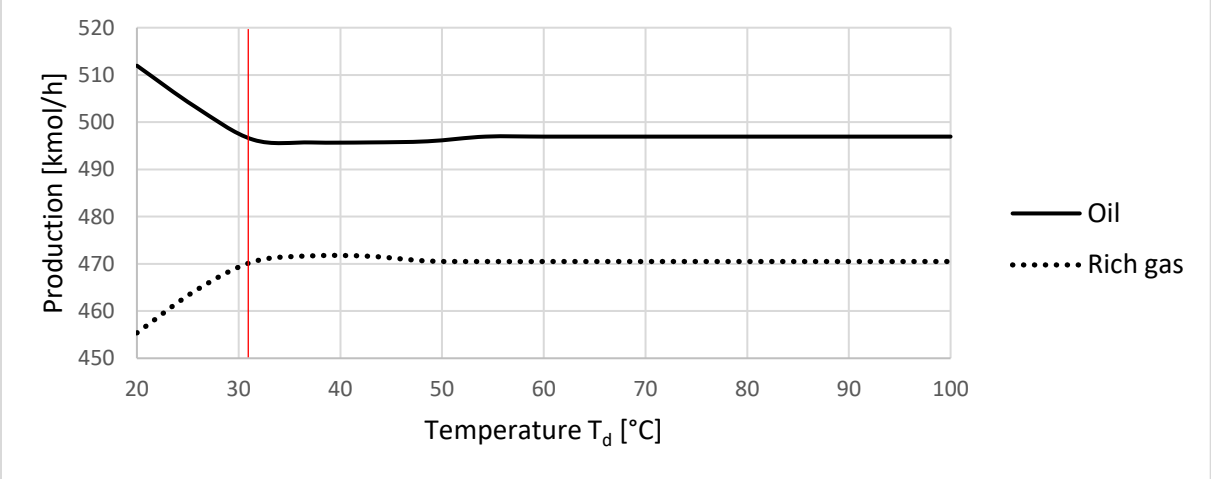

Figure 43: influence of T_d on production rates

Appendix 3: rich gas production maximisation

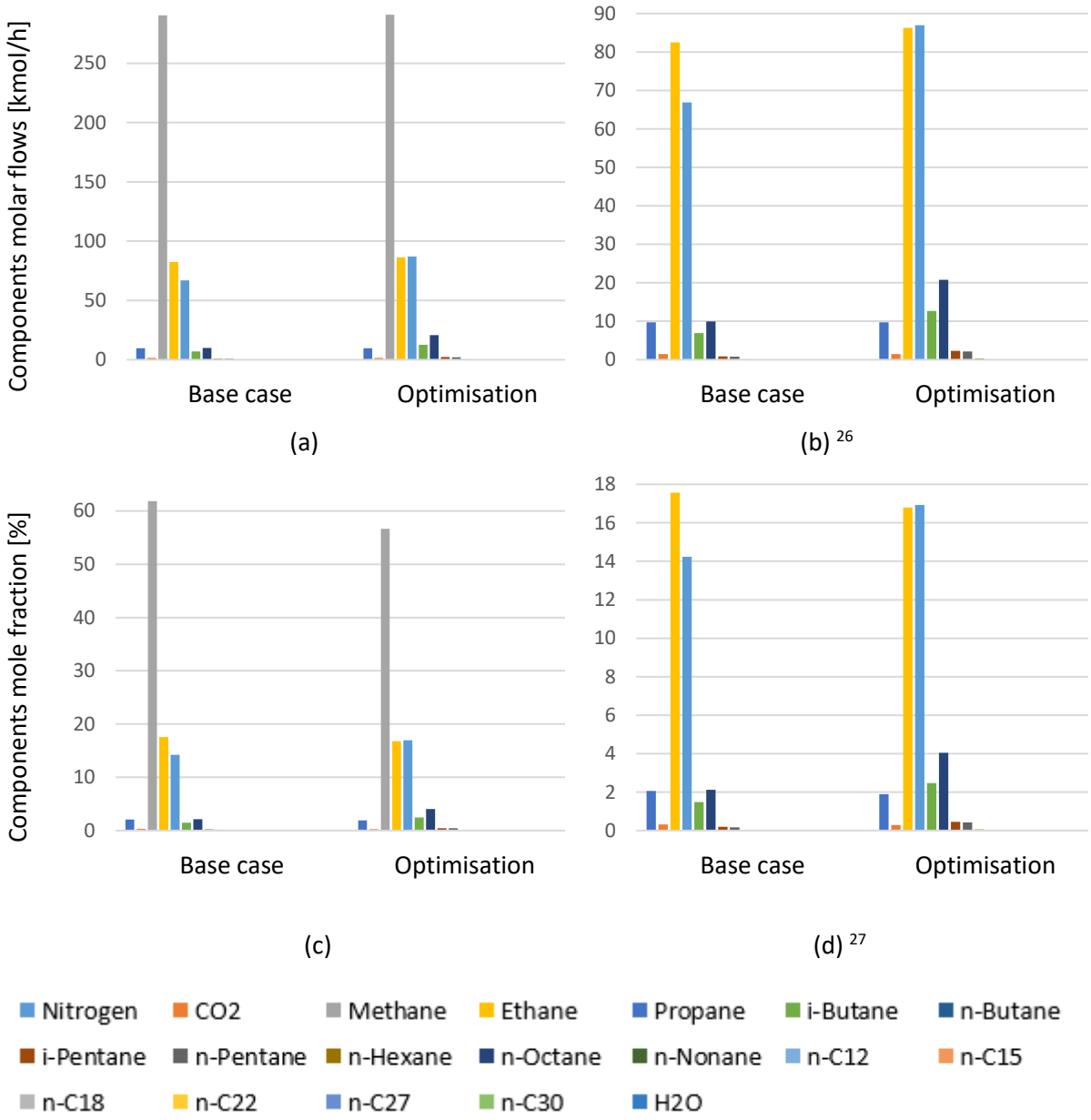

Figure 44: rich gas components behaviour with production maximisation

[26] The figure (b) is the same as the figure (a) except that methane behaviour is not represented to have a better view of the other components.

[27] The figure (d) is the same as the figure (c) except that methane behaviour is not represented to have a better view of the other components.

Appendix 4: energy consumption – parametric studies

A4.1 Condensate stabilization unit: second level of pressure P_2

With P_3 = 2.56 bar, $T_1 = T_2 = T_f = T_d$ = 30°C, T_h = 82°C.

Units	Name	P_2 ↘	Power variation [kW]
pumps	p-1	↗	0.339
	p-2	↘	0.003
compressors	C_1	↘	224.5
	C_2	↗	419.5
	C_3	↗	171.0
	C_4	↗	3.220
heater	heater	↗	1 379

Table 29: influence of P_2 reduction on energy consumption

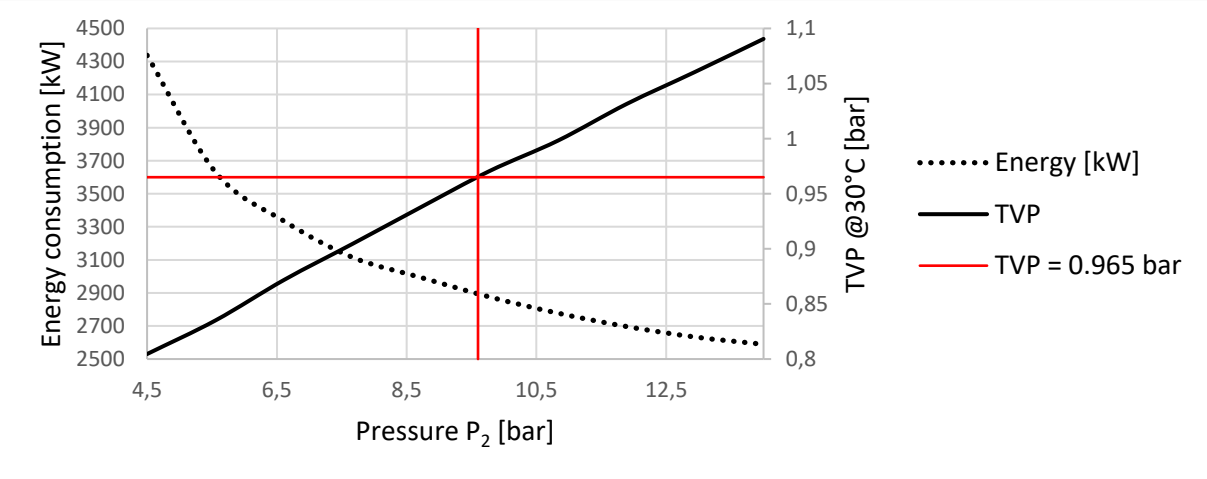

Figure 45: new P_2 for energy consumption minimisation

A4.2 Condensate stabilization unit: third level of pressure P_3

With P_2 = 9.5 bar, $T_1 = T_2 = T_f = T_d$ = 30°C, T_h = 82°C.

Units	Name	P_3 ↘	Power variation [kW]
pumps	p-1	↗	29.28
	p-2	↗	0.006
compressors	C_1	↗	726.7
	C_2	↗	147.0
	C_3	↗	451.8
	C_4	↗	35.30
heater	heater	↗	1 201

Table 30: influence of P_3 reduction on energy consumption

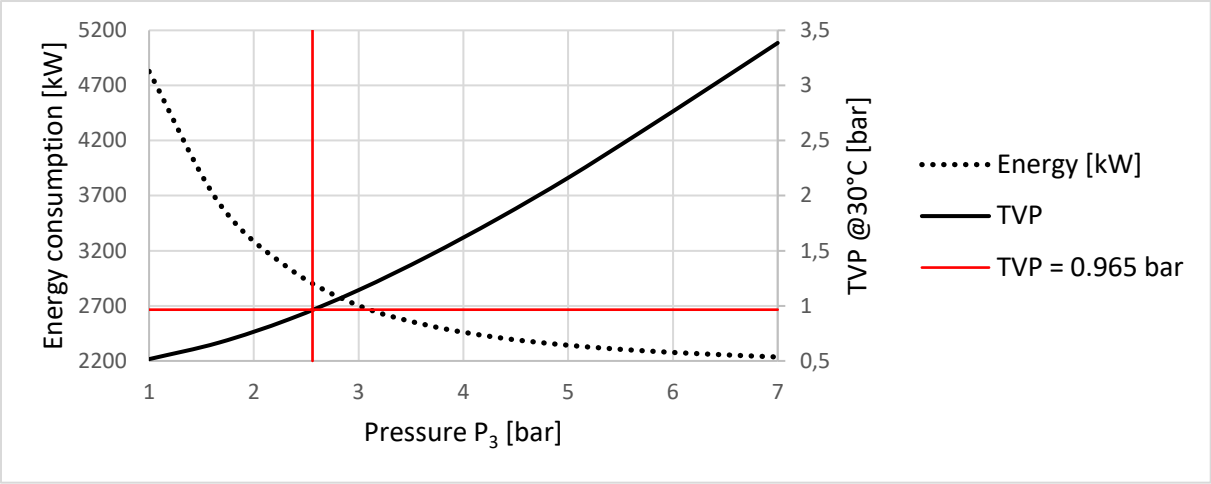

Figure 46: new P_3 for energy consumption minimisation

A4.3 Condensate stabilization unit: heater temperature T_h

With P_2 = 9.5 bar, P_3 = 2.56 bar, $T_1 = T_2 = T_f = T_d$ = 30°C.

Units	Name	T_h ↗	Power variation [kW]
pumps	p-1	↗	0.903
	p-2	↗	0.070
compressors	C_1	↗	268.1
	C_2	↗	121.3
	C_3	↗	404.0
	C_4	↗	15.28
heater	heater	↗	8 648

Table 31: influence of T_h increase on energy consumption

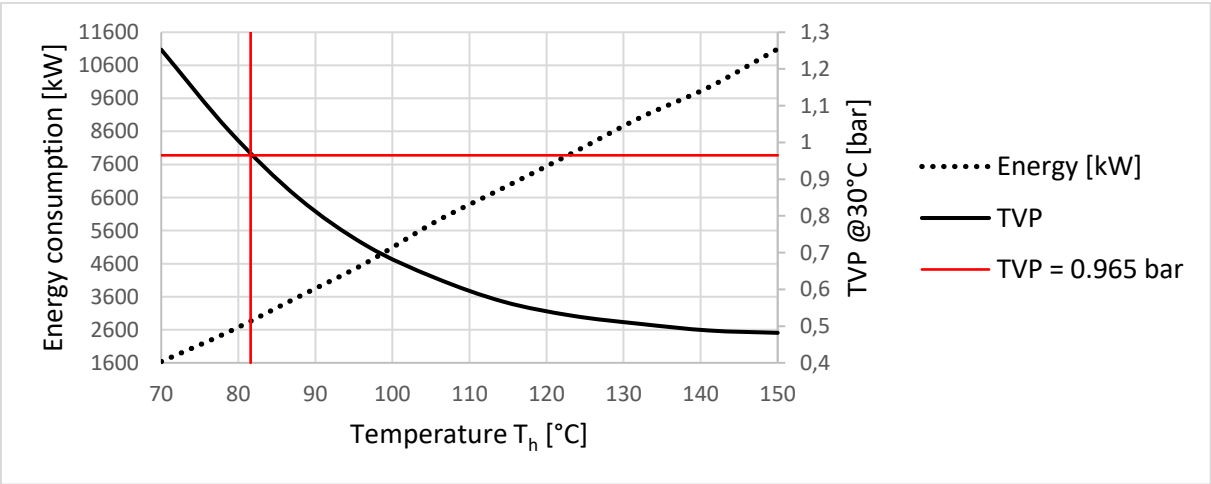

Figure 47: new T_h for energy consumption minimisation

A4.2 Gas recompression train: first cooler temperature T_1

With P_2 = 9.5 bar, P_3 = 2.56 bar, $T_2 = T_f = T_d$ = 30°C, T_h = 82°C.

Units	Name	T_1 ↘	Power variation [kW]
pumps	p-1	↘	0.026
	p-2	↗	0.008
compressors	C_1	↘	48.24
	C_2	↗	0.455
	C_3	↗	0.486
	C_4	↘	0.986
heater	heater	↗	0.193

Table 32: influence of T_1 reduction on energy consumption

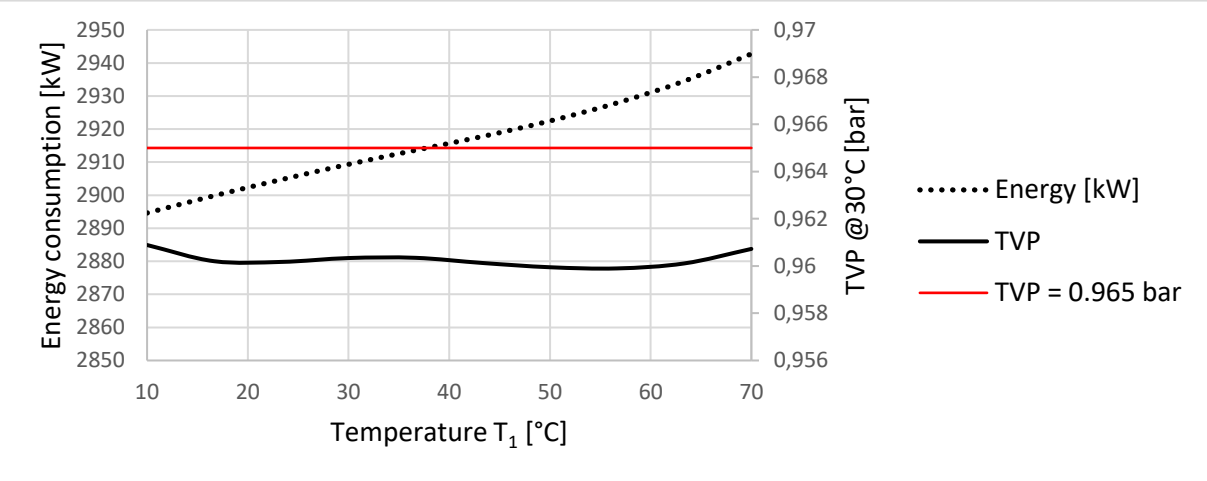

Figure 48: new T_1 for energy consumption minimisation

A4.5 Gas recompression train: second cooler temperature T_2

With P_2 = 9.5 bar, P_3 = 2.56 bar, $T_1 = T_f = T_d$ = 30°C, T_h = 82°C.

Units	Name	T_2 ↘	Power variation [kW]
pumps	p-1	↗	0.008
	p-2	↘	$2x10^{-4}$
compressors	C_1	↗	14.60
	C_2	↘	61.75
	C_3	↘	105.8
	C_4	↗	1.193
heater	heater	↘	336.9

Table 33: influence of T_2 reduction on energy consumption

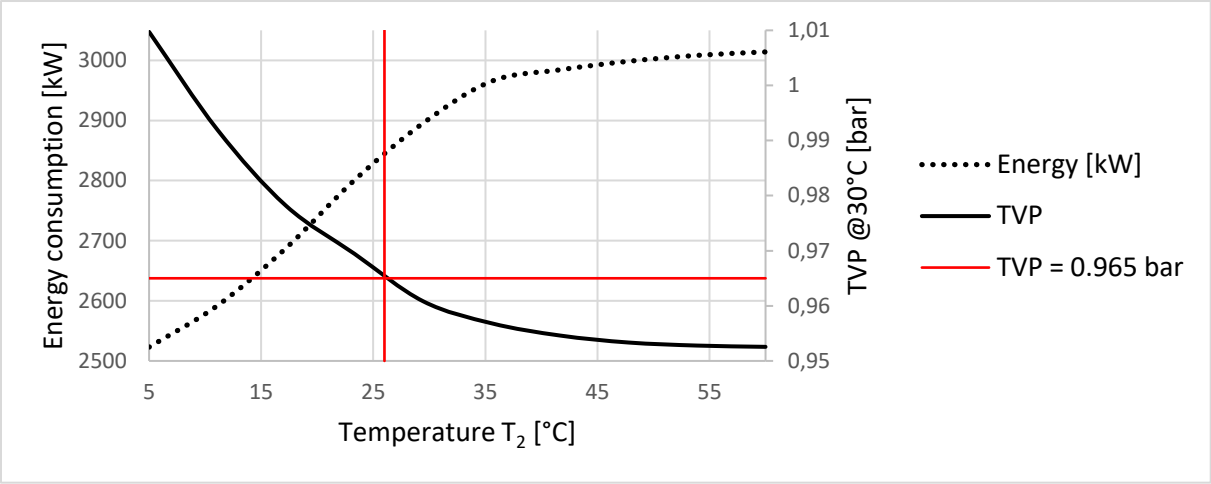

Figure 49: new T_2 for energy consumption minimisation

A4.6 Gas processing: feed gas cooler temperature T_f

With P_2 = 9.5 bar, P_3 = 2.56 bar, $T_1 = T_2 = T_d$ = 30°C, T_h = 82°C.

Units	Name	T_f ↘	Power variation [kW]
pumps	p-1	↗	0.002
	p-2	↘	$9.5x10^{-4}$
compressors	C_1	↘	10.47
	C_2	↘	5.315
	C_3	↘	208.7
	C_4	↗	0.973
heater	heater	↘	42.29

Table 34: influence of the T_f reduction on energy consumption

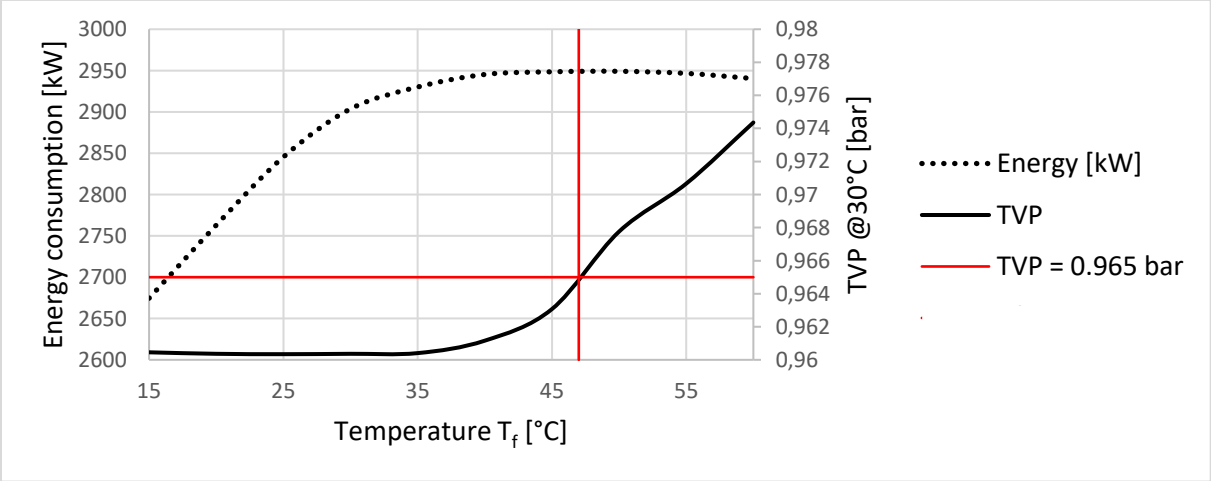

Figure 50: new T_f for energy consumption minimisation

A4.7 Gas processing: temperature before dehydration T_d

With P_2 = 9.5 bar, P_3 = 2.56 bar, $T_1 = T_2 = T_f$ = 30°C, T_h = 82°C.

Units	Name	T_d ↘	Power variation [kW]
pumps	p-1	↗	1.018
	p-2	↗	0.001
compressors	C_1	↗	60.91
	C_2	↗	68.30
	C_3	↗	328.8
	C_4	↘	259.4
heater	heater	↗	1 075

Table 35: influence of T_d on energy consumption

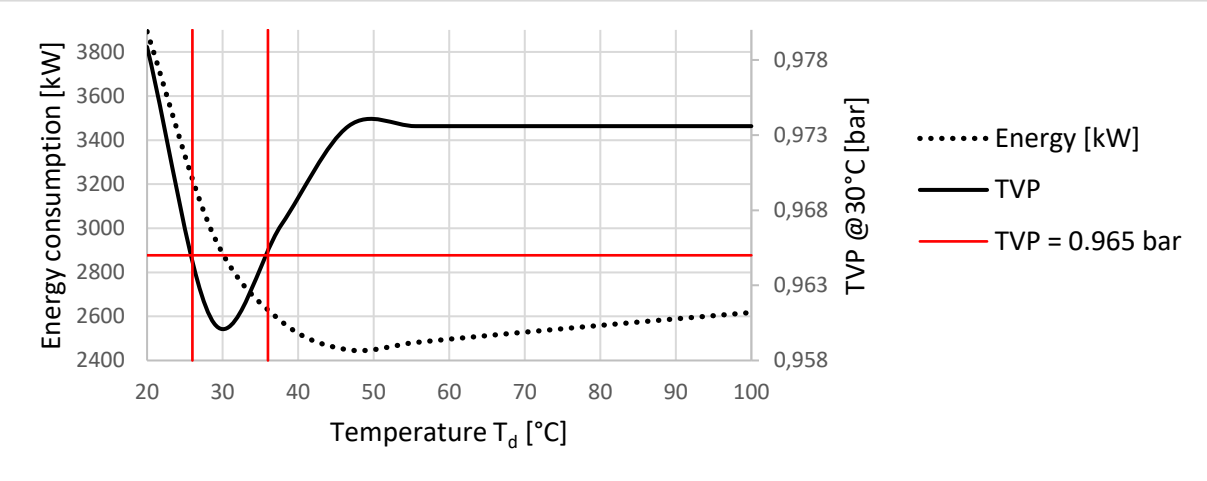

Figure 51: new T_d for energy consumption minimisation

Appendix 5: energy consumption minimisation

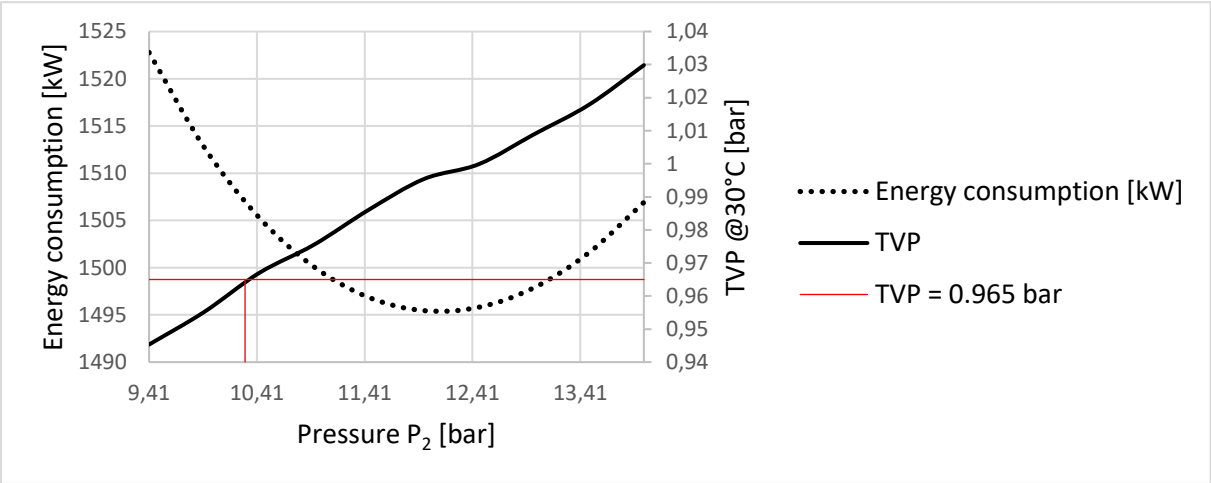

Figure 52: P_2 influence on TVP and energy consumption

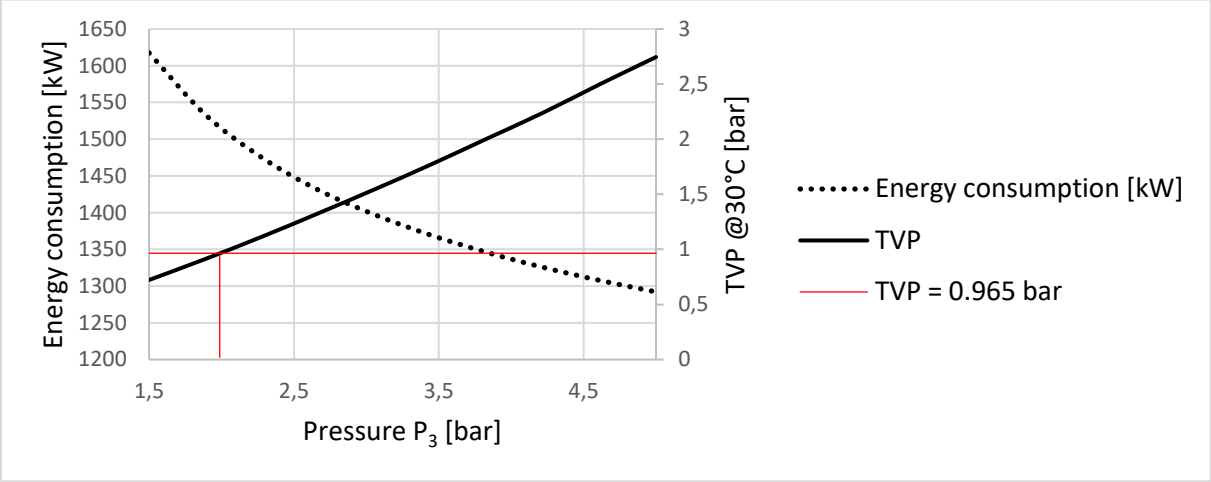

Figure 53: P_3 influence on TVP and energy consumption

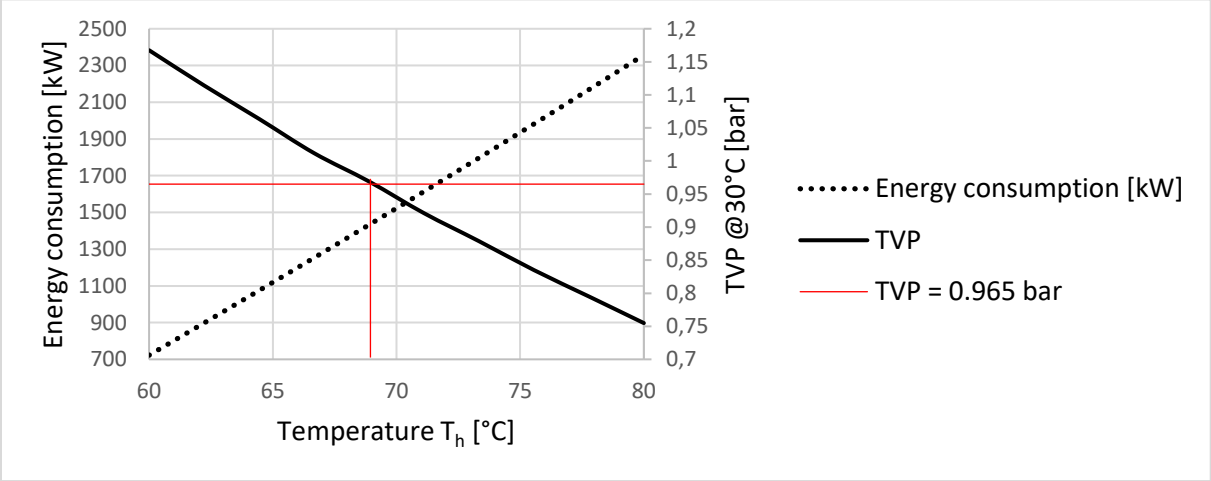

Figure 54: T_h influence on TVP and energy consumption

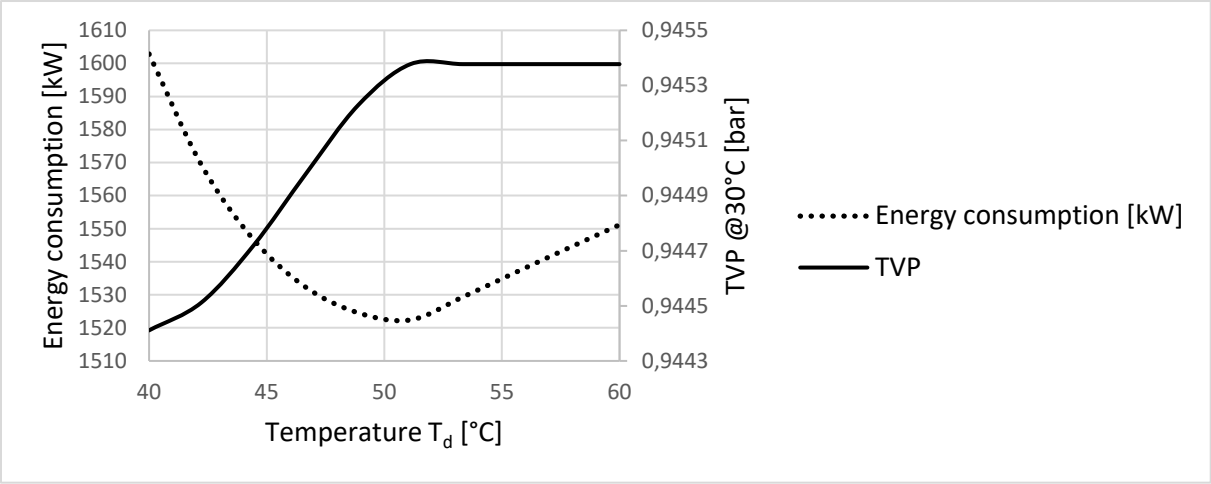

Figure 55: T_d influence on TVP and energy consumption

Appendix 6: energy consumption distribution

	P_2 [bar]	P_3 [bar]	T_h [°C]	T_1 [°C]	T_2 [°C]	T_f [°C]	T_d [°C]
(a)	9.50	2.56	82	30	30	30	30
(b)	9.41	1.95	70	30	30	30	50
(c)	10.3	1.95	70	30	30	30	50
(d)	9.41	1.98	70	30	30	30	50
(e)	9.41	1.95	69.1	30	30	30	50
(f)	9.43	1.95	69.1	30	30	30	50
(g)	9.41	1.95	70	26	25	13	50
(h)	9.41	1.95	70	5	25	13	50
(i)	9.41	1.95	70	26	8.3	13	50
(j)	9.41	1.95	70	26	25	11	50

Table 36: process parameters for energy optimisation

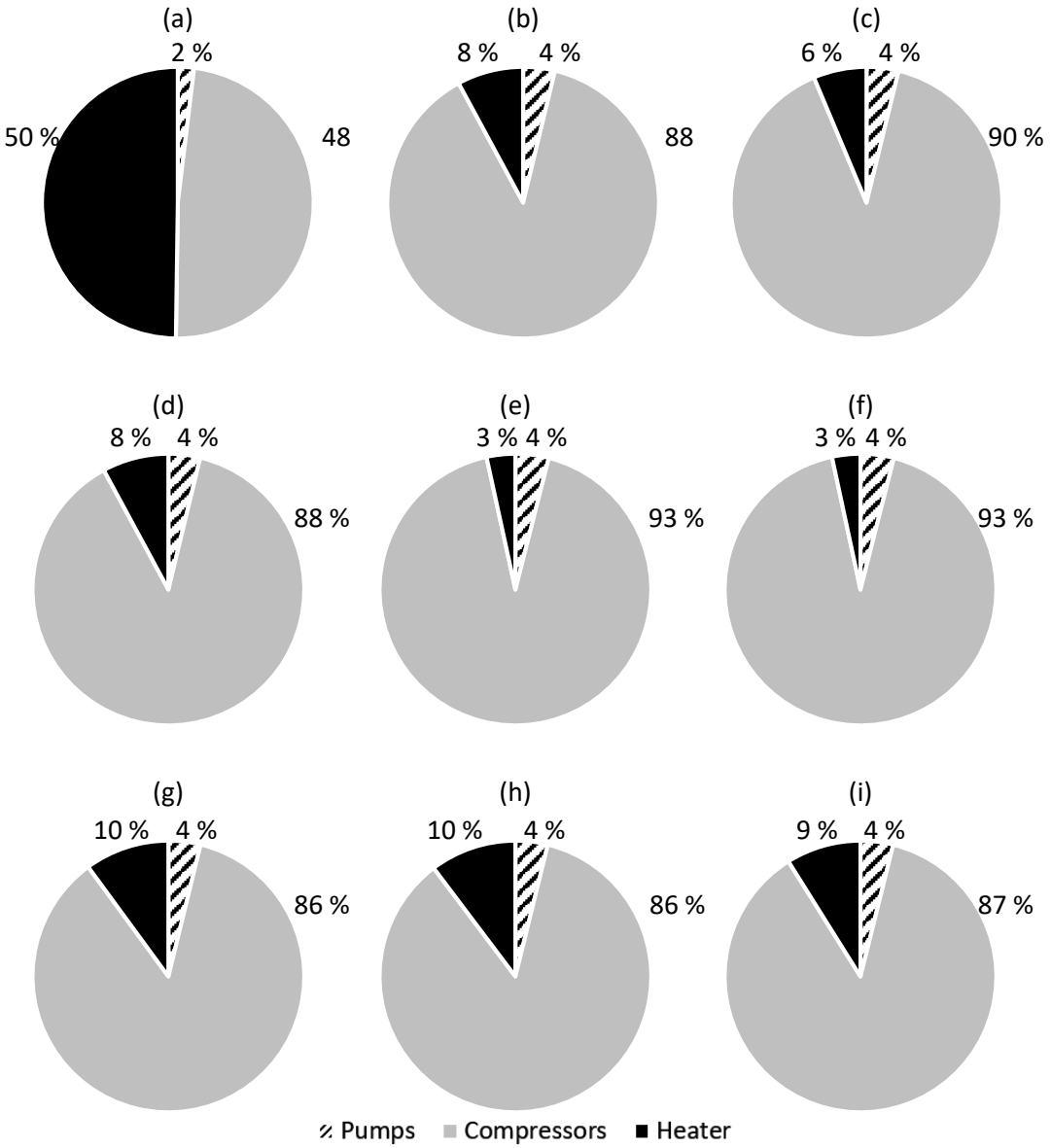

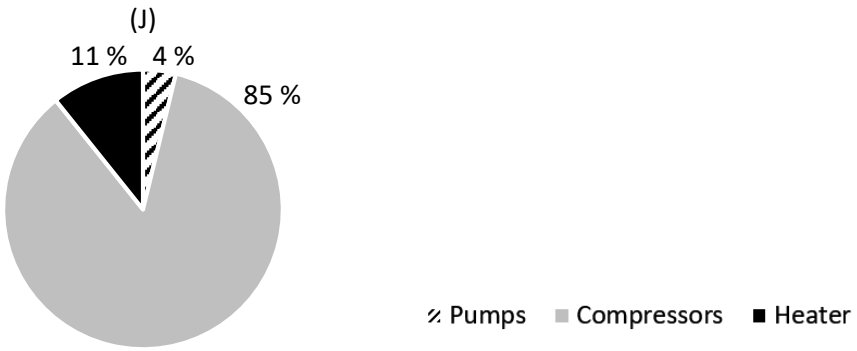

Figure 56: energy consumption distribution for the different optimisations

Appendix 7: heat integration of the base case model

Step 1: identify the hot and cold streams

Same as *Figure 20*.

Step 2: levels of temperature

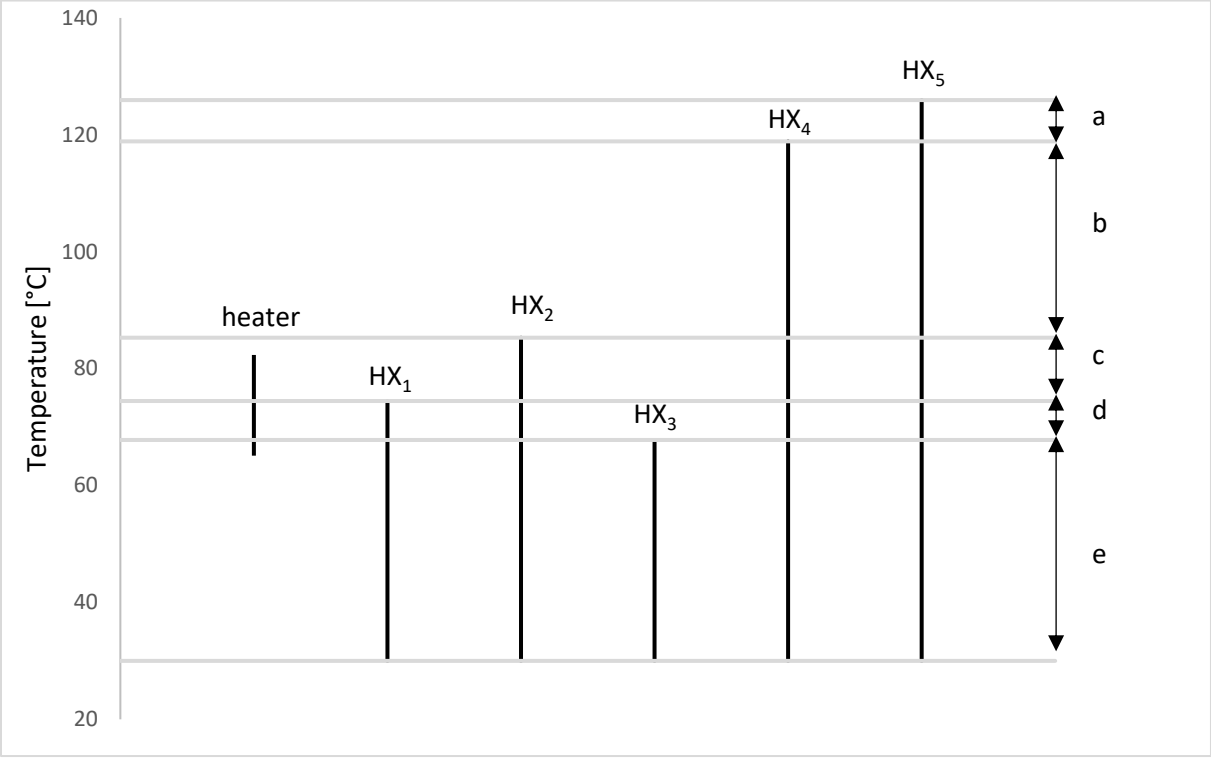

Figure 57: temperature levels in the base case model

Step 3: energy consumption

	$\dot{Q}$ [kW]	T_{in} [°C]	T_{out} [°C]	$\dot{m} * \overline{C_p}$ [kW/°C]
heater	1 442	65.4	82.0	87.2
HX_1	- 253.8	74.5	30.0	5.71
HX_2	- 324.4	85.3	30.0	5.87
HX_3	- 470.8	67.8	30.0	12.46
HX_4	- 1 346	119	30.0	15.15
HX_5	- 1 025	126	30.0	10.69

Table 37: power consumption in heat exchangers in the base case model

		$\dot{m} * \overline{C_p}$ **to consider**	$\dot{Q}$ [KW]
Cold stream		$(\dot{m} * \overline{C_p})_{heater}$	1 442
Hot streams	a	$(\dot{m} * \overline{C_p})_{HX5}$	75.51
	b	$(\dot{m} * \overline{C_p})_{HX4} + (\dot{m} * \overline{C_p})_{HX5}$	867.6
	c	$(\dot{m} * \overline{C_p})_{HX2} + (\dot{m} * \overline{C_p})_{HX4} + (\dot{m} * \overline{C_p})_{HX5}$	343.5
	d	$(\dot{m} * \overline{C_p})_{HX1} + (\dot{m} * \overline{C_p})_{HX2} + (\dot{m} * \overline{C_p})_{HX4} + (\dot{m} * \overline{C_p})_{HX5}$	249.3
	e	$(\dot{m} * \overline{C_p})_{HX1} + (\dot{m} * \overline{C_p})_{HX2} + (\dot{m} * \overline{C_p})_{HX3} + (\dot{m} * \overline{C_p})_{HX4} + (\dot{m} * \overline{C_p})_{HX5}$	1 885

Table 38: power consumption in each part of the composite curves in the base case model

Step 4: pinch analysis

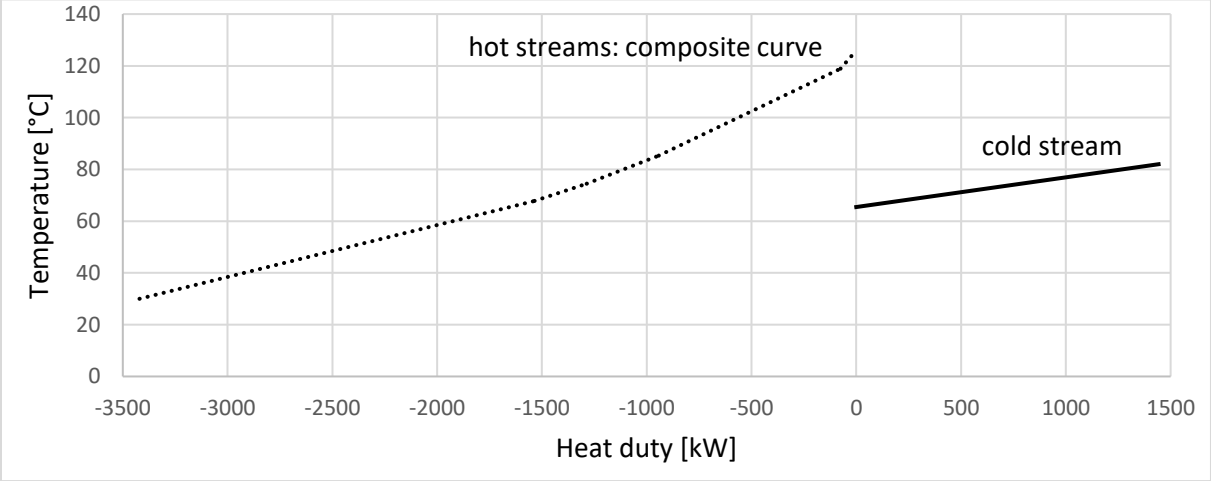

Figure 58: composite curves for the base case model

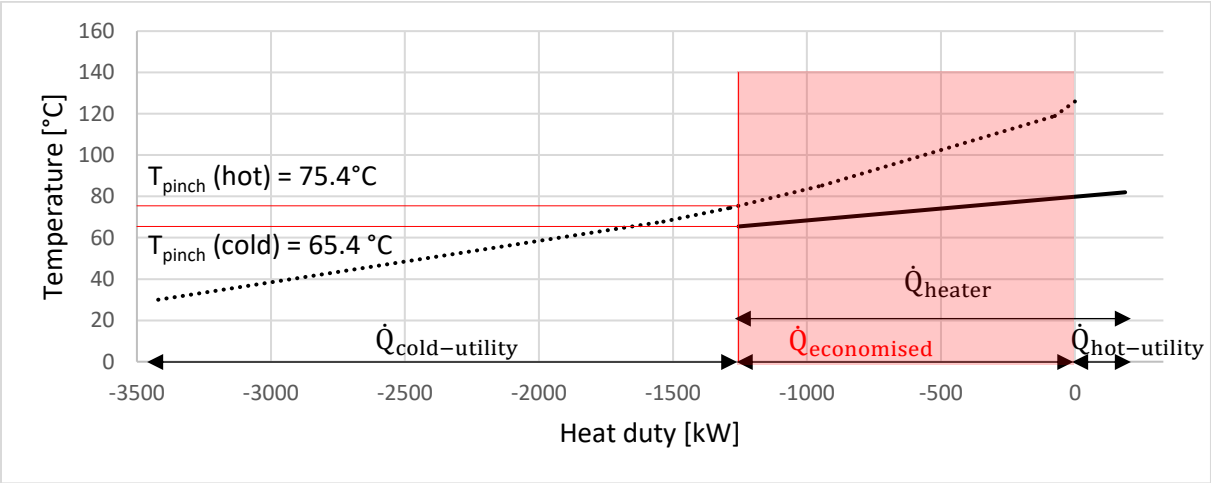

Figure 59: pinch identification for the base case model

In comparison with the optimized model (*Figure 23*), the utilization of hot streams is not sufficient to heat the cold stream until 82°C. Hence, hot utility is required.

$\dot{Q}_{cold-utility}$	$\dot{Q}_{economised}$	$\dot{Q}_{hot-utility}$
2 166 kW	1 255 kW	187.4 kW

Table 39: minimum heat duty consumption in the base case model

Step 5: new network of heat exchangers

Three hot streams can be used to heat the cold one: from the coolers HX_2, HX_4 and HX_5. The way to combine streams has an influence on the amount of energy that can be saved. Using the stream from HX_2, then the one from HX_4 and finally the one from HX_5 is the best combination to save energy. With this combination, 284 kW of hot utility are required to heat the condensate from 78.7°C to 82°C.

Network	$\dot{Q}_{economised}$ [kW]
$HX_2/HX_4/HX_5$	1 159
$HX_2/HX_5/HX_4$	1 145
$HX_4/HX_2/HX_5$	1 129
$HX_5/HX_2/HX_4$	1 121
HX_4/HX_5	1 117
HX_5/HX_4	1 104

Table 40: new network of heat exchangers for the base case model

The following figure is a representation of how fluids are combined with the new temperature levels.

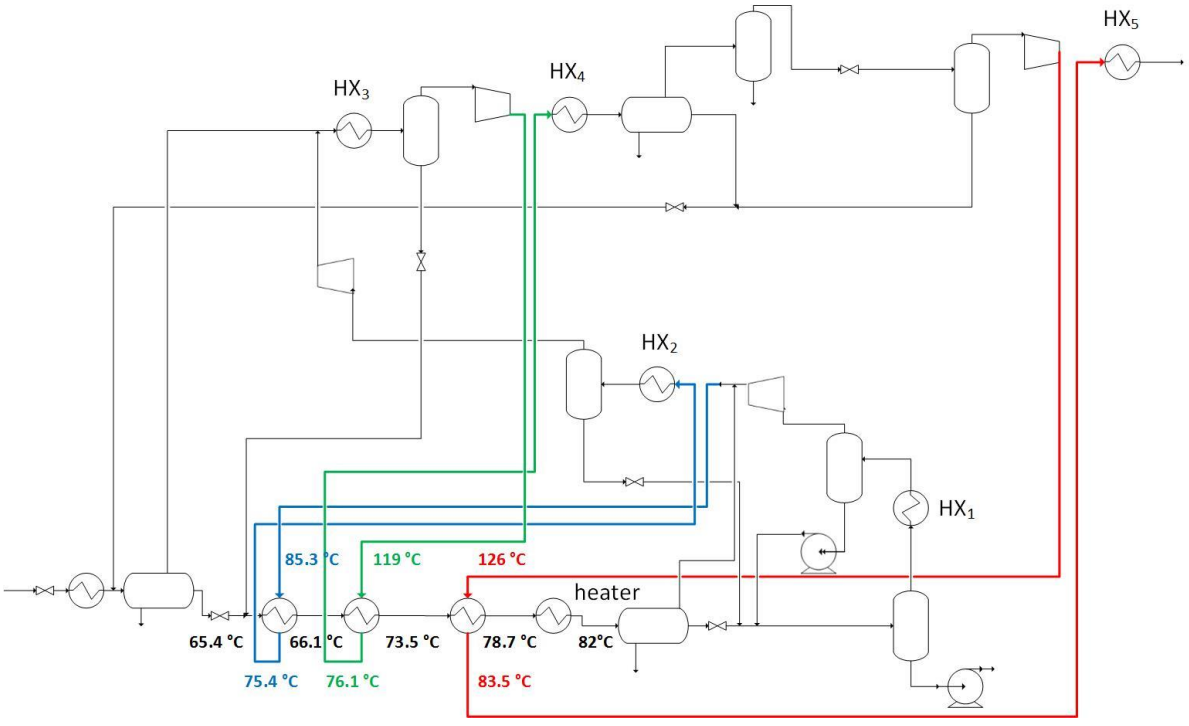

Figure 60: base case model with heat integration

Appendix 8: recirculation studies

In green is identified the minimum value of the total energy consumption of the process. In red is underlines the specifications that are not met.

Numerical values are obtained with the process parameters from the base case meaning P_2 = 9.5 bar, P_3 = 2.56 bar, $T_1 = T_2 = T_f = T_d$ = 30°C, T_h = 82°C.

	Total energy consumption [kW]	Cricondenbar [bar]	TVP @30°C [bar]
1st stage	2 750	99.00	1.024
2nd stage (base case)	2 898	98.85	0.9604
3rd stage	2 799	98.85	0.9798

Table 41: influence of the stage where R_1 is sent on energy consumption and specifications

	Total energy consumption [kW]	Cricondenbar [bar]	TVP @30°C [bar]
1st stage (base case)	2 898	98.85	0.9604
2nd stage	3 127	98.94	0.9687
3rd stage	2 804	99.13	1.278

Table 42: influence of the stage where R_2 is sent on energy consumption and specifications

	Total energy consumption [kW]	Cricondenbar [bar]	TVP @30°C [bar]
1st stage	2 856	98.95	1.003
2nd stage	2 859	98.95	1.003
3rd stage (base case)	2 898	98.85	0.9604

Table 43: influence of the stage where R_3 is sent on energy consumption and specifications

	Total energy consumption [kW]	Cricondenbar [bar]	TVP @30°C [bar]
1st stage [28]	2 927	98.88	0.9886
2nd stage [28]	2 912	98.88	0.9890
3rd stage (base case)	2 898	98.85	0.9604

Table 44: influence of the stage where R_4 is sent on energy consumption and specifications

[28] If R_4 is sent to the first or second stage, an additional pump is required. The total energy consumption includes this new pump.

Appendix 9: new process parameters for the recirculation studies

A9.1 Condensate stabilization unit

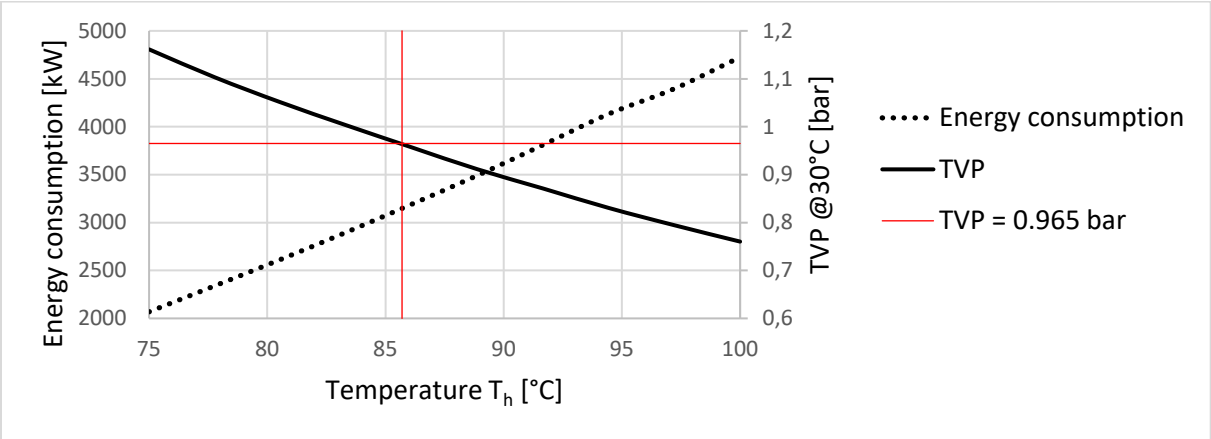

Figure 61: new T_h for recirculation studies [29]

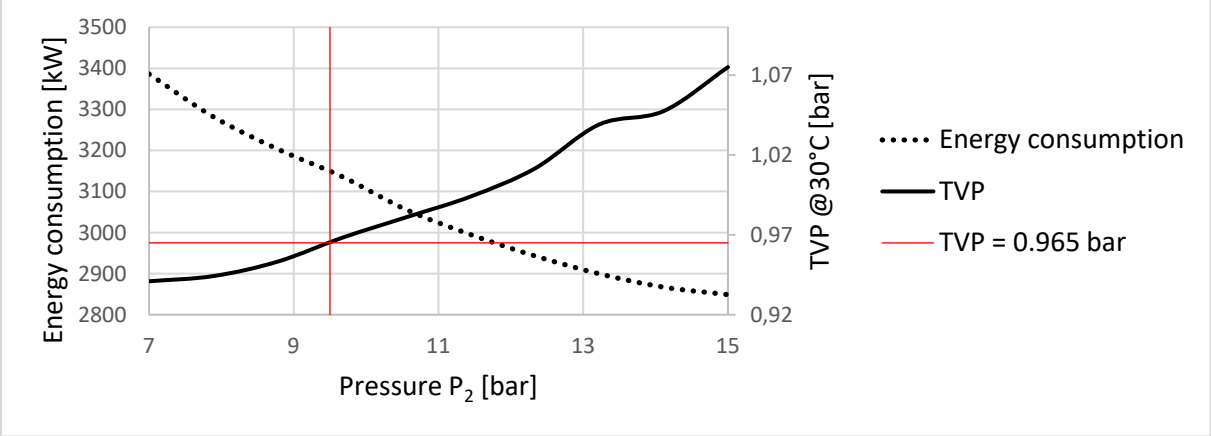

Figure 62: new P_2 for the recirculation studies [30]

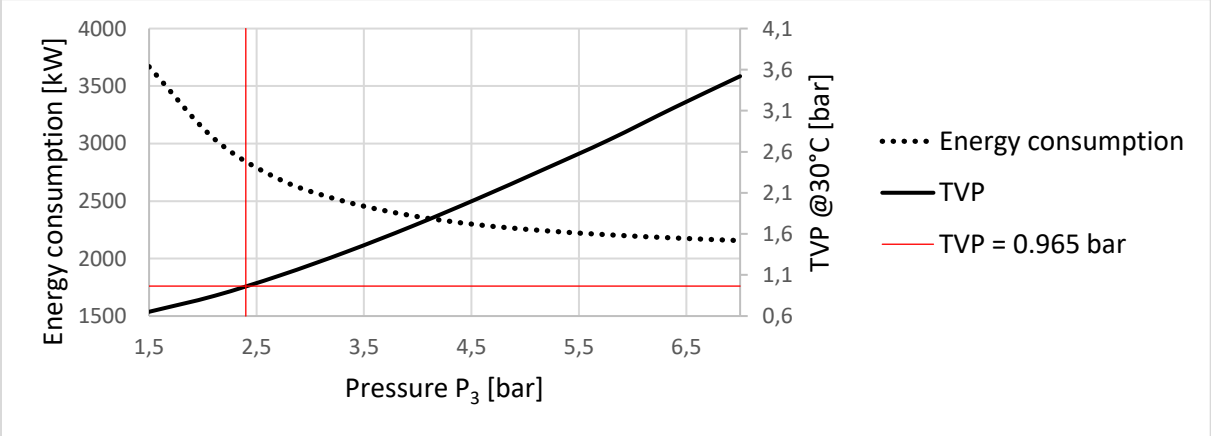

Figure 63: new P_3 for the recirculation studies [31]

[29] P_2 = 9.5 bar, P_3 = 2.56 bar, $T_1 = T_2 = T_f = T_d$ = 30°C
[30] P_3 = 2.56 bar, T_h = 85.7°C, $T_1 = T_2 = T_f = T_d$ = 30°C
[31] P_2 = 9.5 bar, T_h = 82°C, $T_1 = T_2 = T_f = T_d$ = 30°C

A9.2 Gas recompression train

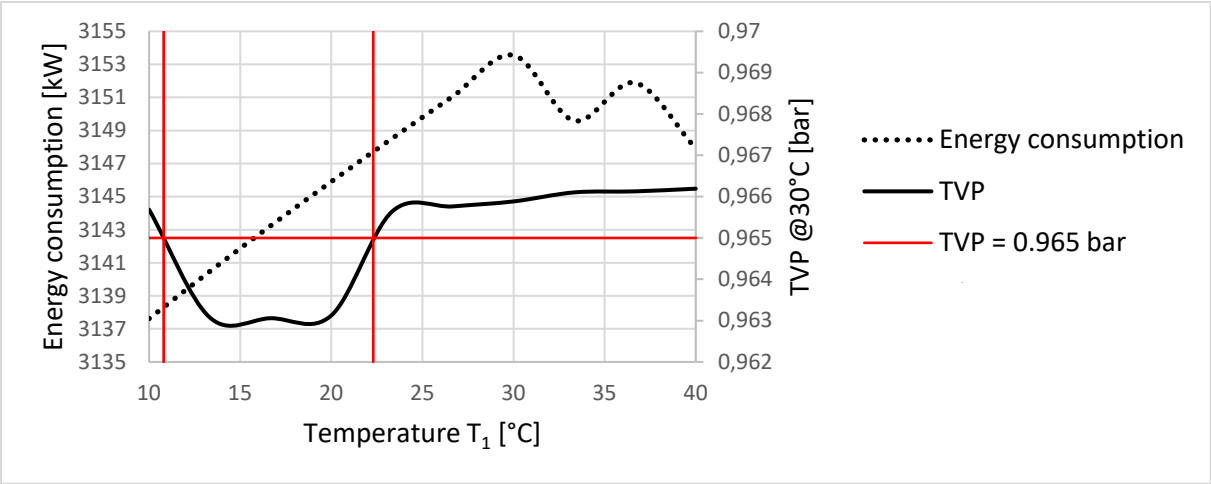

Figure 64: new T_1 for the recirculation studies [32]

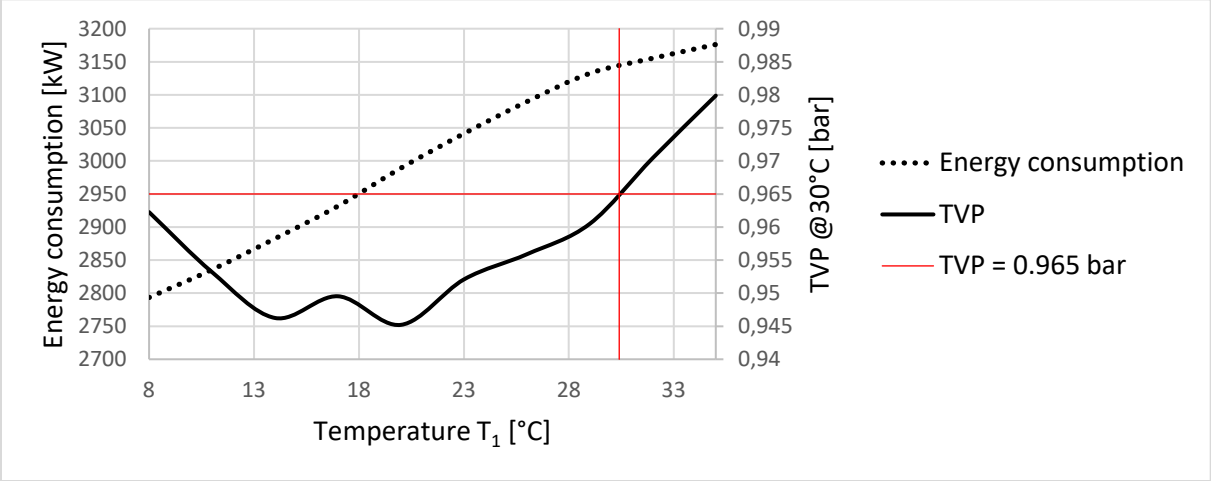

Figure 65: new T_2 for the recirculation studies [33]

[32] P_2 = 9.5 bar, P_3 = 2.56 bar, T_h = 85.7°C, $T_2 = T_f = T_d$ = 30°C
[33] P_2 = 9.5 bar, P_3 = 2.56 bar, T_h = 85.7°C, $T_1 = T_f = T_d$ = 30°C

A9.3 Gas processing

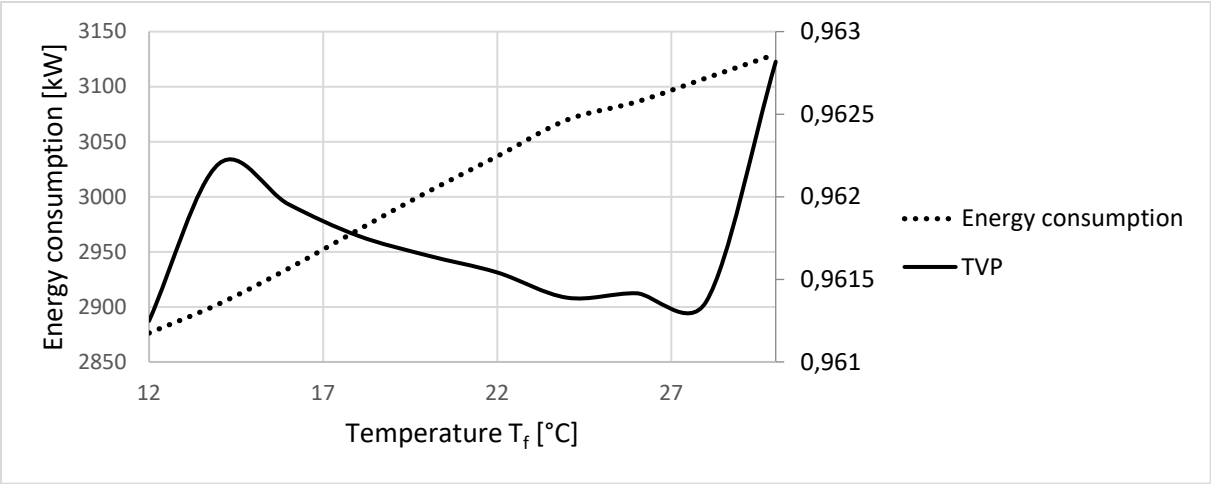

Figure 66: new T_f for the recirculation studies [34]

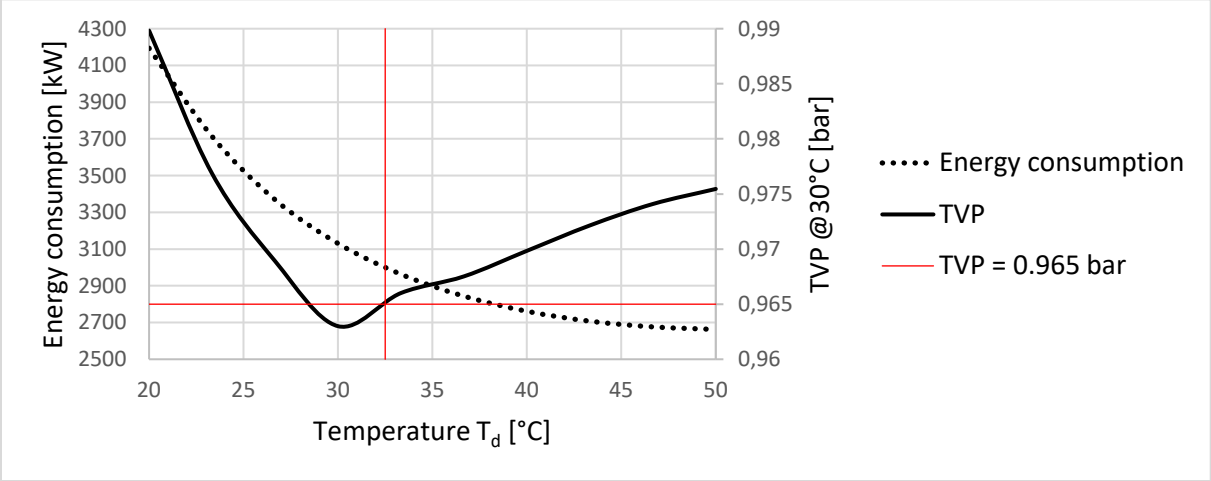

Figure 67: new T_d for the recirculation studies [35]

[34] P_2 = 9.5 bar, P_3 = 2.56 bar, T_h = 85.7°C, $T_1 = T_2 = T_d$ = 30°C
[35] P_2 = 9.5 bar, P_3 = 2.56 bar, T_h = 85.7°C, $T_1 = T_2 = T_f$ = 30°C

Appendix 10: heat integration of the optimised recirculation model

Step 1: identify the hot and cold streams

Same as *Figure 20*.

Step 2: levels of temperature

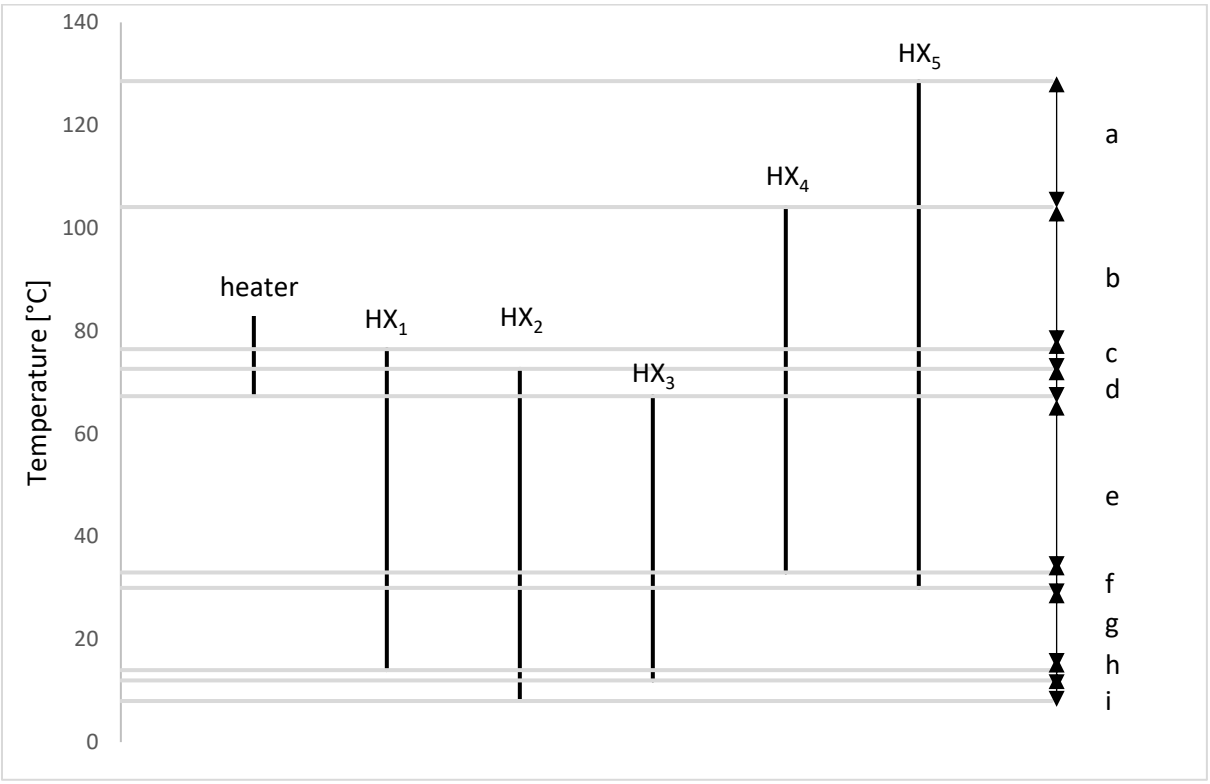

Figure 68: temperature levels in the recirculation optimisation model

Step 3: energy consumption

	$\dot{Q}$ [kW]	T_{in} [°C]	T_{out} [°C]	$\dot{m} * \overline{C_p}$ [kW/°C]
heater	1 185	67.8	82.5	80.9
HX_1	- 223.0	76.4	14.0	3.57
HX_2	- 284.7	72.6	8.00	4.41
HX_3	- 570.6	67.3	12.0	10.32
HX_4	- 679.8	104.1	33.0	9.56
HX_5	- 1 081	128.6	30.0	10.97

Table 45: power consumption in heat exchangers in the recirculation optimisation model

		$\dot{m} * \overline{C_p}$ to consider	$\dot{Q}$ [KW]
Cold stream		$(\dot{m} * \overline{C_p})_{heater}$	1 185
Hot streams	a	$(\dot{m} * \overline{C_p})_{HX5}$	268.6
	b	$(\dot{m} * \overline{C_p})_{HX4} + (\dot{m} * \overline{C_p})_{HX5}$	567.4
	c	$(\dot{m} * \overline{C_p})_{HX1} + (\dot{m} * \overline{C_p})_{HX4} + (\dot{m} * \overline{C_p})_{HX5}$	78.81
	d	$(\dot{m} * \overline{C_p})_{HX1} + (\dot{m} * \overline{C_p})_{HX2} + (\dot{m} * \overline{C_p})_{HX4} + (\dot{m} * \overline{C_p})_{HX5}$	151.4
	e	$(\dot{m} * \overline{C_p})_{HX1} + (\dot{m} * \overline{C_p})_{HX2} + (\dot{m} * \overline{C_p})_{HX3} + (\dot{m} * \overline{C_p})_{HX4} + (\dot{m} * \overline{C_p})_{HX5}$	1 332
	f	$(\dot{m} * \overline{C_p})_{HX1} + (\dot{m} * \overline{C_p})_{HX2} + (\dot{m} * \overline{C_p})_{HX3} + (\dot{m} * \overline{C_p})_{HX5}$	87.79
	g	$(\dot{m} * \overline{C_p})_{HX1} + (\dot{m} * \overline{C_p})_{HX2} + (\dot{m} * \overline{C_p})_{HX3}$	292.7
	h	$(\dot{m} * \overline{C_p})_{HX2} + (\dot{m} * \overline{C_p})_{HX3}$	29.45
	i	$(\dot{m} * \overline{C_p})_{HX2}$	17.62

Table 46: power consumption in the composite curves in the recirculation optimisation model

Step 4: pinch analysis

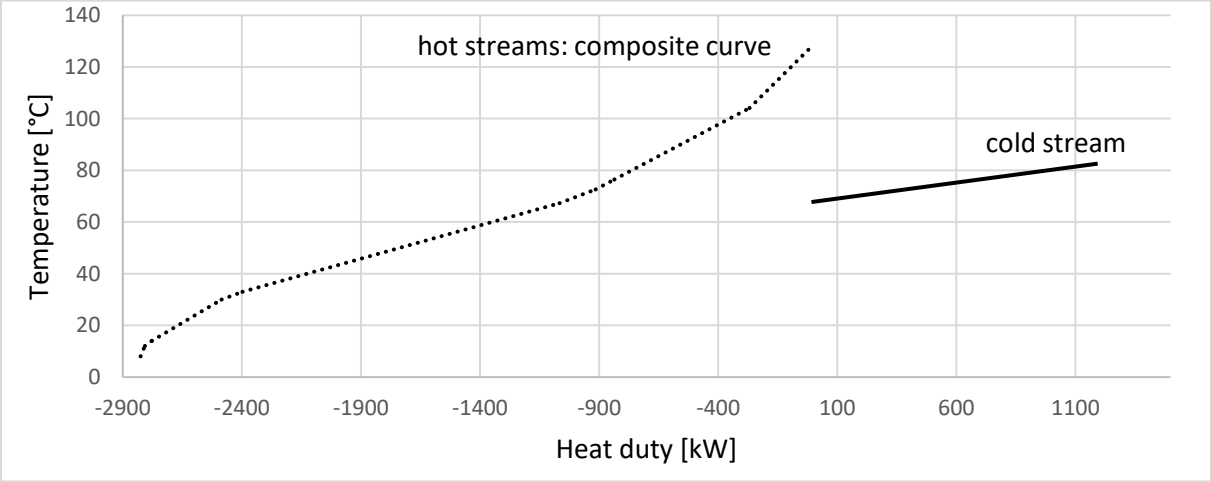

Figure 69: composite curves for the recirculation optimisation model

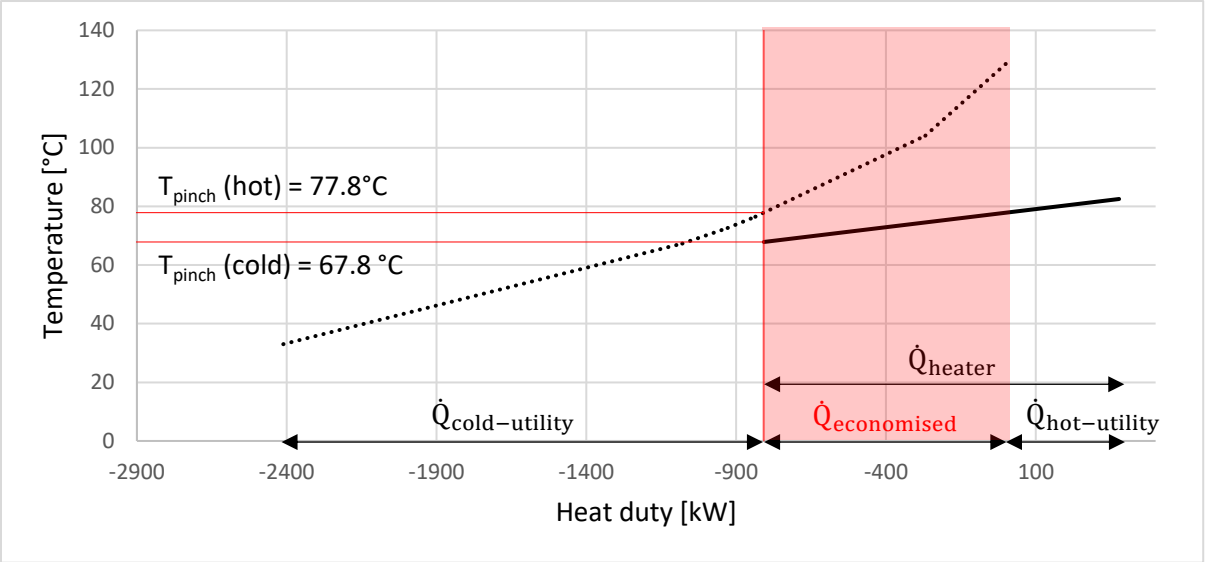

Figure 70: pinch identification for the recirculation optimisation model

$\dot{Q}_{cold-utility}$	$\dot{Q}_{economised}$	$\dot{Q}_{hot-utility}$
2 032 kW	807.3 kW	378.1 kW

Table 47: minimum heat duty consumption in the recirculation optimisation model

Step 5: new network of heat exchangers

Two hot streams can be used to heat the cold one: from the coolers HX_4 and HX_5. The way to combine streams has an influence on the amount of energy that can be saved. Using the stream from HX_4, then the one from HX_5 is the best combination to save energy. With this combination, 412 kW of hot utility are required to heat the condensate from 77.4°C to 82.5°C.

Network	$\dot{Q}_{economised}$ [kW]
HX_4/HX_5	773.3
HX_5/HX_4	741.5

Table 48: new network of heat exchangers for the recirculation optimisation model

The following figure is a representation of how fluids are combined with the new temperature levels.

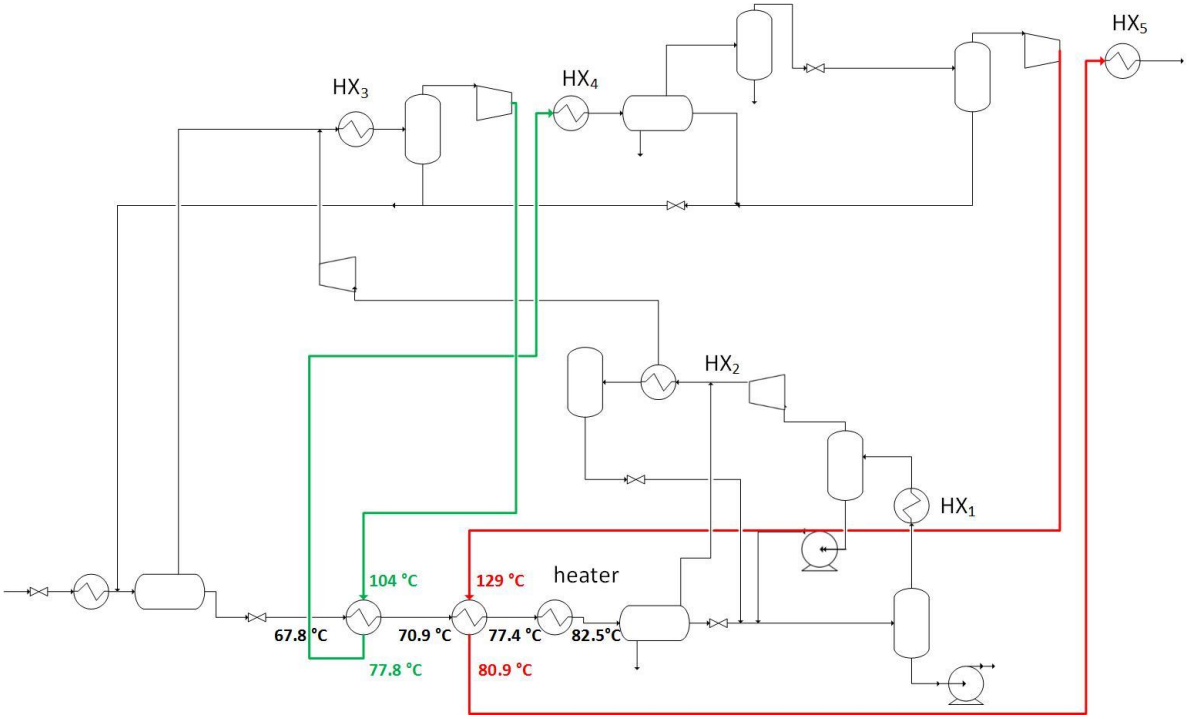

Figure 71: recirculation optimisation model with heat integration

Appendix 11: NG2 composition

Component	Mole fraction
Nitrogen	0.0036
CO_2	0.0123
Methane	0.7750
Ethane	0.1031
Propane	0.0485
i-Butane	0.0056
n-Butane	0.0125
i-Pentane	0.0030
n-Pentane	0.0037
n-Hexane	0.0034
n-Heptane	0.0049
n-Octane	0.0047
n-Nonane	0.0026
C_{10-12}	0.0041
C_{13-15}	0.0030
C_{16-22}	0.0023
C_{19-22}	0.0022
C_{23-25}	0.0012
C_{26-30}	0.0015
C_{31-36}	0.0011
C_{37-46}	0.0010
C_{47-80}	0.0007

Table 49: reservoir composition (NG2)

Appendix 12: parametric studies with NG2 composition

A12.1 Condensate stabilization unit

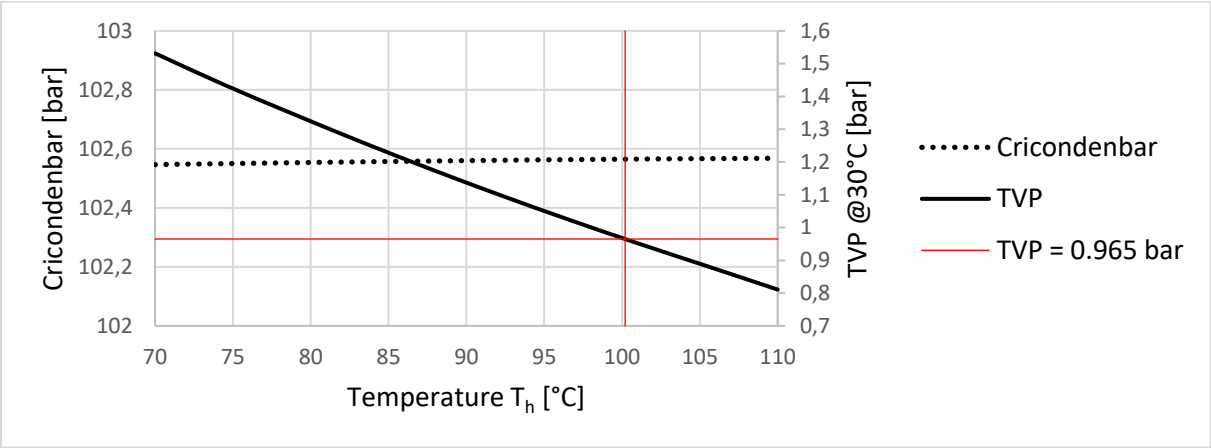

Figure 72: T_h study for NG2 [36]

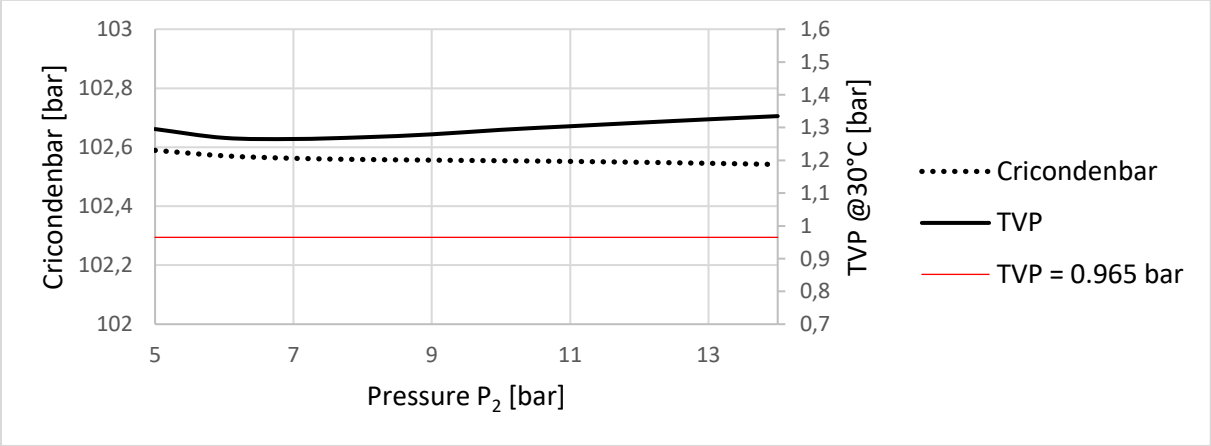

Figure 73: P_2 study for NG2 [37]

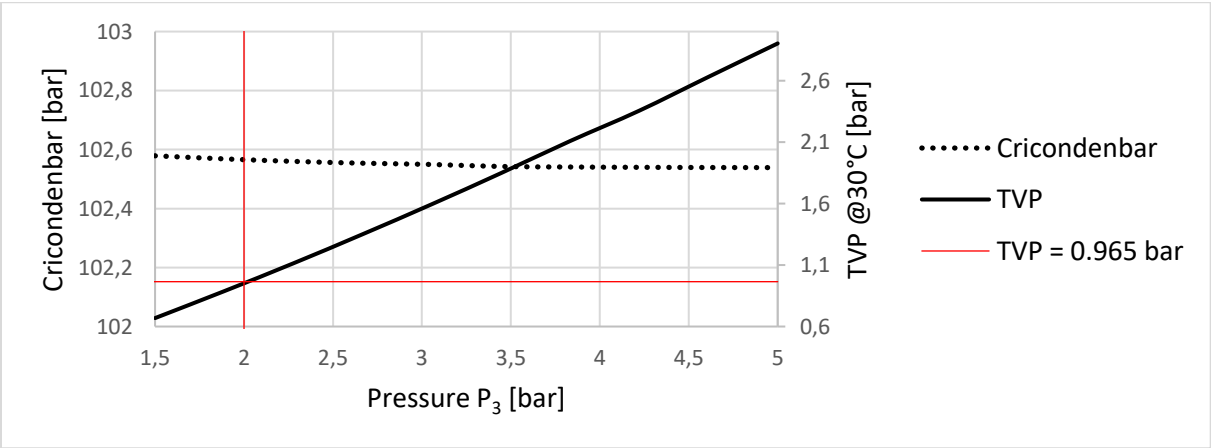

Figure 74: P_3 study for NG2 [38]

[36] P_2 = 9.5 bar, P_3 = 2.56 bar, $T_1 = T_2 = T_f = T_d$ = 30°C
[37] P_3 = 2.56 bar, T_h = 82°C, $T_1 = T_2 = T_f = T_d$ = 30°C
[38] P_2 = 9.5 bar, T_h = 82°C, $T_1 = T_2 = T_f = T_d$ = 30°C

A12.2 Gas recompression stage

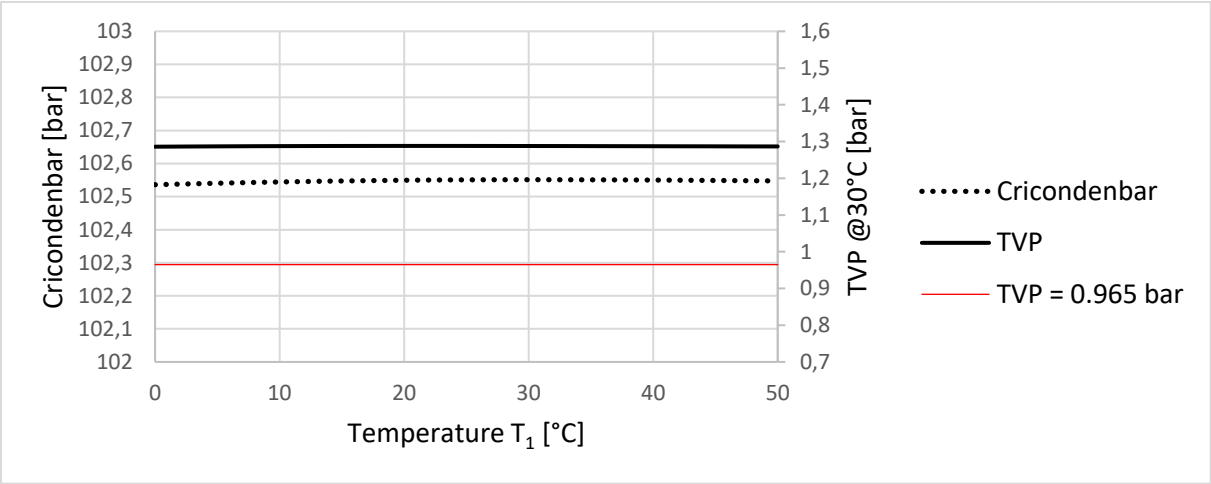

Figure 75: T_1 study for NG2 [39]

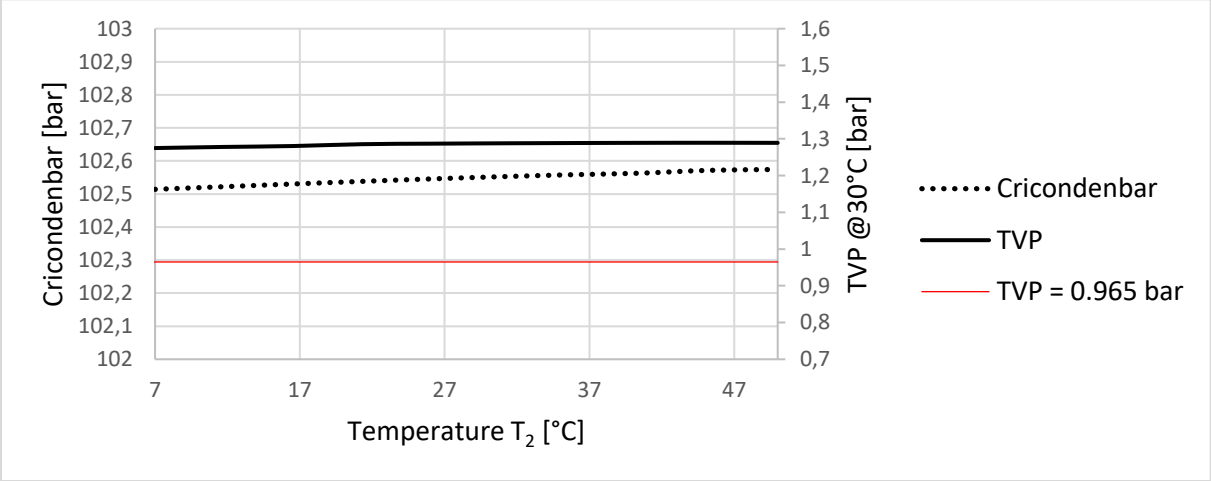

Figure 76: T_2 study for NG2 [40]

[39] P_2 = 9.5 bar, P_3 = 2.56 bar, T_h = 82°C, $T_2 = T_f = T_d$ = 30°C
[40] P_2 = 9.5 bar, P_3 = 2.56 bar, T_h = 82°C, $T_1 = T_f = T_d$ = 30°C

A12.3 Gas processing

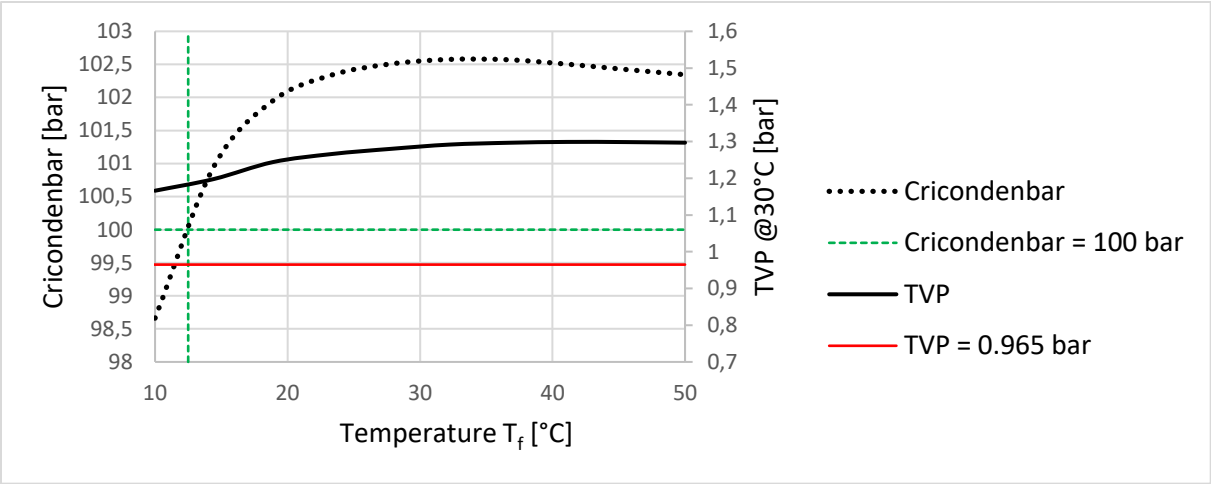

Figure 77: T_f study for NG2 [41]

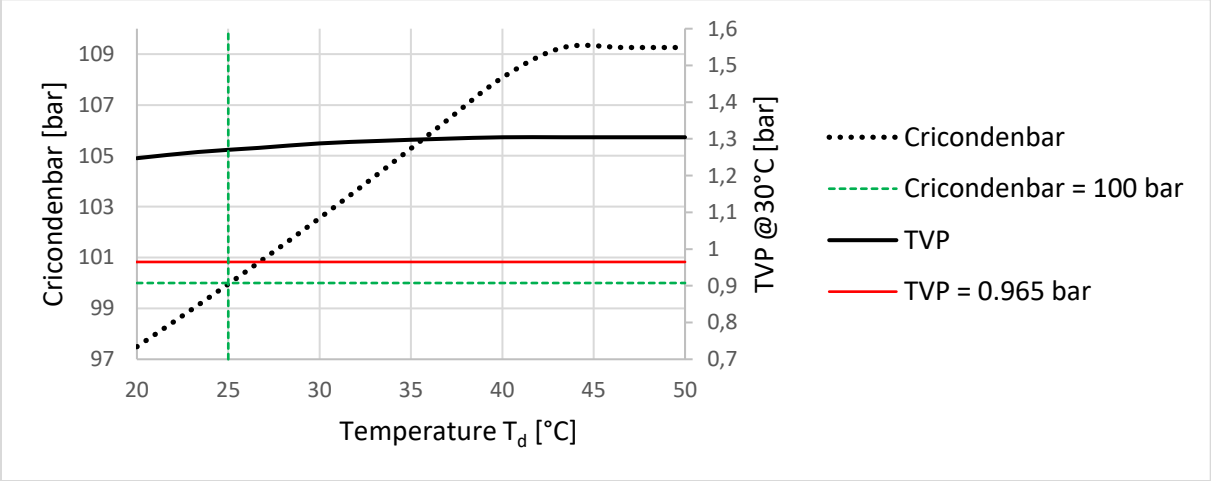

Figure 78: T_d study for NG2 [42]

[41] P_2 = 9.5 bar, P_3 = 2.56 bar, T_h = 82°C, $T_1 = T_2 = T_d$ = 30°C
[42] P_2 = 9.5 bar, P_3 = 2.56 bar, T_h = 82°C, $T_1 = T_2 = T_f$ = 30°C

Appendix 13: cricondenbar specification of 100 bar

A13.1 Cricondenbar controlled by T_f

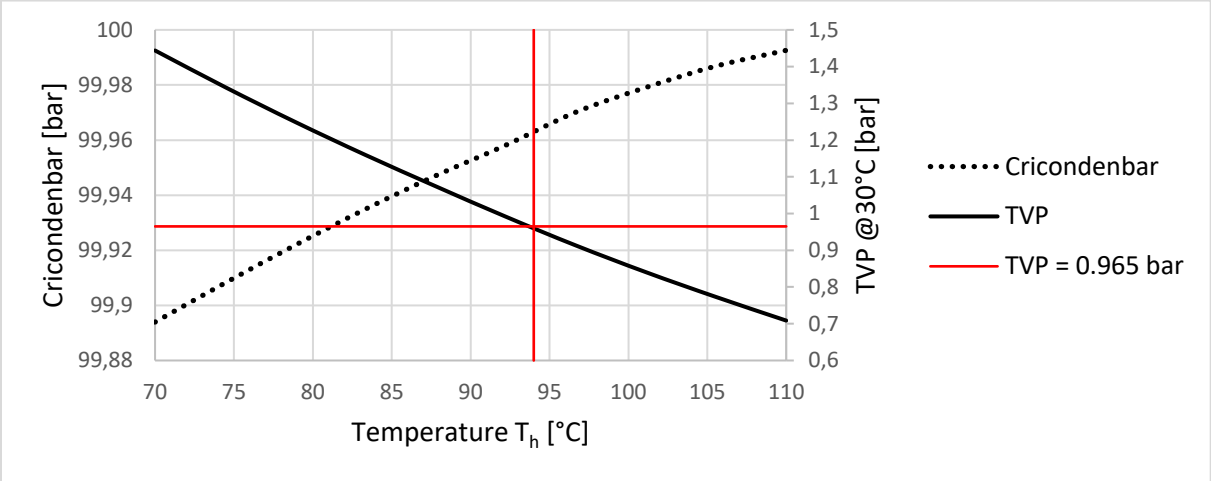

Figure 79: T_h study with cricondenbar controlled by T_f [43]

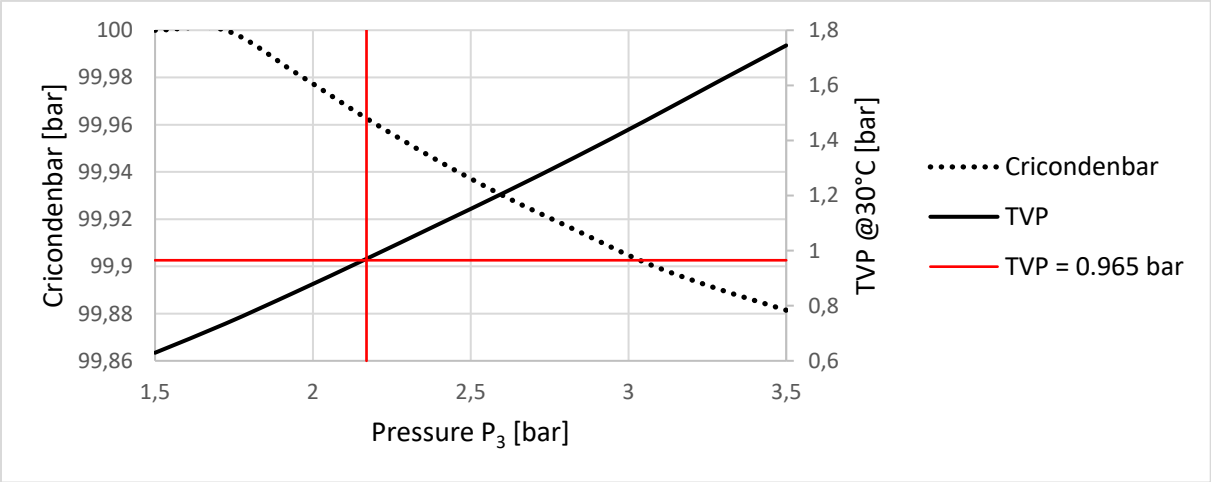

Figure 80: P_3 study with cricondenbar controlled by T_f [44]

[43] P_2 = 9.5 bar, P_3 = 2.56 bar, $T_1 = T_2 = T_d$ = 30°C, T_f = 12.5°C
[44] P_2 = 9.5 bar, T_h = 82°C, $T_1 = T_2 = T_d$ = 30°C, T_f = 12.5°C

A13.2 Cricondenbar controlled by T_d

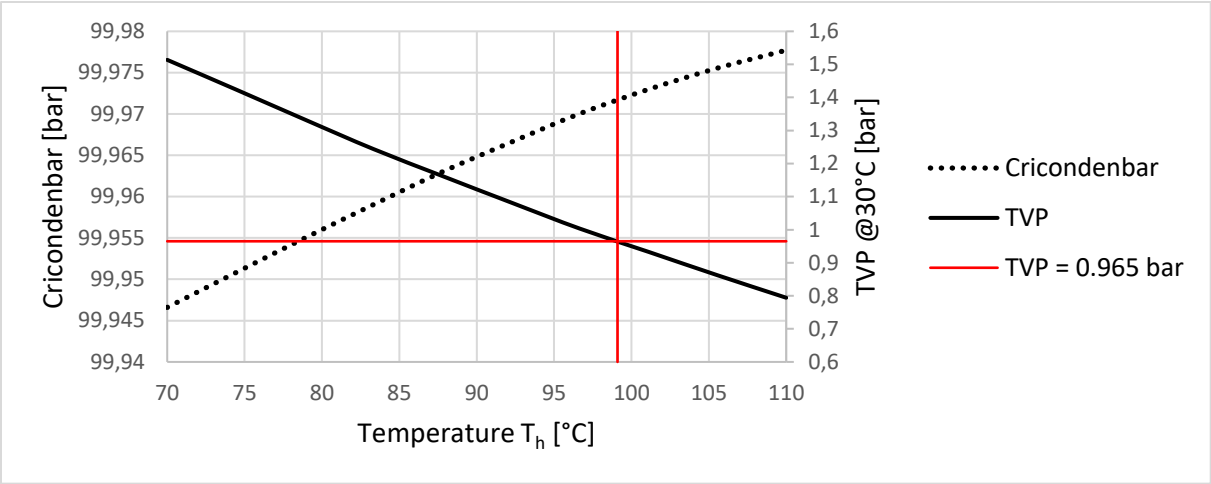

Figure 81: T_h study with cricondenbar controlled by T_d [45]

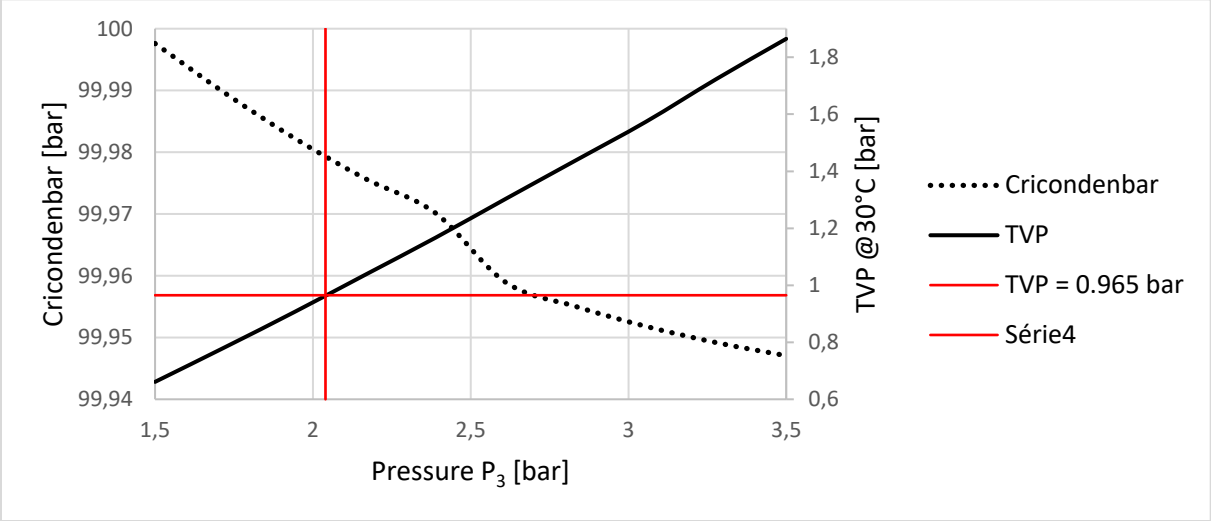

Figure 82: P_3 study with cricondenbar controlled by T_d [46]

[45] P_2 = 9.5 bar, P_3 = 2.56 bar, $T_1 = T_2 = T_f$ = 30°C, T_d = 25°C

[46] P_2 = 9.5 bar, T_h = 82°C, $T_1 = T_2 = T_f$ = 30°C, T_d = 25°C

Mélanie Jaspart

Optimisation of offshore oil and gas processing plants

NTNU
Norwegian University of
Science and Technology

equinor